AD A114516

(12)

# INVESTIGATION OF MODELING CONCEPTS FOR PLUME-AFTERBODY FLOW INTERACTIONS

Final Technical Report

by

Sven-Erik Nyberg and Johan Agrell

November 1981

EUROPEAN RESEARCH OFFICE
United States Army
London England

GRANT NUMBER DA-ERO-78-G-028

Grantee: Georg Drougge, Dr., Deputy Director
THE AERONAUTICAL RESEARCH INSTITUTE OF SWEDEN (FFA)
Box 11021, S - 161 11 BROMMA, Sweden

Approved for Public Release; distribution unlimited

DTIC
ELECTE
MAY 18 1982
S D
E

DTIC FILE COPY

This research has been sponsored jointly by the US Army European Research Office and by the FFA.

82 05 17 090

UNCLASSIFIED

SECURITY CLASSIFICATION OF THIS PAGE (When Data Entered)

| REPORT DOCUMENTATION PAGE | | READ INSTRUCTIONS BEFORE COMPLETING FORM |
|---|---|---|
| 1. REPORT NUMBER | 2. GOVT ACCESSION NO. AD-A114 546 | 3. RECIPIENT'S CATALOG NUMBER |
| 4. TITLE (and Subtitle) Investigation of Modeling Concepts for Plume-Afterbody Flow Interactions | | 5. TYPE OF REPORT & PERIOD COVERED Final Technical Report Jan 78 - Apr 81 |
| | | 6. PERFORMING ORG. REPORT NUMBER FFA Technical Note AU-1384 |
| 7. AUTHOR(s) Sven-Erik Nyberg and Johan Agrell | | 8. CONTRACT OR GRANT NUMBER(s) DA-ERO-78-G-028 |
| 9. PERFORMING ORGANIZATION NAME AND ADDRESS The Aeronautical Research Institute of Sweden (FFA), Box 11021, S - 161 11 BROMMA, Sweden | | 10. PROGRAM ELEMENT, PROJECT, TASK AREA & WORK UNIT NUMBERS 6.11.02A 1T161102BH57-06 |
| 11. CONTROLLING OFFICE NAME AND ADDRESS USARDSG-UK Box 65, FPO NY 09510 | | 12. REPORT DATE November 1981 |
| | | 13. NUMBER OF PAGES 80 |
| 14. MONITORING AGENCY NAME & ADDRESS(if different from Controlling Office) | | 15. SECURITY CLASS. (of this report) Unclassified |
| | | 15a. DECLASSIFICATION/DOWNGRADING SCHEDULE |

16. DISTRIBUTION STATEMENT (of this Report)

Approved for Public Release; distribution unlimited

17. DISTRIBUTION STATEMENT (of the abstract entered in Block 20, if different from Report)

18. SUPPLEMENTARY NOTES

19. KEY WORDS (Continue on reverse side if necessary and identify by block number)

Plume Modeling Laws; Plume-induced Separation

20. ABSTRACT (Continue on reverse side if necessary and identify by block number)

A high pressure hot gas supply system has been developed for the FFA $0.5 \times 0.5\ m^2$ S5 wind tunnel to allow the study of aerodynamic interference effects caused by plume induced separation from propulsive afterbodies. Capable of operating with a variety of gases covering a wide range of specific heat ratios, the facility serves to evaluate the merits and potential of a new plume simulation methodology suggested by Korst. The program has been carried out in close cooperation with the Gas Dynamics Laboratory,

DD FORM 1 JAN 73 1473 EDITION OF 1 NOV 65 IS OBSOLETE

SECURITY CLASSIFICATION OF THIS PAGE (When Data Entered)

the University of Illinois at Urbana-Champaign.

Experimental programs carried out with air and Freon-22 for the jet simulation confirmed the correctness of the theory. The accuracy of the modeling extended over wide ranges of jet-to-ambient pressure ratios straddling the design points. Limited tests at small angles of attack ($-6^{o} \leq \alpha \leq +6^{o}$) and with external disturbances in the vicinity of the base plane (fins) appear to support the applicability of the modeling scheme for more complex flow field geometries. Beyond the ability to correctly model and interpret near wake pressures and slipstream separation locations, the new methodology allows experiments to be conducted with diatomic gases (air or nitrogen, $\gamma = 1.4$) at much lower stagnation pressures as would be required for propellants of lower specific heat ratios.

Accession For
NTIS GRA&I [X]
DTIC TAB [ ]
Unannounced [ ]
Justification
By
Distribution/
Availability Codes
Dist | Avail and/or Special
A

DTIC COPY INSPECTED 2

# INVESTIGATION OF MODELING CONCEPTS FOR PLUME-AFTERBODY FLOW INTERACTIONS

Final Technical Report

Sven-Erik Nyberg and Johan Agrell

SUMMARY

A high pressure hot gas supply system has been developed for the FFA 0.5 × 0.5 $m^2$ S5 wind tunnel to allow the study of aerodynamic interference effects caused by plume induced separation from propulsive afterbodies. Capable of operating with a variety of gases covering a wide range of specific heat ratios, the facility serves to evaluate the merits and potential of a new plume simulation methodology suggested by Korst. The program has been carried out in close cooperation with the Gas Dynamics Laboratory, the University of Illinois at Urbana-Champaign.

Experimental programs carried out with air and Freon-22 for the jet simulation confirmed the correctness of the theory. The accuracy of the modeling extended over wide ranges of jet-to-ambient pressure ratios straddling the design points. Limited tests at small angles of attack ($-6° \leq \alpha \leq +6°$) and with external disturbances in the vicinity of the base plane (fins) appear to support the applicability of the modeling scheme for more complex flow field geometries. Beyond the ability to correctly model and interpret near wake pressures and slipstream separation locations, the new methodology allows experiments to be conducted with diatomic gases (air or nitrogen, $\gamma = 1.4$) at much lower stagnation pressures as would be required for propellants of lower specific heat ratios.

LIST OF CONTENTS

Page

REPORT DOCUMENTATION PAGE

SUMMARY ..... 1

LIST OF CONTENTS ..... 3

NOMENCLATURE ..... 5

1. INTRODUCTION ..... 7

2. SIMULATION TEST FACILITY ..... 9

3. REVIEW OF THE PLUME MODELING METHODOLOGY SUGGESTED BY KORST ..... 13

4. EXPERIMENTAL EQUIPMENT ..... 17

4.1 Wind tunnel models ..... 17

4.2 Strut interference tests ..... 19

5. PLUME MODELING EXPERIMENTS ..... 21

5.1 Test conditions ..... 21

5.2 Modeling from Air to Freon ..... 21

5.3 Modeling from Freon to Air ..... 23

5.31 Zero angle of attack tests ..... 23

5.32 Effects of small angles of attack ..... 24

5.33 Effects of fins at zero angle of attack ... 25

5.4 Plume modeling experience ..... 26

6. CONCLUSIONS ..... 27

REFERENCES ..... 29

ACKNOWLEDGEMENT ..... 33

FIGURES ..... 35

APPENDIX 1. TABLES OF BASIC TEST DATA, MODELING FROM AIR TO FREON..... 53

APPENDIX 2. TABLES OF BASIC TEST DATA, MODELING FROM FREON TO AIR..... 67

PRECEDING PAGE BLANK-NOT FILMED

NOMENCLATURE

Geometry

| | |
|---|---|
| | Afterbody |
| D | Forebody diameter [m] |
| L | Boattail length [m] |
| M, N | Pressure tap location index, see Fig. 7 |
| X | Axial coordinate [m], see Fig. 6 |
| $\alpha$ | Angle of attack [deg.] |
| $\beta$ | Boattail angle [deg.] |
| $\varphi$ | Circumferential angle [deg.], see Fig. 7 |
| | Nozzle |
| $R_L$ | Exit or lip radius [m] |
| $\theta_L$ | Conical divergence angle [deg.] |

Tunnel Flow

| | |
|---|---|
| $P_0$ | Stagnation pressure [Pa] |
| $P_E$, $P_e$ | Freestream static pressure [Pa] |
| $M_E$ | Freestream Mach No. [-] |

Nozzle Flow

| | |
|---|---|
| $M_L$ | Lip Mach No. [-]*) |
| $P_{0I}$ | Nozzle stagnation pressure [Pa] |
| $P_L$ | Lip pressure [Pa] |
| $T_{0I}$ | Nozzle stagnation temperature [°C] |
| $\gamma$ | Specific heat ratio [-] |
| $\omega_L$ | Prandtl-Meyer angle corresponding to $M_L$ [deg.] |

*) Conical source flow assumed, otherwise nozzle geometry and lip conditions have to be specified in greater detail, see Reference [21]

PRECEDING PAGE BLANK-NOT FILMED

Plume

| | |
|---|---|
| $M_F$ | Surface Mach No. [-] |
| $\theta_F$ | Initial surface slope [deg.] |
| $R_C$ | Initial surface curvature [m] |
| $r_c$ | $R_C/R_L$ [-] |
| $\omega_F$ | Prandtl-Meyer angle corresponding to $M_F$ [deg.] |

Wake Conditions

| | |
|---|---|
| S | Separation distance measured from end of boat-tail [m] |
| $P_b, P_B$ | Base pressure [Pa] |

Subscripts

| | |
|---|---|
| M | Model |
| P | Prototype |
| A | Air |
| F | Freon |

## 1. INTRODUCTION

The interaction of rocket or jet plumes with the external flow over a vehicle as well as surrounding equipment or surfaces is important to system performance [1].*) In particular, such interactions are critical in their effects on the near wake base temperature and pressure, flow over the vehicle itself due to external flow separation, wake flow field at angle of attack, afterbody fin effectiveness, and launch equipment performance. Thus, the jet-slipstream interaction can give rise to undesirable aerodynamic performance by introducing drag penalties through lower than ambient pressures or, as the ratio of jet stagnation pressure to ambient pressure increases, plume induced separation [2]. In extreme cases, plume induced separation can result in catastrophic pitch-up of missiles because of loss of stability of degradation or control effectiveness [3].

Rocket or jet plumes have been treated in wind tunnel tests using a variety of methods which include the use of cold or heated air through geometrically modeled nozzles, small rocket motors, radial gas injection and solid surfaces with simulated plume shape (either calculated or determined from Schlieren photographs of jet plumes). Shortcomings inherent in these methods can be traced to failure to account for all, or part, of such factors as plume deflections, mass entrainment, wake closure, influence of specific heat ratio, viscous effects, geometry and temperature. It is, of course, not feasible to take account of all the contributing parameters simultaneously in a simulation test. While some methods of plume simulation appear to be more appropriate than others, i.e., cold gas rather than solid surfaces, only limited comparisons have been undertaken between results for simulation models and for actual prototypes. In addition, documentation

---

*)Numbers in square brackets refer to entries in REFERENCES

of the importance of individual factors such as plume geometry, plume stiffness (i.e. jet surface Mach number), and wake closure conditions for the various Mach number regimes has been lacking.

It is the purpose of this project to undertake, in close cooperation with the Gas Dynamics Laboratory at University of Illinois at Urbana-Champaign, the evaluation of modeling techniques and importance of primary and secondary factors.

The project has been going on for three years. During the first year the design and construction of a facility for the use of superheated Freon ($\gamma \approx 1.16$) at high pressure was carried out, to be used for jet simulation in the FFA $0.5 \times 0.5$ $m^2$ S5 wind tunnel. Shake-down testing of the facility was started and an existing strut-supported axi-symmetric model was modified for tests with heated Freon [4, 5]. Plume modeling experiments were started during the second year with tests at the design Mach number $M_E = 2.0$, zero angle of attack and modeling from air as prototype, to Freon, as model [6, 7]. During the third year the same nozzles were tested at an off-design free stream Mach number $M_E = 3.0$ [8]. The major part of the third year activities, however, was the study of the plume modeling from a Freon prototype nozzle (combustion product simulation) to air model nozzles. The investigation was carried out at the design free stream Mach number $M_E = 2.0$ for the angles of attack $\alpha = 0, \pm 3°$ and $\pm 6°$. A few tests were also made at zero angle of attack to examine the effects of aft-mounted control surfaces.

This final report briefly describes the simulation test facility. The analytical basis for the plume modeling methodology proposed by Korst [9, 10] is also reviewed. Results of the plume modeling tests obtained during the second and third year program with nozzles designed in accordance with this method are presented and discussed.

Reports and other publications resulting from the work sponsored by this Grant are in chronological order References Nos: 27, 4, 5, 6, 24, 7, 22, 28, 8, 25 and 29.

## 2. SIMULATION TEST FACILITY

A jet simulation test facility has been designed and constructed for use with the FFA 0.25 $m^2$ and 1.0 $m^2$ wind tunnels [5, 11]. It has been designed for various types of heated Freon but can in principle also be used in future investigations for other gases (e.g. Argon) with small changes in the instrumentation. The unit has been constructed for this research program exclusively with the object of allowing critical evaluation of the merits and limitations of plume modeling techniques, such as outlined in Section 3.

For this purpose, it is essential to have accurate test results and well controlled operating conditions for both prototype and model. The test conditions should be well known in terms of the wind tunnel slipstream flow and should allow for careful control of the modeled propulsive jet, influence of transonic throat flow, nozzle design methodology, and working fluid. The design concept draws on the extensive test program on missile afterbody-jet performance which the FFA has carried out and reported on over the last ten years [12,13,14]. This approach provides a wide base of well documented results to be used as prototypes as well as allowing the use of a considerable portion of existing wind tunnel models and supporting equipment. The latter, in addition to reducing cost, guarantees that such factors as external boundary layer thickness remain largely unchanged in prototype and modeled configurations.

The selection of the test gas was based on availability, cost, non-toxicity, having an appropriate ratio of specific heats and not having serious real gas effects. After an examination of alternatives Freon-22 was chosen. Cost and chemical stability - which allows it to be heated to sufficiently high temperatures without chemical breakdown - were major factors in its selection. The latter should allow expansion up to approximately Mach number 5 without crossing the condensation line. Fig. 1 shows a simplified pressure-enthalpy diagram for Freon-22 illustrating the thermodynamic paths for the heating and nozzle expansion processes. The ratio of specific heats at nozzle exit and plume expansion conditions, $\gamma_F$, is in the range of 1.16 to 1.18 which is appropriate for simulation of combustion type jet products.

The modeled nozzles were designed using the modeling procedures discussed in Section 3 and their mass flow requirements were based on configurations run with air (prototype) in the earlier FFA programs [12,13,14]. Shown in Fig. 2 is a systems performance diagram having the nozzle exit (lip) Mach number as abscissa, the nozzle mass flow rate as ordinate and driver pressure level as a parameter. Mapped into this diagram are the operating conditions required for the modeling scheme. The nozzle configurations in the higher lip Mach number range (greater than approximately 4) require impractically high pressure levels but, fortunately, are physically unrealistic as models since the nozzle divergence angles are generally excessive (greater than 40 degrees half angle).

The basic system makes use of the high pressure storage of the FFA's hypersonic facilities [11] which allows the storage of 50 $m^3$ of air at a pressure of 25 MPa. This is used in the simulation system as an essentially constant pressure driver for the Freon. Fig. 3 is an annotated schematic of the Freon

system, the test model and the high pressure driver. Details of component design, construction and operating procedures are given in Ref. [5] along with a discussion of the temperature control requirements and the system developed for this purpose.

The facility consists of two parts: the unheated driver section and the heated and insulated section containing the test gas. Referring to the schematic (Fig. 3), the unheated pressure section and the heated and insulated part are constructed in a similar manner using vertical arrays of high-pressure tubes. The thermodynamic paths followed by the test gas are shown in Fig. 1 and consist of a constant volume heating process from points 0 to 1 and the essentially isentropic expansion through the nozzle from 1 to 2. The system is designed to provide the maximum supply capacity indicated (dashed line) in Fig. 2 with the upper limit determined by choking and the varying pressure line established by the maximum driving pressure and flow rate-pressure loss characteristics of the entire system. It can be seen in Fig. 2 that the design points of the selected simulation nozzles fall within the system operating range while allowing considerable off-design testing.

The basic design concepts of the system can best be illustrated by a brief discussion of the operational procedure: Prior to a run, the system is charged by the charging pump to the state where the heated portion contains the correct amount of Freon to reach the desired pressure and temperature after being heated at constant volume, that is process 0-1 shown in Fig. 1. The required volume for the system described is approximately 0.16 $m^3$. The determination of the amount of Freon charged is facilitated by use of a pump revolution counter serving for metering purposes.

The hot and cold portions are now isolated and charging is continued until the unheated portion of the system has reached the pressure prescribed for the run (state 1 in Fig. 1). Small pressure corrections may be necessary and these can be made using either the needle valve, the discharge line, or the charging pump as may be appropriate.

The heating process is accomplished by heating only a portion of the tubes, thus producing thermal circulation within the high temperature tube array. The convection persists until the desired temperature is reached.

During a run, the cold Freon serves as a cushion between the air and test gas to prevent mixing of the driver air and hot test gas. The density relations between the cold Freon cushion and hot gas are such that thermal convection at the interface is inhibited.

An individual run may last as long as the gas temperature remains constant (the system is designed for 15 second tests). A small portion of the cold Freon will be sufficiently heated by entering and traversing the warm tube array to also serve as test gas and thus allowing slightly increased run times over the nominal design value. The latter has been found to contribute to slow pressure variations during a typical run. Fast pressure transducers for measurement of model pressures affected by the jet stagnation pressure in combination with synchronized Schlieren photographs allow a range of pressure conditions to be monitored in a single run as the jet stagnation pressure varies.

## 3. A REVIEW OF THE PLUME MODELING METHODOLOGY SUGGESTED BY KORST

Integral and component approaches to near wake solutions, with their wake closure conditions linked to second law concepts, have led to a basic understanding of the problem and even to the establishment of relations [15] accounting for the influence of all pertinent variables. The difficulty of making specific assessments concerning the wake closure has led to extensive experimental studies in support of semi-empirical relations to account for the incomplete realignment of streamlines during recompression [16].

Experimental programs require proper plume simulation whenever the use of prototype propellant is not feasible. The modeling of plume interactions requires in principle geometrically similar inviscid jet contours and correct pressure rise-jet boundary deflection characteristics (plume stiffness) as well as mass entrainment along the wake boundaries. Thus modeling with gaseous plumes is needed and normally involves dissimilar specific heat ratios.

The importance of generating the correct jet plume geometry has been stressed in prior efforts to establish modeling laws between propellant gases having dissimilar specific heat ratios [17,18,19]. However, the geometrical requirements were only formulated for the initial deflection angle of the jet, a condition not stringent enough to cope with plume induced separation [17].

A second order approximation for dealing with axi-symmetric centered expansions [20] forms in Korst's method the basis for geometrical jet plume surface modeling [9]. This approach allows matching not only initial deflection angle but also plume radius of curvature (shape), see Fig. 5. It can

be shown that the accuracy obtained by such a procedure extends well beyond the range of convergence for the corner expansion itself [21].

The plume expansion derives its initial conditions from the flow approaching the end of the nozzle. For the case where exit conditions can be sufficiently well described, locally, by conical source flow ($M_L, \theta_L$), sweeping simplifications in the interpretation of results are possible [21]. The solutions lead to a direct correspondence of nozzle shapes producing the same plume boundary geometry with one free parameter remaining available for satisfying the inviscid recompression conditions at the end of the separated flow region. It is thus possible to determine nozzle exit conditions in terms of Mach number at the nozzle lip and the nozzle divergence angle at the lip which will geometrically duplicate the jet contour produced by a gas with different specific heat ratio as it expands from a given nozzle under specific adjacent conditions (within the present degree of approximation), that is

$$\theta_{F,M} = \theta_{F,P} \quad \text{and} \quad R_{C,M} = R_{C,P} \tag{1}$$

where the geometry and notation are shown in Fig. 5 and subscripts M and P are for model and prototype respectively. The downstream condition should properly account for the interaction of the (viscous) wake flow with the inviscid flow. With only one choice available as a result of the geometric requirements, it is obvious that one has to account above all, for the proper pressure rise in the external flow [17]. The recompression mechanism of the dissipative boundary of the jet, as a consequence of its mass entrainment, will, however, generally not be simultaneously satisfied. While this effect may be expected to be small for cases involving strongly underexpanded plumes [21], it is possible

to account for it in principle by introducing mass bleed. The concept of equivalent mass bleed has been shown [16] to be useful for both mass and temperature effect simulations.

The effect of plume stiffness has been examined in some detail [22] in tests carried out at FFA and at Calspan [23]. The results underscore the importance of the selection of plume flexibility characteristics to the simulation process particularly at supersonic Mach numbers. Selection of the pressure rise-deflection characteristics of the plume leads to the inviscid specifying relations [9]:

$$[\gamma_M M_{F,M}^2/(M_{F,M}^2-1)^{\frac{1}{2}}] = [\gamma_P M_{F,P}^2/(M_{F,P}^2-1)^{\frac{1}{2}}] \qquad (2)$$

for weak shock recompression and

$$[2\gamma_M M_{F,M}^2-(\gamma_M-1)]/(\gamma_M+1) = [2\gamma_P M_{F,P}^2-(\gamma_P-1)]/(\gamma_P+1) \qquad (3)$$

when a strong shock occurs.*)

It is now necessary to identify the type of separation phenomenon to be investigated in order to establish design criteria for proper modeling. For a known pressure distribution over the prototype afterbody due to the non-separated slipstream, one can estimate the pressure rise due to separation by using information on free interactions [16] or slight modifications thereof due to local pressure gradients and/or surface slope discontinuities [14]. The resulting plateau pressure determines the jet surface Mach number $M_{F,P}$ so that the prototype conditions (nozzle flow, $M_{L,P}$ $\theta_{L,P}$ especially

---

*) It should be noted that the concept of weak or strong shock design as used in this repeort has been redefined based on weak shock conditions only. Thus pressure rises can be treated on a consistent basis, see Reference [29] for details.

for conical source flow) are all given and the model nozzle exit conditions $M_{L,M}$; $\theta_{L,M}$ as well as the model jet surface Mach number $M_{F,M}$ (Eqs. (2) or (3)) are determined [9]. Thus, for this "design point", Eqs. (1) and either (2) or (3) are satisfied.

In the vicinity of the design point, only the more stringent condition of plume slope matching is retained. This can be expressed in the form

$$\theta_{F,M} = \theta_{F,P} \tag{4}$$

and

$$\omega_{F,P} = \theta_{L,M} - \theta_{L,P} + \omega_{L,P} - \omega_{L,M} + \omega_{F,M} \tag{5}$$

Since the nozzle flows - and therefore $\theta_{L,M}$, $\theta_{L,P}$, $\omega_{L,M}$, $\omega_{L,P}$ remain identical for design and off-design operation then one may expect that the wake pressure ratios will still be closely modeled

$$\left(P_b/P_E\right)_P = \left(P_b/P_E\right)_M = f\left(P_{0I,M}/P_{0E}\right) \tag{6}$$

Thus, one finds the pressure ratio for the prototype flow from the Prandtl-Meyer relation

$$M_{F,P} = f(\gamma_P, \omega_{F,P}) \tag{7}$$

and the identity

$$P_{0I,P}/P_{0E} = \left(P_{0I,P}/P_b\right)_{M_{F,P}} \cdot \left(P_b/P_E\right)_M \cdot \left(P_E/P_{0E}\right)_{M_E} \tag{8}$$

Thus, for each model flow experiment series for which the relations

$$(P_b/P_E)_M = f[M_E, (P_{OI,M}/P_{OE}), \gamma_M] \quad (9)$$

has been established, the corresponding operating condition of the prototype flow can be determined.

## 4. EXPERIMENTAL EQUIPMENT

### 4.1 Wind tunnel models

A strut supported wind tunnel model, as shown in Fig. 6, earlier used for the study of plume interference effects with air as the propellant gas [12], was modified to allow high mass flow of heated high pressure Freon to be introduced into the model with acceptably low pressure losses. The model is composed of a 14 degree half-angle nose cone, a cylindrical center body of 50 mm diameter and a set of interchangeable afterbodies. The overall model length is 9.5 diameters.

The basic afterbody configuration is an 8 degree boattail with L/D = 1 [12,13]. The rear part of model body, the boattail and the base region are all instrumented with pressure taps (Fig. 7). The individual pressures are recorded from a series of rapid response transducers. Combined with Schlieren photographs (and in some cases oil-flow photographs), this allows the accurate determination of the external flow-jet interference pattern, in particular the plume induced separation on the afterbody. A set of four stabilizing or control surfaces can be attached to the afterbody as shown in Fig. 6. In this test the fins were fixed at zero incidence positioned circumferentially at $\varphi = \pm 45°$ and $\pm 135°$.

The first series of plume modeling tests was carried out with $\text{air}_{|\text{prototype}}$ to $\text{Freon}_{|\text{model}}$ nozzles. Based on the earlier series of experiments conducted with air nozzles [12,13,14] calculations were carried out according to the methodology of Section 3 to select the best suited prototype configuration for the initial Freon 22 modeling tests. The results mapped into the Freon facility performance diagram are shown in Fig. 2. Based on these calculations, the air nozzle with a nominal exit Mach number of 2.5 and a conical wall angle of 10° was selected as the prototype (see Fig. 8a). Design conditions were chosen to allow for both design and off-design experimentation with the Freon nozzles for weak shock modeling ($M_{L,M} = 3.9$, $\theta_{L,M} = 19.76°$, see Fig. 8b, corresponding to $p_L/P_{E|P} = 6.1$) and for strong shock modeling ($M_{L,M} = 3.19$, $\theta_{L,M} = 14.19°$, see Fig. 8c, corresponding to $p_L/P_{E|P} = 9.2$). Operating ranges for these model tests are also shown in Fig. 2.

A second series of plume modeling tests was carried out with $\text{Freon}_{|\text{prototype}}$ to $\text{air}_{|\text{model}}$ nozzles. As the specific heat ratio for Freon 22 is $\gamma = 1.16$, which is appropriate for simulation of combustion type jet products, this modeling is relevant for typical plume simulation in wind tunnels. The geometry of the prototype was chosen to be as realistic as possible, e.g. to have a shape similar to a typical rocket nozzle (see Fig. 9a, $M_{L,P} = 2.60$, $\theta_{L,P} = 15°$, and $p_L/P_{E|P} = 3.48$). The calculated data of the model air nozzles are $M_{L,M} = 1.41$, $\theta_{L,M} = 3.07°$ and $p_L/P_{E|M} = 6.03$ for weak shock modeling and $M_{L,M} = 2.03$, $\theta_{L,M} = 10.47°$ and $p_L/P_{E|M} = 5.07$ for strong shock modeling. Unfortunately the calculated air nozzles could not be accommodated in the existing afterbody due to the large throat areas. It was therefore necessary to construct two new afterbodies with integrated nozzles, see Fig. 9b and c. Each afterbody was provided with the pressure tubing needed for measurement of the surface pressure distribution at angle of attack.

## 4.2 Strut interference tests

Fig. 6 shows both the original configuration and the modified version of the model support strut. The modified strut section is thicker and has larger chord due to the additional Freon piping and its fairing, which increase the interference of the strut on the model afterbody flow field. During the facility calibration tests the strut interference was determined for the zero angle of attack case with air as propellant. The axial pressure distribution along the generator opposite to the strut was measured and was compared with earlier measurements with the original strut. While the earlier strut configuration produced negligible interference effects as has been confirmed by comparison with sting mounted runs [24], the new, enlarged fairing led to small but measurable differences in afterbody pressure distributions [7] as shown in Fig. 10.

The small difference noted for the pressure distribution due to the modified strut required that the air prototype tests be repeated over the range reported in earlier publications to ensure that strut effects did not introduce unanticipated changes. The results from the current air tests are shown in Fig. 11 and the results from the earlier tests are also shown for comparison.

When the second series of plume modeling tests started and pressures at different circumferential body angles were measured, it was revealed that quite appreciable strut interference affected the pressure distributions on the side of the model. During these tests the pressure measurements were made in a quadrant on the opposite side to the supporting strut. In the angle of attack tests the wind and lee sides were accounted for by testing at negative and positive angles

of attack respectively. Some results of the interference measurements are shown in Fig. 12 [25]. Also shown in the figure are the experimental data corrected for the theoretically determined primary non-viscous influence of the strut, as calculated by small disturbance potential flow theory [26]. From the $\alpha = 0$ case, where the unaffected pressure should be constant around the model, the conclusion can be drawn that not only the effects from the non-viscous strut flow field are present, but also effects induced by this flow field on the model boundary layer. This is demonstrated in Fig. 13, where oil flow pictures at zero angle of attack are shown. For the original strut configuration the boundary layer flow is nearly parallel to the axis and the separation line is straight except right behind the strut. For the modified model, however, the strut induced boundary layer flow tends to thicken the boundary layer at the model side ($\varphi = 90°$) and the separation line is curved.

A number of modifications to the geometry of the strut trailing edge were tested. The interference could be appreciably decreased, but unfortunately it turned out that the best configuration for the $\alpha = 0$ case had an interference, which varied strongly with angle of attack. As determination of the angle of attack effects on the plume-simulation is one important objective, it was preferred to use the strut without further modifications and accept an appreciable interference from a strut, for which there is evidence that the interference does not vary much with angle of attack within the range investigated. It is, however, recommended that, in any future extension of this work to higher angles of attack, a more slender strut be used.

# 5. PLUME MODELING EXPERIMENTS

## 5.1 Test conditions

The tests were carried out in the 0.5×0.5 $m^2$ S5 wind tunnel, which operates at atmospheric stagnation pressure [11]. The major part of the tests was accomplished at $M_E = 2.0$ and a corresponding Reynolds number based on the model length $Re = 6\times10^6$ extended by a few tests at $M_E = 3.0$ and $Re = 4\times10^6$. The nozzle stagnation pressures were varied over a wide range; the nozzle stagnation temperatures were -20° - +20°C for air and 200-250°C for Freon.

## 5.2 Modeling from air to Freon

Base pressure ratios obtained for the two model cases, i.e. weak shock modeling (nozzle, Fig. 8b) and strong shock modeling (nozzle, Fig. 8c), are most appropriately interpreted in comparison to the prototype. Consequently the test results presented below are compared on the basis of the corresponding prototype (air) or model (Freon) pressure ratios as determined by the methods of Section 3, Eqs. (4) to (9).

The model pressures recorded at $M_E = 2.0$ [7] and at $M_E = 3.0$ [8] are presented in Tables 1-9, APPENDIX 1. A sample of the agreement achieved between the prototype air plume and model Freon plume shapes is shown in Fig. 14. The Schlieren photos, Figs. 14a,b, are seen to be nearly identical. A direct comparison of the essential features of the two flow fields from photo overlays (Fig. 14c) shows the agreement is also satisfactory for slipstream and plume geometries for the entire near wake region.

Shown in Figs 15 and 16 is the base pressure ratio $P_B/P_E$ versus the Freon jet stagnation pressure $P_{0I}$ as measured in the settling chamber of the nozzle. For the weak shock modeling nozzle, the plume surface Mach numbers are in some cases at the higher stagnation pressures so high that, combined with the temperature loss in the model and its support, condensation has been found to occur in some tests and those points are flagged in Fig. 15.

Transformation of the air prototype results into the Freon model plane are shown for comparison. The base pressure results are also presented with the Freon model results transformed into the air model plane, versus stagnation pressure in Fig. 17 and versus lip pressure in Fig. 18 and the design points are identified. The agreement between prototype and model experiments for base pressures is satisfactory not only for the design point but also for a rather wide range of off-design conditions.

Also shown are a few results for the Freon nozzles run with air to illustrate the shortcomings of retaining nozzle similarity. Slope modeling of these results gives reasonable correspondence to the prototype data but at effectively much lower pressure ratios. At these conditions, with essentially no separation, the radius of curvature is less important. In contrast to the proposed technique based on distorted nozzle geometries, very high stagnation pressures would be required for modeling with gases of higher than prototype specific heat ratios. This in turn would restrict experimentation to lower than ambient base pressures in accordance with the limitations anticipated and stated in Reference [17].

The separation locations S/D for the air (prototype) and Freon (model) nozzles are shown as a function of lip pressure

in Fig. 19. For the separation location the weak shock nozzle provides the best correlation, particularly near the design pressure ratio.

Some tests at off-design free stream Mach number conditions were undertaken to gain insight into the range of applicability of the plume deflection angle-radius of curvature (shape) model method. Thus while the nozzles were designed for $M_E$ = 2.0 free stream condition tests were also run at $M_E$ = 3.0. Fig. 20 shows the base pressure, which can be seen to be satisfactory particularly in the lower base pressure regime. The more sensitive separation distance as, however, shows poorer correlation (Fig. 21).

## 5.3 Modeling from Freon to Air

### 5.31 Zero angle of attack tests

Base pressure ratios measured for the Freon (prototype) and the air (model) nozzles versus the jet stagnation pressure $P_{0I}$ as measured in the settling chamber of the nozzle are shown in Fig. 22. A detailed study of the internal flow in the low Mach number air nozzle (see Fig. 8b) revealed that the baffle upstream of the nozzle had at this Mach number not been sufficiently effective in smoothing out the stagnation pressure distribution and that the stagnation pressure measured by the installed probe was not representative of the average stagnation pressure over the nozzle exit area. The stagnation pressure results presented in this report have been corrected correspondingly. It was also established that the exit plane Mach number distribution was distorted. The average Mach number over the exit area was however M = 1.41,

which is equal to the design Mach number. This Mach number has been used when the air jet results have been transformed into the Freon plane.

Base pressure ratios $P_B/P_E$ with the air (model) results transformed into the Freon (prototype) plane versus stagnation pressure $P_{0I|P}$ are shown in Fig. 23. The agreement is as good as it was in the tests modeling from air to Freon. Also shown are a few results for the Freon nozzle run with air which as in the first test series were run to illustrate the shortcomings of retaining nozzle similarity only.

The separation locations S/D as determined from Schlieren photographs for the Freon (prototype) and air (model) nozzles are shown versus lip pressure in Fig. 24. The agreement is satisfactory for the design point and for a rather wide range of off-design conditions. It should be pointed out, however, that at the design condition the prototype operates with a rather limited afterbody separation and that therefore this might not be a severe test case.

## 5.32 Effects of small angles of attack

Base pressure ratios $P_B/P_E$ versus stagnation pressure $P_{0I|P}$ at different circumferential angles $\varphi$ and angles of attack $\alpha$ are presented for Freon (prototype) in Fig. 25 and for air (model) nozzles in Figs 26 and 27. The effect of angle of attack on the base pressure evaluated as the pressure difference $\Delta(P_B/P_E) = (P_B/P_E)_\alpha - (P_b/P_E)_{\alpha=0}$ at the stagnation pressure $P_{0I|P} = 0.75$ MPa is shown versus angle of attack in

Fig. 28 for the three nozzles. It can be seen that the effect of angle of attack obtained with the Freon (prototype) nozzle is simulated satisfactorily with the air (model) nozzles.

Shown in Fig. 29 is the separation location S/D at the circumferential angle of $\varphi = 0$ versus jet stagnation pressure $P_{0I|P}$ for the Freon (prototype) and air (model) nozzles at different angles of attack. A comparison of the separation location S/D for three nozzles at the design pressure $P_{0I|P} =$ 1.0 MPa is presented in Fig. 30. It can be seen that the agreement is reasonably good within the angle of attack range investigated.

## 5.33 Effects of fins at zero angle of attack

Shown in Fig. 31 is the base pressure ratio $P_B/P_E$ for Freon (prototype) and air (model) nozzles versus jet stagnation pressure $P_{0I}$ with and without fins at zero angle of attack. The four fins are at $\varphi = \pm 45°$ and $\varphi = \pm 135°$. The base pressure shown is measured at $\varphi = 0$. It can be seen that the effect of the fins is small but noticable for this configuration. The effect of the fins obtained with the Freon (prototype) is satisfactorily simulated by the air (model) nozzles, both the magnitude of the deviation and the cross-over base pressure. An oil flow picture showing the disturbance of the afterbody boundary layer flow induced by the fins is shown in Fig. 32.

## 5.4 Plume modeling experience

The modeling methodology [9, 21] examined during this study has been shown to correlate wind tunnel tests successfully for propulsive nozzles using either low or high specific heat ratio prototype gases and with the converse model gas. The utilization of a wide base of experimental data using cold air as the propulsive gas gathered over many years made the initial modeling from air (prototype) to Freon (model) the logical test sequence. Completion of the test program with modeling from a low gamma (Freon with $\gamma \simeq 1.16$) to high gamma (air, $\gamma = 1.40$), the normal wind tunnel problem, provided a broader base of support for the wider validity of the methodology. Modeling from low to high gamma values, however, introduces difficulties particularly for wind tunnel testing in that modeling leads to nozzles that have lower exit Mach numbers and smaller exit angles than the prototype. The design point operating pressure ratio is also smaller but this is advantageous since it reduces the need for high pressure instrumentation and equipment. For prototypes with low supersonic Mach number exit values, $M < 2.50$ and exit angles of less than approximately 15 degrees and combustion gas ($\gamma \simeq 1.16$ to 1.18) to air modeling, the model nozzles for base pressure simulation have exit Mach numbers near unity and exit angles near zero degrees. These types of nozzles raise a number of severe problems for wind tunnel testing due to the large throat sizes in relation to exit area which when combined with internal model instrumentation and construction requirements may make them practically impossible to be utilized. Further, the internal model propulsion gas flow field coupled with the large throat may also lead to unsatisfactory exit plane Mach number distributions and poor quality of the plume compared to the prototype. See, e.g., the difficulties described in Section 5.31.

Fortunately, however, off-design operating conditions have been shown to provide excellent results due to the closeness of the plume curvature (relaxed constraint) if initial slope correlation is retained. Selection of a higher prototype design point pressure ratio leads to increased model exit Mach number and exit angle, which coupled with the range of applicability of the modeling results on either side of the design point using slope correction can allow for satisfactory testing even for apparently difficult prototype conditions. In severe conditions, actual prototype geometries and Freon or other suitable gases may be required rather than modeling. Consequently, the Freon hot gas facility retains importance beyond the current studies.

## 6. CONCLUSIONS

The hot gas facility and the test program reported on in this and previous reports have provided a capability and a solid data base on which to evaluate jet plume modeling. A careful analysis of the system performance and experimental results obtained allows the formulation of the following conclusions and recommendations.

1. The hot gas facility constructed to determine the validity of propulsive nozzle modeling successfully meets its design objectives.
2. While allowing testing with Freon as a combustion product simulant, $\gamma \approx 1.16$, the hot gas facility retains its usefulness in being able to test with a variety of gases over a wide range of pressure ratios and is thus an extremely flexible research and development tool.
3. The modeling methodology concept of similar plumes as determined by radius of curvature and initial slope with proper consideration of plume pliability at the

design condition for prototype and modeled nozzles successfully correlates both base pressures and flow separation in the vicinity of the base.

4. Design point conditions can be selected to represent conditions from the base pressure to large external flow field separation depending on their relation to the vehicle operating conditions.

5. It is possible to relax the radius of curvature constraint while relating initial expansion angle and still successfully model and correlate results in the vicinity of the design point.

6. Tests carried out using prototype and modeled nozzles designed for a free stream of Mach number 2.0 showed excellent agreement for base pressure and extent of afterbody separation for both $air_{|prototype}$ to $Freon_{|model}$ and $Freon_{|model}$ to $air_{|prototype}$.

7. The Mach number 2.0 tests showed that the modeled results were good over a range of pressure ratios extending on either side of the design condition.

8. Limited tests at small angles of attack ($-6° \leq \alpha \leq \pm 6°$) and with external disturbances in the vicinity of the base plane (fins) appear to support the modeling scheme for more complex flow field geometries.

9. Tests at Mach number 3.0 using the same nozzles designed for and tested at Mach number 2.0 show that retention of the initial expansion angle matching produces acceptable results for base pressure but poor correlation of separation distance. The latter may be explained by the increasing importance of plume curvature for large separated regions.

10. When modeling from low specific heat ratio prototypes to high specific heat ratio models, it may be necessary to place restrictions on the practicality of the model

nozzles for testing due to the low lip Mach number and small exit angles required. This is particularly true for prototype nozzles with low supersonic exit Mach numbers and/or small exit angles. However, the existence of a wide range of applicability of the modeled nozzles through initial plume slope retentions allows, to some degree, this difficulty to be circumvented through the use of nozzles designed for higher operating pressure ratios.

11. Tests with complex and inter-related flow fields such as occur at larger angles of attack (vortex generation and separation) and with control surfaces (multi-dimensional flow separation geometries) should be carried out to determine the range and validity of the modeling methodology into the regimes where wind tunnel testing is the only available tool for examining vehicle performance characteristics.

REFERENCES


1. Addy, A.L.; Korst, H.H.; Walker, B.J.; White, R.A. — A Study of Flow Separation in the Base Region and its Effects During Powered Flight. AGARD Conf. Proc. No. 124 on Aerodynamic Drag, AGARD-CP-124, Specialists' Meeting held at Izmir, Turkey, 10-13 April 1973.

2. Alpinieri, L.J.; Adams, R.M. — Flow Separation due to Jet Pluming. AIAA J., Oct. 1966 (4), pp. 1865-6.

3. Deep, R.A.; Henderson, J.H.; Brazzel, C.E. — Thrust Effects on Missile Aerodynamics. U.S. Army Missile Command Report No RD-TR-71-9, May 1971, Redstone Arsenal. Ala., USA.

4. Nyberg, S.-E. — Investigation of Modeling Concepts for Plume-Afterbody Flow Interactions. Grant DAERO-78-G-028, 1st Semi-Annual Status Report, 1 Jan 1978-30 June 1978. Internal report for ERO and FFA.

5. Nyberg, S.-E.
Agrell, J.
Hevreng, T.
Investigation of Modeling Concepts for Plume-Afterbody Flow Interactions. Grant DAERO-78-G-028, 1st Annual Technical Report, February 1979.

6. Nyberg, S.-E.
Investigation of Modeling Concepts for Plume-Afterbody Flow Interactions. Grant DAERO-78-G-028, 2nd Semi-Annual Status Report, 1 Jan 1979-20 June 1979. Internal report for ERO and FFA.

7. Nyberg, S.-E.
Agrell, J.
Hevreng, T.
Investigation of Modeling Concepts for Plume-Afterbody Flow Interactions. Grant DAERO-78-G-028, 2nd Annual Technical Report, February 1980.

8. Nyberg, S.-E.
Investigation of Modeling Concepts for Plume-Afterbody Flow Interactions. Grant DAERO-78-G-028, 3rd Semi-Annual Status Report, 1 Jan 1980-30 June 1980. Internal report for ERO and FFA.

9. Korst, H.H.
Approximate Determination of Jet Contours Near the Exit of Axially Symmetrical Nozzles as a Basis for Plume Modeling. TR-RD-72-14, August 1972, US Army Missile Command, Redstone Arsenal, Ala., USA.

10. Korst, H.H.
An Analysis of Jet Plume Modeling by Dissimilar Propellant Gases. Proc., 43rd Semi-Annual Meeting, Supersonic Tunnel Association, 2-3 April 1975, Pasadena, Cal., USA.

11.
FFA Wind Tunnel Facilities. FFA Memorandum 93, Stockholm 1974.

12. Agrell, J.
White, R.A.
An Experimental Investigation of Supersonic Axisymmetric Flow over Boattails Containing a Centered Propulsive Jet. The Aeronautical Research Institute of Sweden, FFA, Technical Note AU-913, Dec. 1974.

13. White, R.A.
The Calculation of Supersonic Axisymmetric Afterbody Flow with Jet Interference and Possible Flow Separation.
The Aeronautical Research Institute of Sweden, FFA, Technical Note AU-912, 1974.

14. White, R.A.
Agrell, J.
Boattail and Base Pressure Prediction Including Flow Separation for Afterbodies with a Centered Propulsive Jet and Supersonic External Flow at Small Angles of Attack.
AIAA/SAE 13th Propulsion Conference, Orlando, Florida, 11-13 July 1977.

15. Korst, H.H.
Chow, W.L.
Zumwalt, G.W.
Research on Transonic and Supersonic Flow of a Real Fluid at Abrupt Increases in Cross Section (with Special Consideration of Base Drag Problems).
Final Report. Report No. ME-TR-329-5.
University of Ill., Urbana, Ill., USA, Dec. 1959.

16. Carrière, P.
Siriex, M.
Delery, J.
Methodes de Calcul des Ecoulements Turbulents Decolles en Supersonique.
Prog. in Aerospace Sci., 1975, Vol. 16, No. 4, pp. 385-429.

17. Goethert, B.H.
Barnes, L.T.
Some Studies of the Flow Pattern at the Base of Missiles with Rocket Exhaust Jets.
Arnold Engr. Development Center, Tullahoma, Tenn., AEDC-TR-58-12, June 1960.

18. Herron, R.D.
Investigation of Jet Boundary Simulation Parameters for Underexpanded Jets in a Quiescent Atmosphere.
AEDC-TR-65-6, Tullahoma, Sept. 1968.

19. Sims, J.L.
Blackwell, K.L.
Base Pressure Correlation Parameters, presented at the Workshop on Missile and Plume Interaction Flow Fields, Redstone Arsenal, Ala., 7-8 June 1977.

20. Johannesen, N.H.
Meyer, R.E.
Axially-Symmetrical Supersonic Flow Near the Centre of an Expansion.
The Aeron. Quarterly (2), 1950, pp. 127-142.

21. Korst, H.H.
Deep, R.A.
Modeling of Plume Induced Interference Problems in Missile Aerodynamics. AIAA Paper No. 790362, 17th Aerospace Sciences Meeting, New Orleans, La., 15-17 Jan. 1979.

22. Korst, H.H.
White, R.A.
Nyberg, S.-E.
Agrell, J.
The Simulation and Modeling of Jet Plumes in Wind Tunnel Facilities. Paper 80-0430 presented at the AIAA 11th Aerodynamic Testing Conference, Colorado Springs, Colorado, USA, 18-20 March 1980.

23. Reid, C.F.
Effects of Jet-Plume and Pressure Distributions over a Cylindrical Afterbody at Transonic Speeds. Calspan Report No. AA-5017-W-15, W.A. T17-160, T17.170, Feb. 1979.

24. Agrell, J.
Experimental Investigation of Flow Separation on Afterbodies with a Central Propulsive Jet and Supersonic External Flow at Small Angles of Attack.
FFAP-A-455, Sept. 1979, presented at DGLR-Symposium "Strömungen mit Ablösung", Munich, 19-20 Sept. 1979.

25. Agrell, J.
The Hot Gas Facility for Jet Plume Simulation in a Supersonic Wind Tunnel at FFA.
FFAP-A-504, March 1981, presented at 15. Sitzung des DGLR-Fachausschusses 2B1 "Flugkörper", DFVLR, Cologne/Porz, 25-26 March 1981.

26. Woodward, F.A.
Analysis and Design of Wing-Body Combinations at Subsonic and Supersonic Speeds.
J. Aircraft, Vol. 5, No. 6, 1968.

27. White, R.A.
Nyberg, S.-E.
Korst, H.H.
Hevreng, T.
Agrell, J.
Development of a Plume Modeling Facility and Test Methodology. Proc. 49th Semi-Annual Meeting of the Supersonic Tunnel Association at El Segundo, Calif., U.S.A., 17-18 April 1978.

28. White, R.A.
Agrell, J.
Operational Experience with the Hot Freon Plume Simulation Facility and Some Initial Test Results.
Proc. 53rd Semi-Annual Meeting of the Supersonic Tunnel Association at Moffett Field, Calif., U.S.A., 26-28 March 1980.

29. Korst, H.H.
White, R.A.
Nyberg, S.-E.
Agrell, J.
Simulation and Modeling of Jet Plumes in Wind Tunnel Facilities.
Journal of Spacecrafts and Rockets, Vol. 18, No. 5, Sept.-Oct. 1981, pp. 427-434.

ACKNOWLEDGEMENT

The authors wish to thank Professor H.H. Korst and Professor R.A. White at the University of Illinois for stimulating and fruitful cooperation and for their contributions to this report.

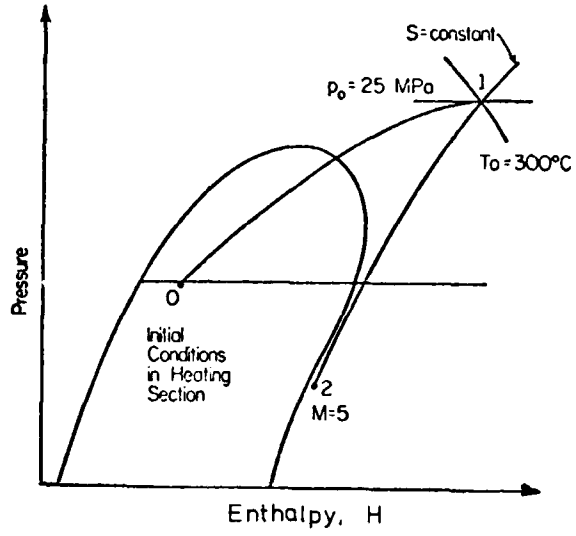


Figure 1. Freon-22 simplified pressure enthalpy diagram with schematic of thermodynamic process of heating at constant volume (Heater) followed by isentropic expansion (Nozzle).

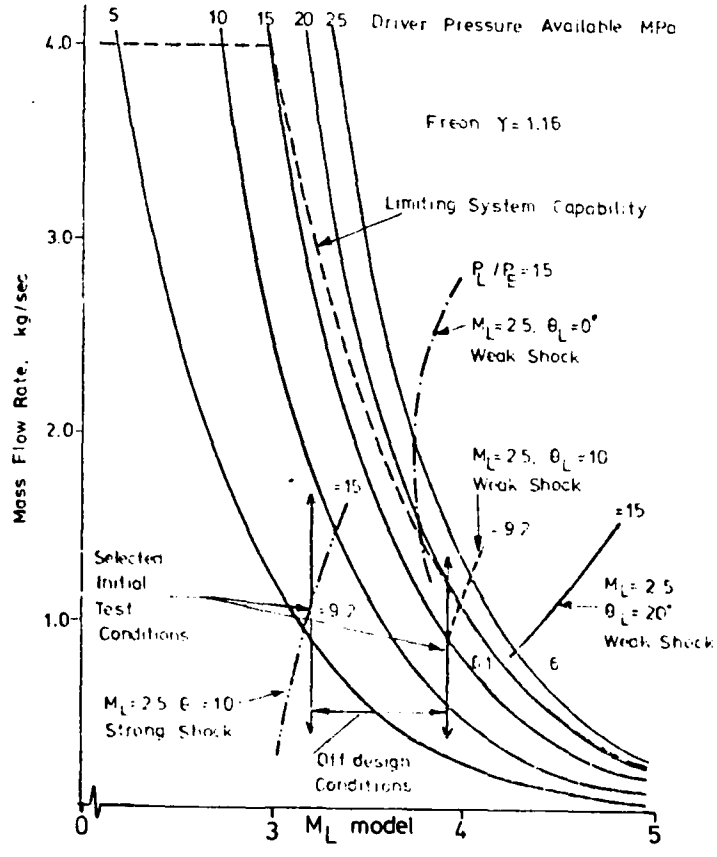


Figure 2. Systems performance diagram showing operating conditions for initial modeling tests (see Fig. 8 for nozzle geometries) (Air nozzle, prototype and design points selected).

PRECEDING PAGE BLANK-NOT FILMED

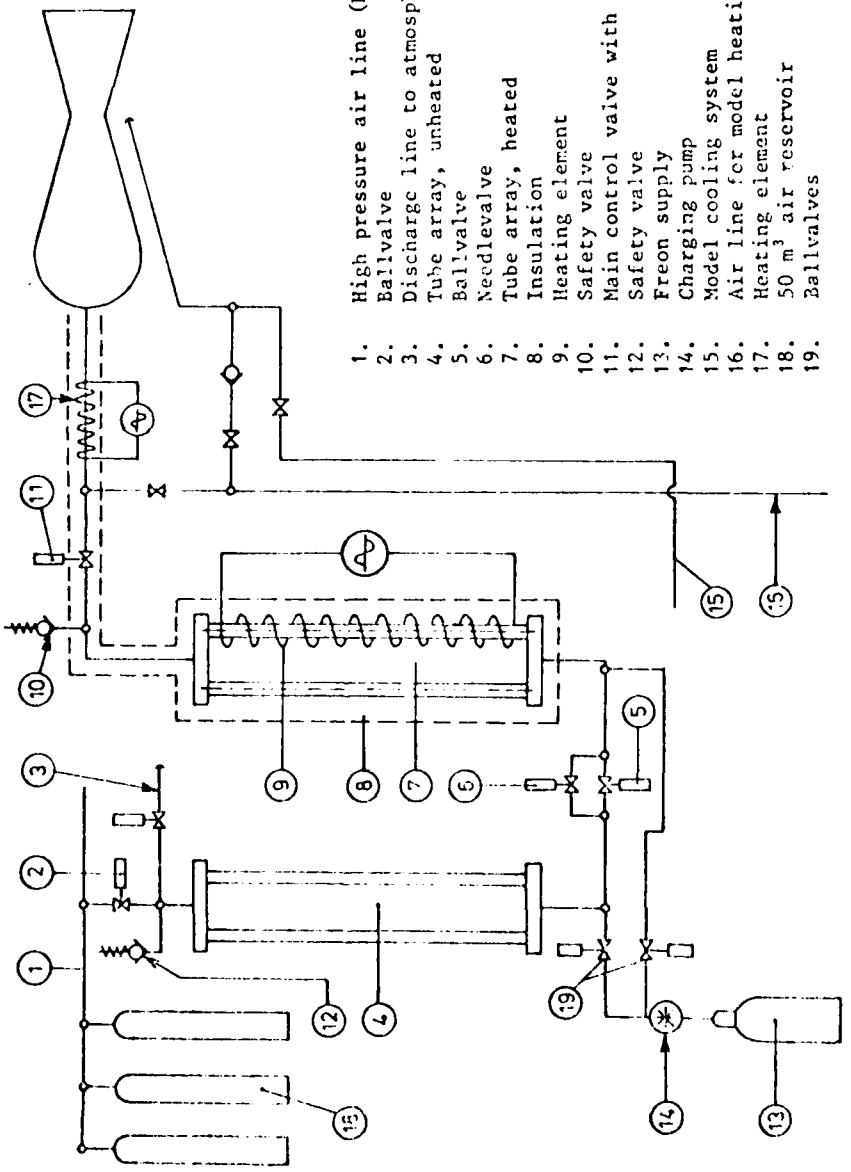


Figure 3. Annotated schematic of air driver system, Freon heater and Nozzle.

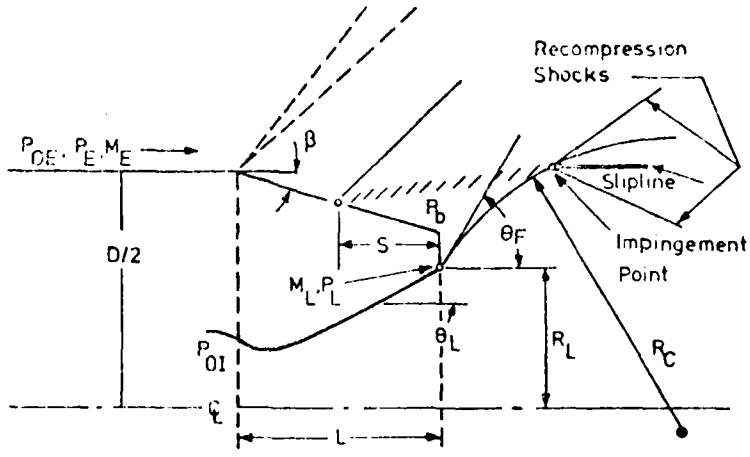


Figure 4. Flow configuration for plume induced separation from conical afterbody (geometrical and operational parameters identified).

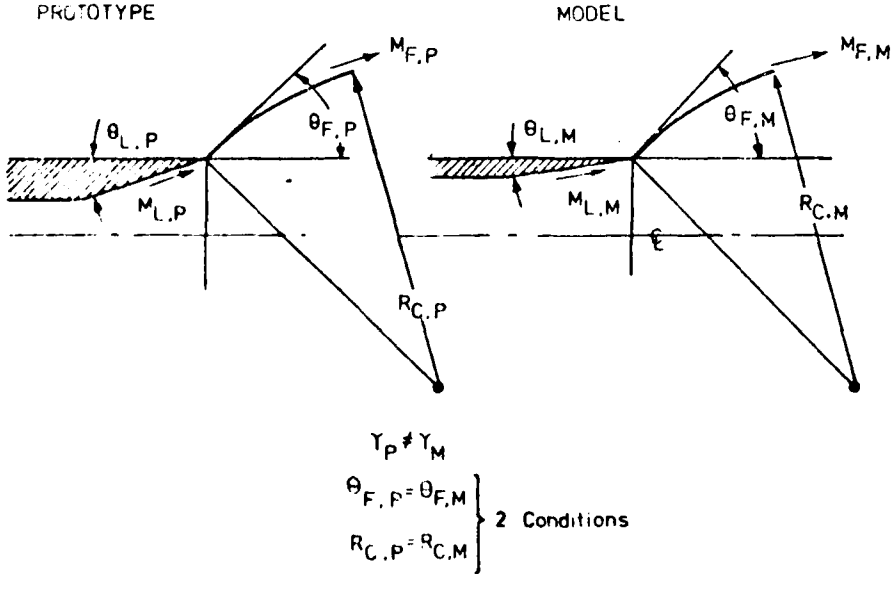


Figure 5. Schematic of geometrical plume modeling [21].

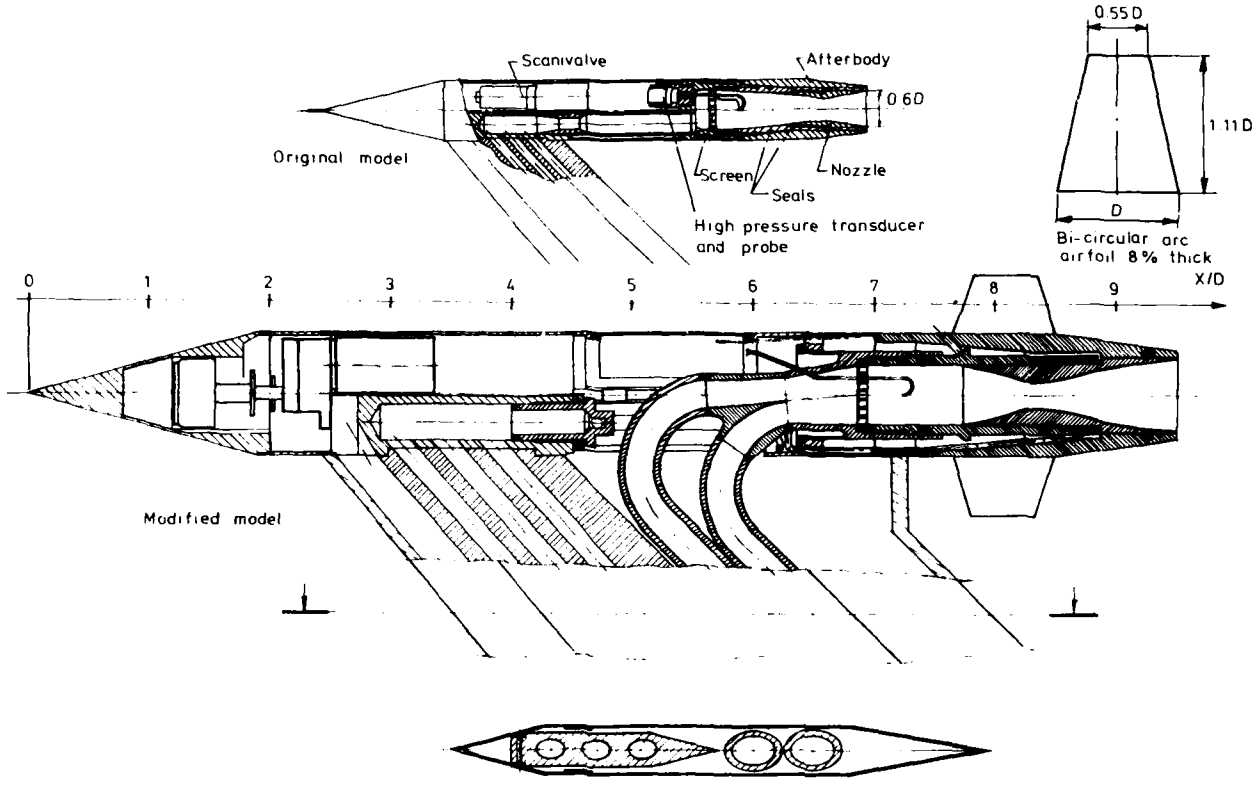


Figure 6. Adaption of propulsive afterbody wind tunnel model for operation with Freon.

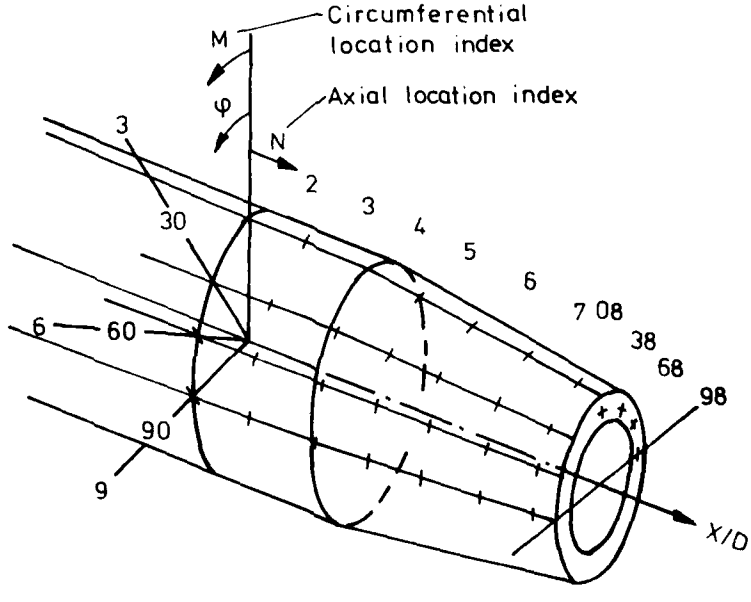


| N | X/D |
|---|---|
| 1 | 8.10 |
| 2 | 8.30 |
| 3 | 8.52 |
| 4 | 8.74 |
| 5 | 8.96 |
| 6 | 9.20 |
| 7 | 9.42 |
| 8 | 9.50 |

Figure 7. Location of pressure taps on boat-tail.

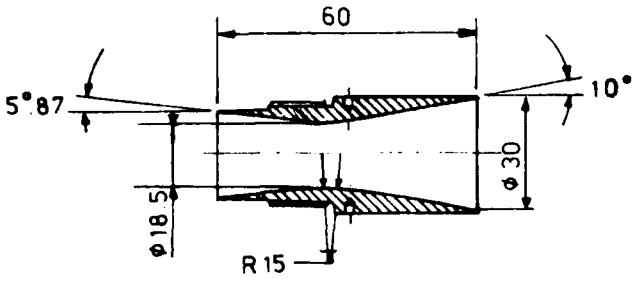


a) $M_L$=2.5; $\theta_L$=10°.

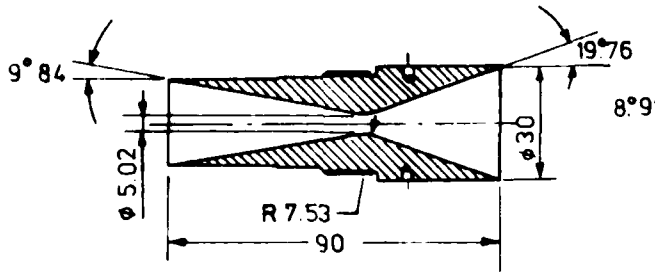


b) Weak shock modeling. $M_L$=3.90; $\theta_L$=19°.79.

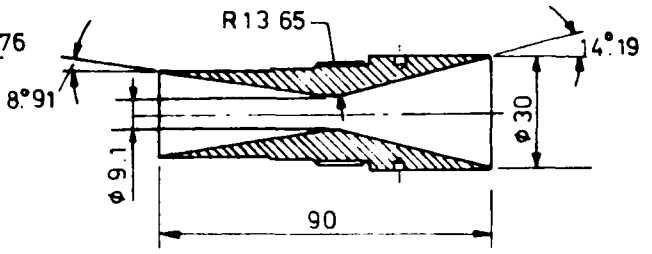


c) Strong shock modeling. $M_L$=3.19; $\theta_L$=14°.19.

Figure 8. Nozzles modeling from air to Freon (a) Prototype nozzle (Air, $\lambda_P = 1.4$). (b,c) Model nozzles (Freon 22, $\lambda_M = 1.16$) (Dimensions are in millimeters)

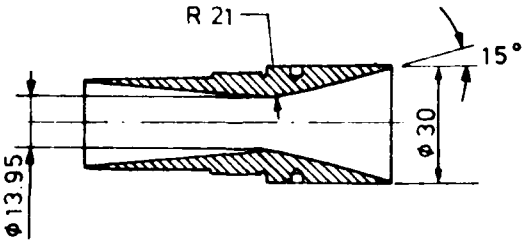


a) $M_L$=2.60; $\theta_L$=15°

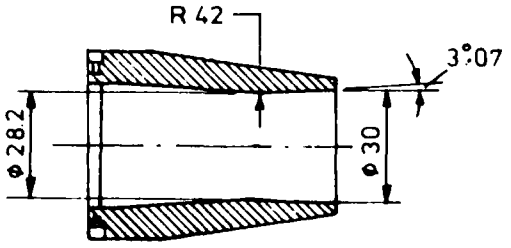


b) Weak shock modeling. $M_L$=1.41; $\theta_L$=3.07.°

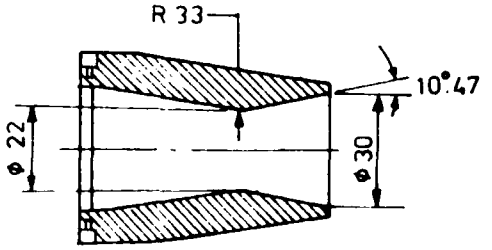


c) Strong shock modeling $M_L$ = 2.03; $\theta_L$ = 10°47.

Figure 9. Nozzles modeling from Freon to air (a) Prototype nozzle (Freon 22, $\lambda_P = 1.16$). (b,c) Model nozzles (Air, $\lambda_M = 1.4$) (Dimensions are in millimeters)

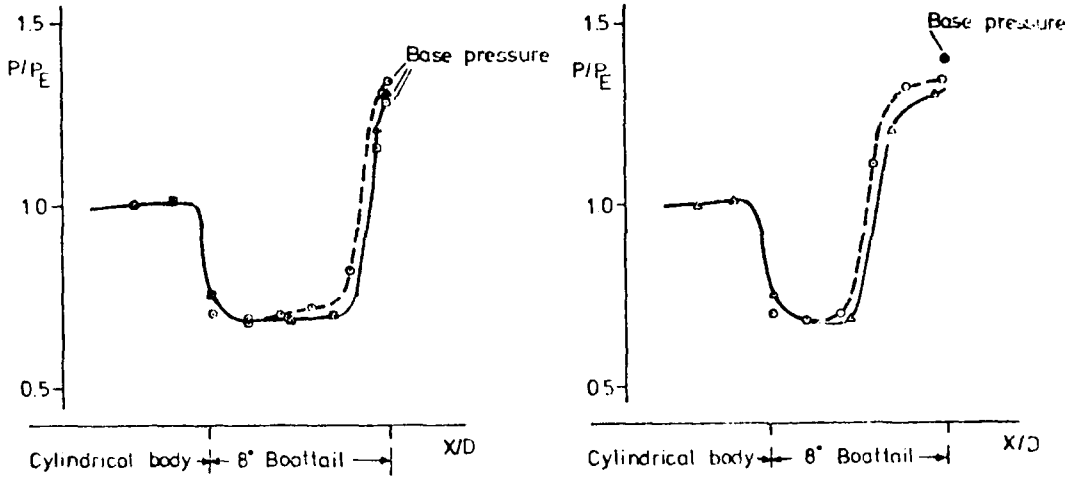


o 31784 Air $M_L$=2.5 $\theta_L$=10° $P_L/P_E$=9.2 earlier test
Δ 35260 Air $M_L$=2.5 $\theta_L$=10° $P_L/P_E$=9.2 current test
□ 35312 Freon $M_L$=3.19 $\theta_L$=14°19 $P_o$~4.8 MPa

o 31751 Air $M_L$=2.5 $\theta_L$=20° $P_L/P_E$=9.1 earlier test
Δ 35268 Air $M_L$=2.5 $\theta_L$=20° $P_L/P_E$=9.2 current test

Figure 10. Pressure distribution on the rear part of the body $M_E = 2.0$; $\alpha = 0$; Effect of redesigned strut (five digit numbers identify runs).

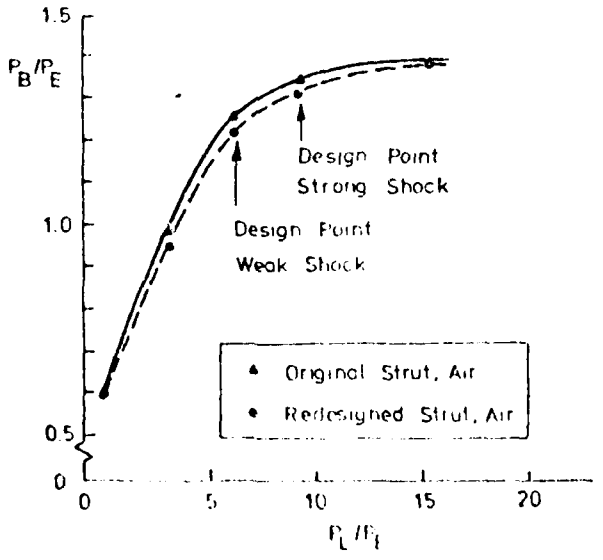


Figure 11. Base pressure ratio versus $P_L/P_E$ for the air prototype nozzle ($\theta_L = 10^o$) showing effect of strut modification.

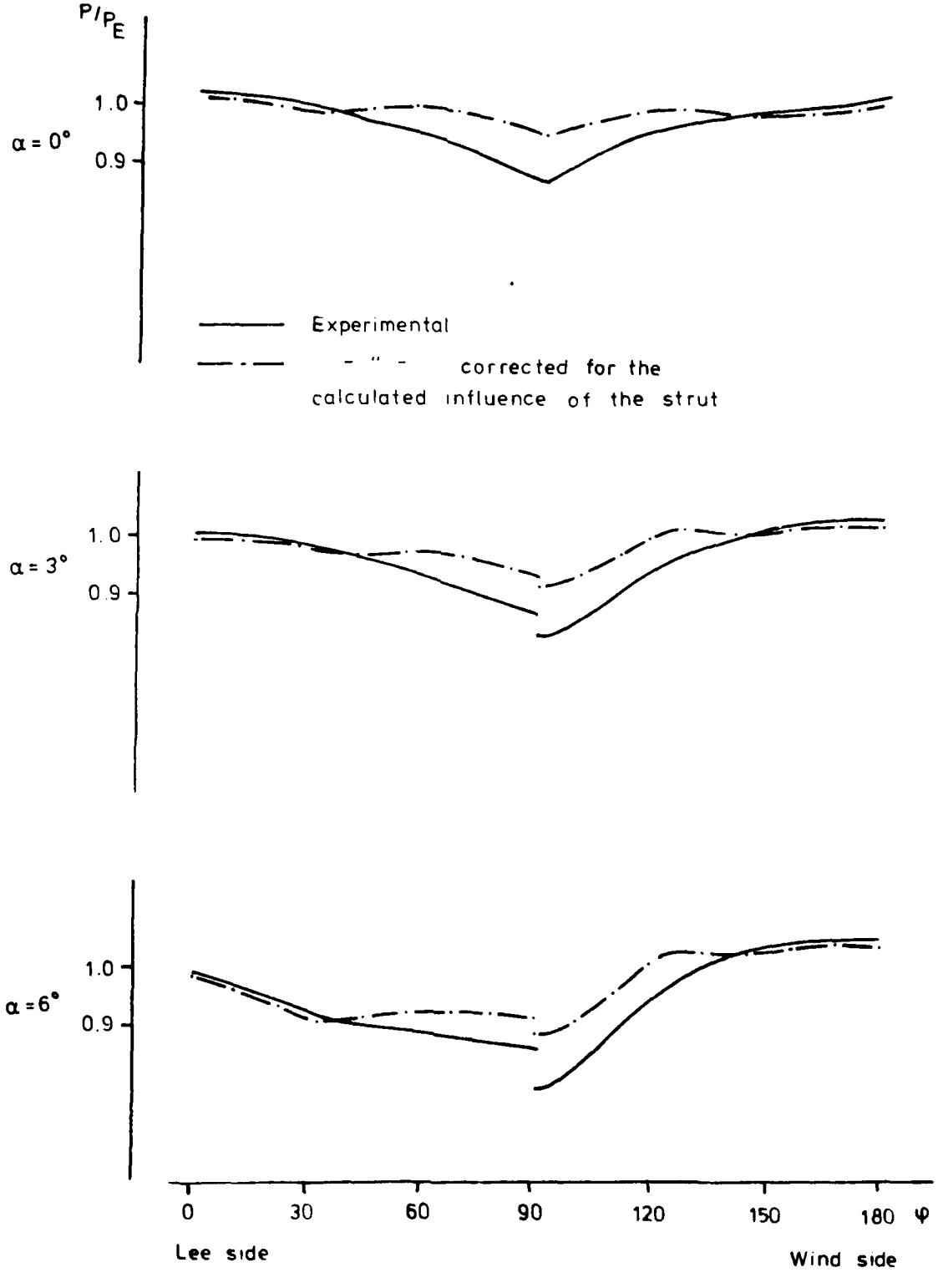


Figure 12. Pressure distributions around the model at X/D = 8.24. $M_E$ = 2.0

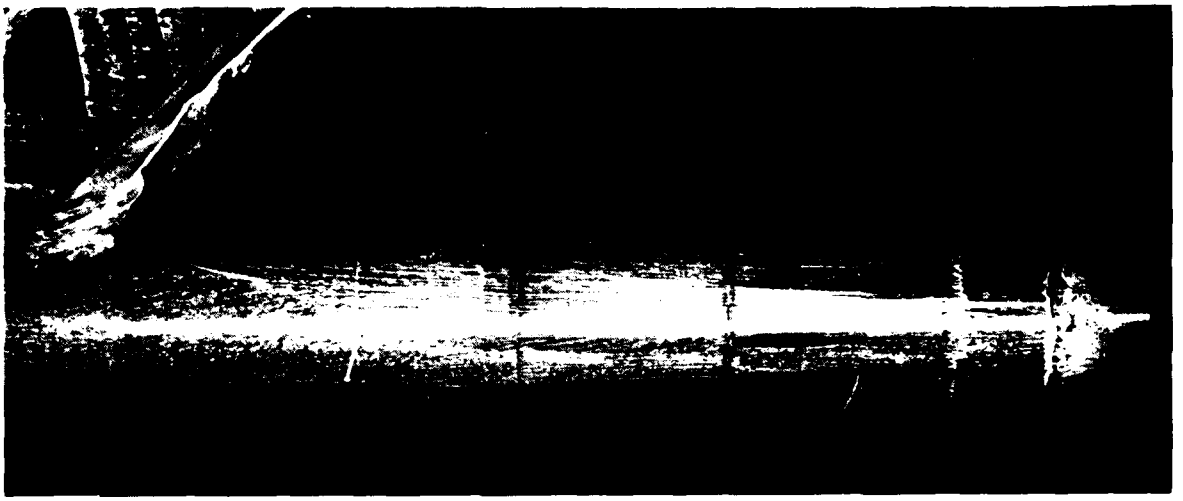

Original model

Air jet $M_I = 2.5$[1], $\beta_I = 20°$, $Po_I = 1.92$ MPa.

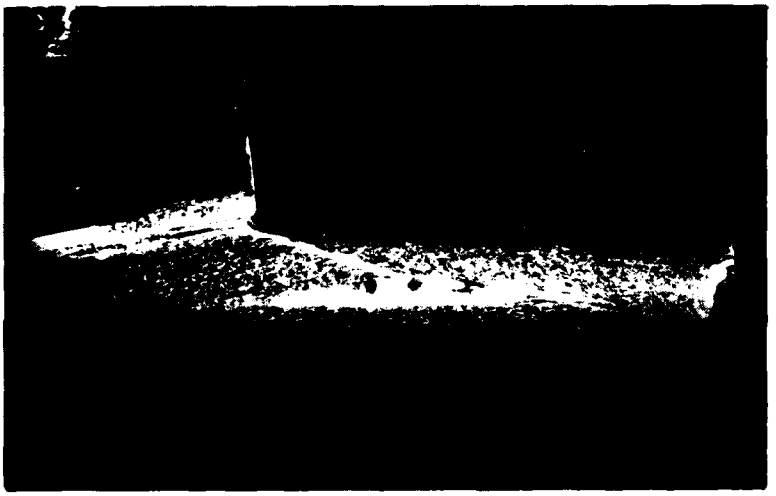

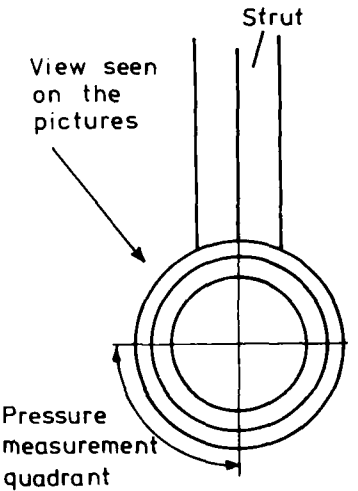


Modified model

Freon jet $M_I = 2.6$, $\beta_I = 15°$, $Po_I = 1$ MPa.

*Figure 13. Oil-flow pictures of the original and modified model at $M_E = 2.0$ and $\alpha = 0$.*

1) not the prototype nozzle.

a) Run 35261 Air $M_L = 2.5$; $\theta_L = 10$: $P_L/P_E = 6.0$.

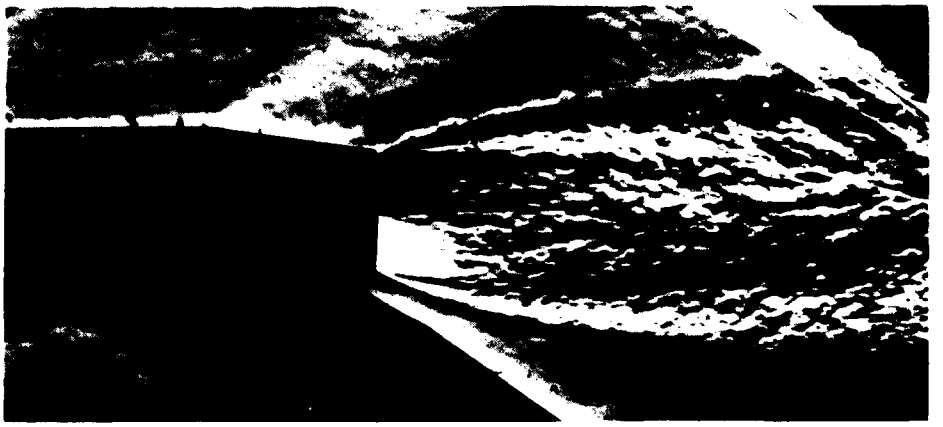

b) Run 35352 Freon 22 $M_L = 3.90$; $\theta_L = 19.76$; $P_{OI} = 13.10$ MPa.

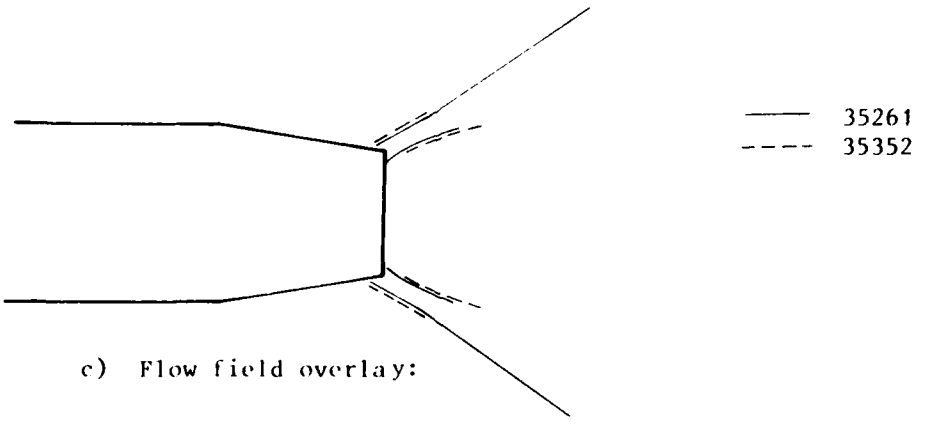


c) Flow field overlay:

Figure 14. Comparison of plume shape from Schlieren photos. $M_E = 2.0$; $\alpha = 0$. (Weak shock modeling)

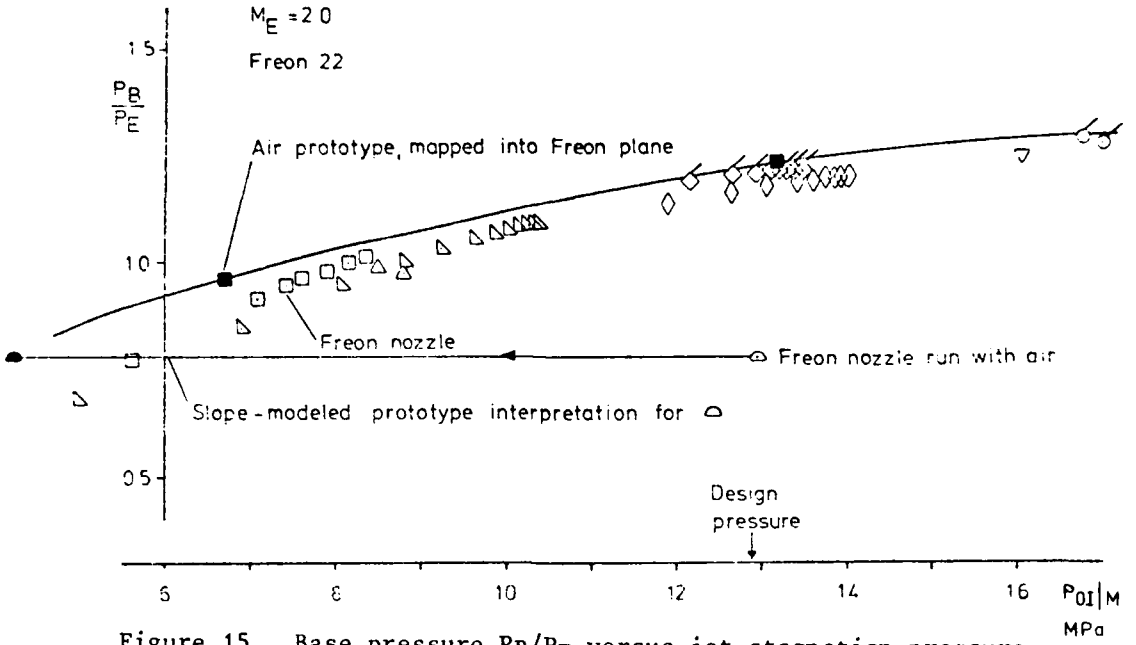


Figure 15. Base pressure $P_B/P_E$ versus jet stagnation pressure $P_{OI}$ for Freon nozzle (Weak shock modeling, Model nozzle Figure 8b).

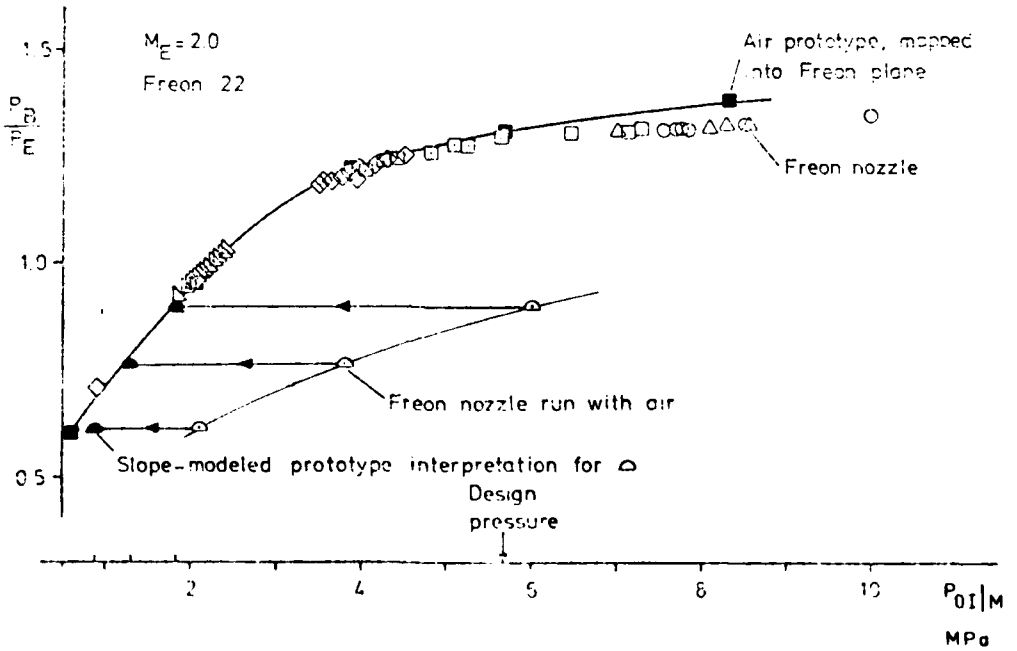


Figure 16. Base pressure $P_B/P_E$ versus jet stagnation pressure $P_{OI}$ for Freon nozzle (Strong shock modeling, Model nozzle Figure 8c).

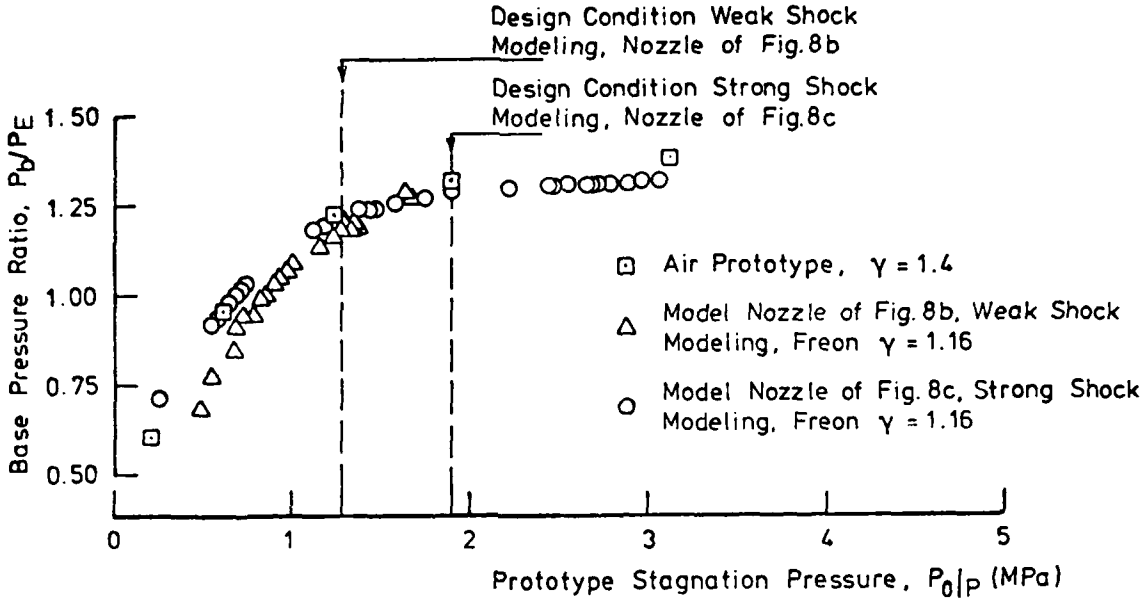


Figure 17. Base pressure ratio for Air (prototype) and Freon (model) tests versus prototype (Air) Nozzle stagnation pressure.

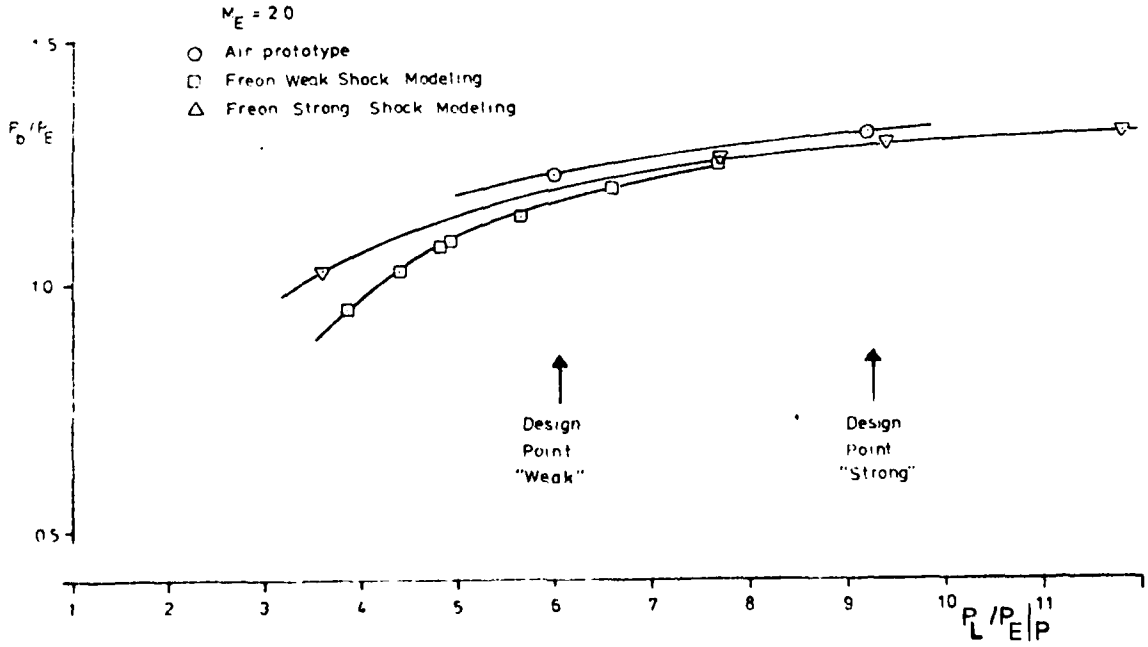


Figure 18. Base pressure versus lip pressure. Comparison of air prototype with Freon models.

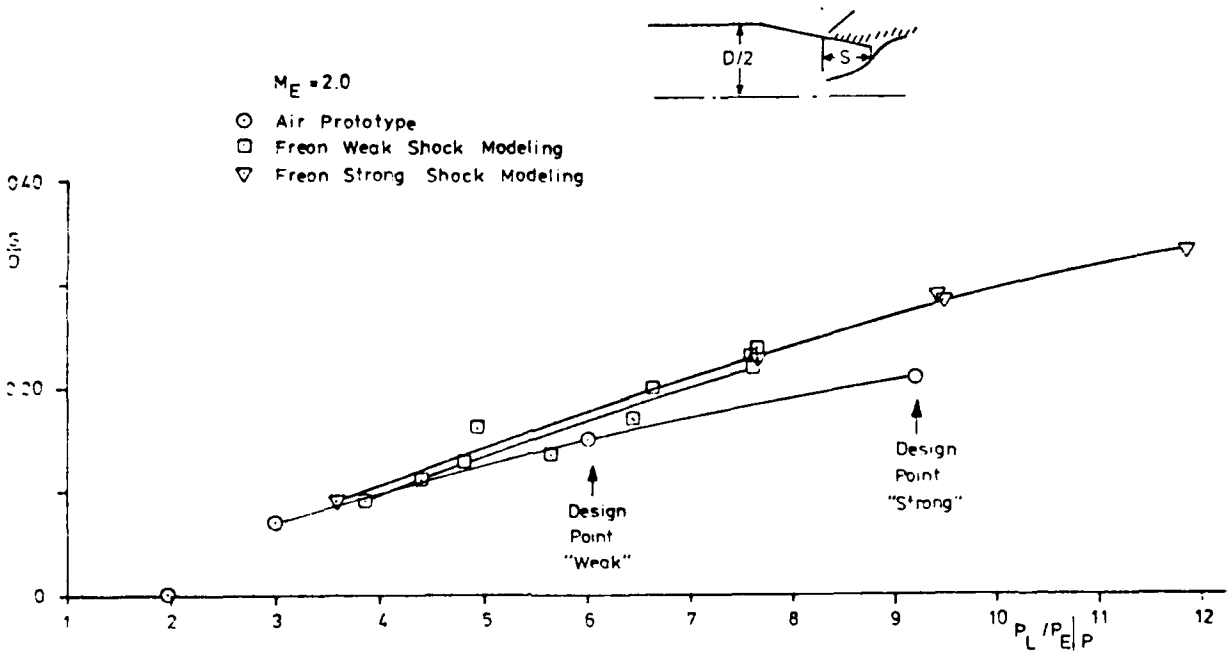


Figure 19. Separation location vs lip pressure for air (prototype) and Freon (model) Nozzles.

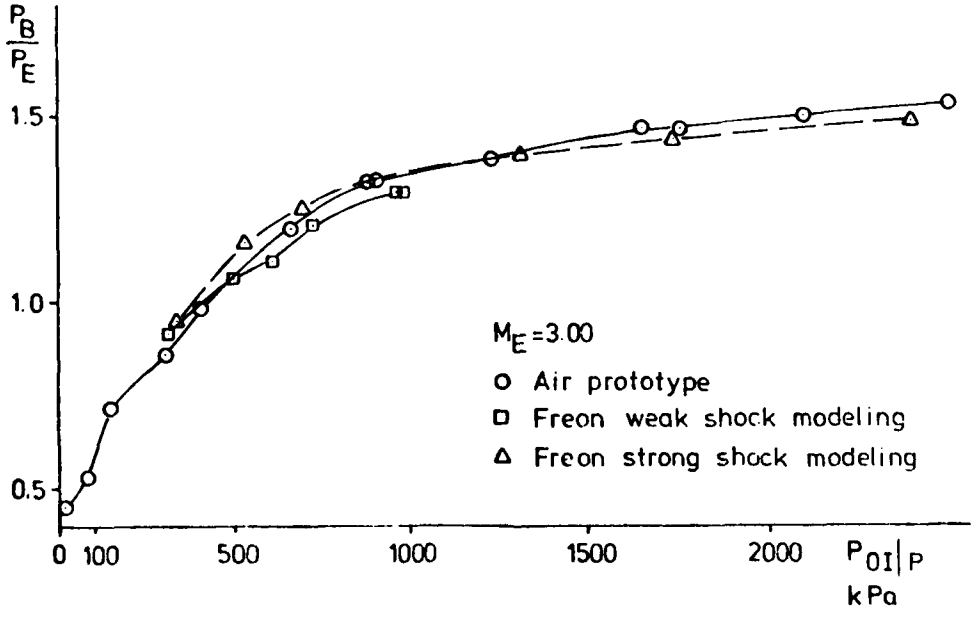


Figure 20. Base pressure versus jet stagnation pressure.

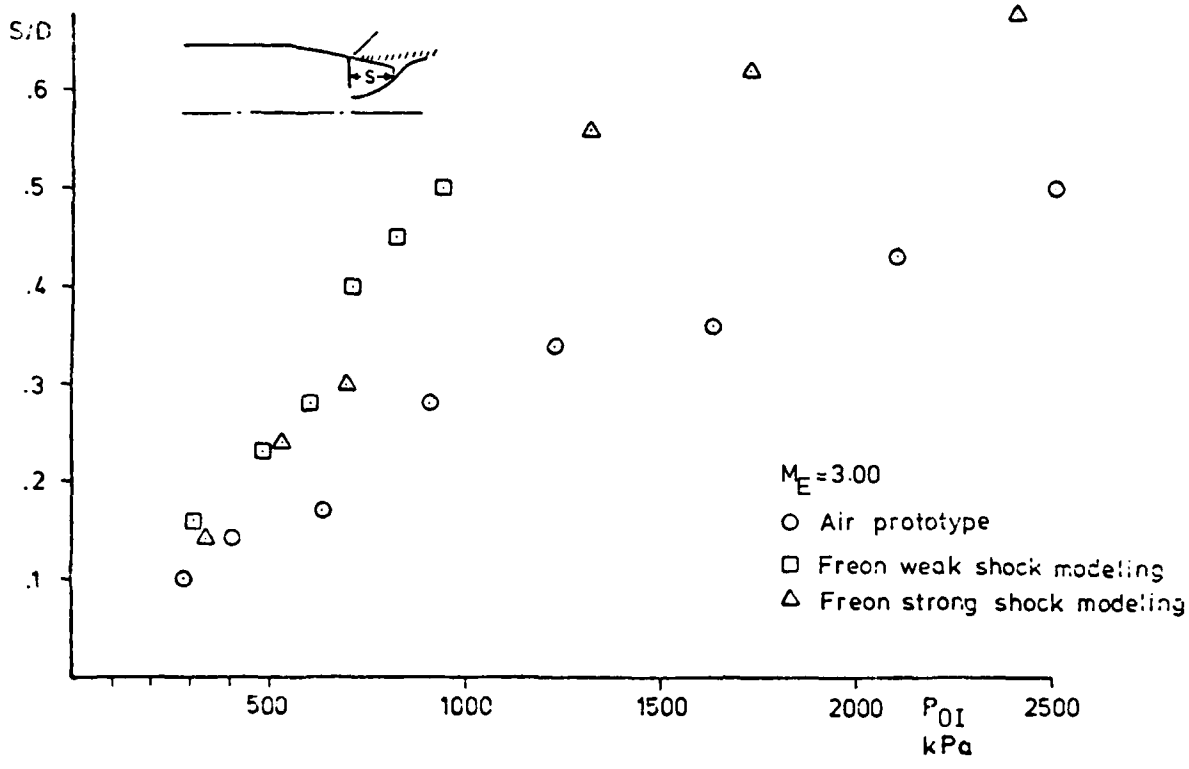


Figure 21. Separation location versus jet stagnation pressure.

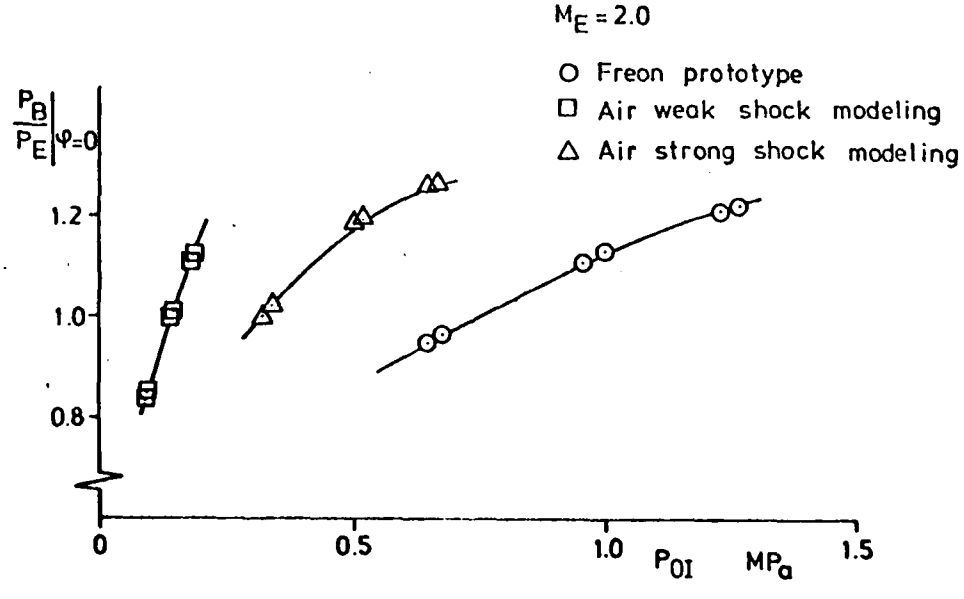


Figure 22. Base pressure ratio for Freon (prototype) and Air (model) tests versus nozzle stagnation pressure.

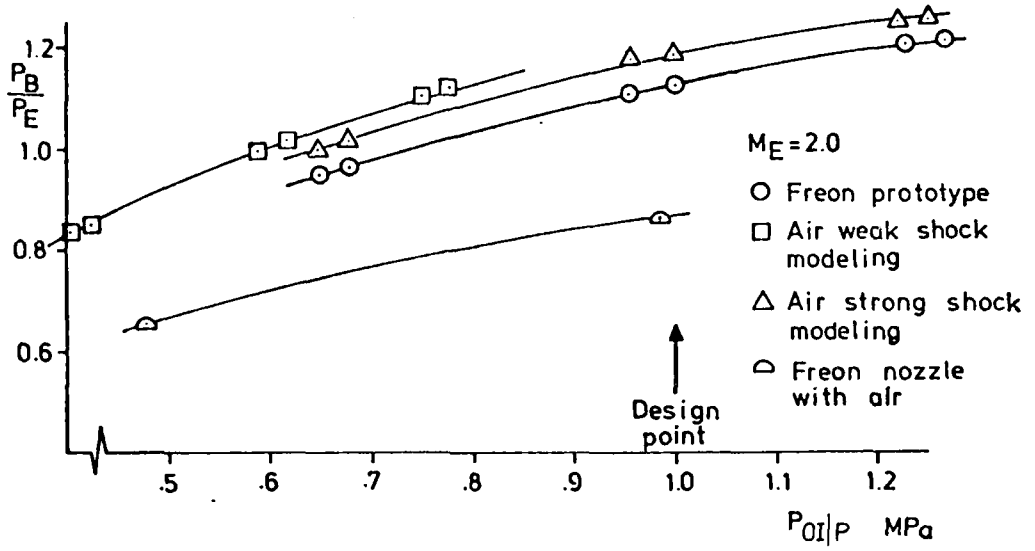


Figure 23. Base pressure ratio for Freon (prototype) and Air (model) tests versus nozzle stagnation pressure in prototype plane.

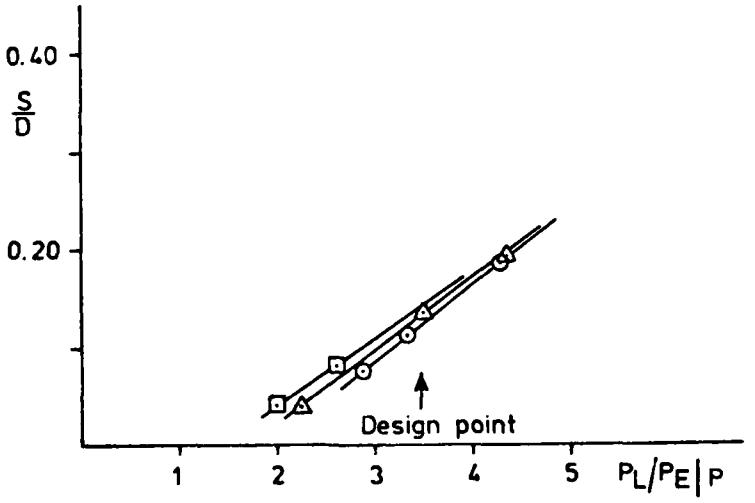


Figure 24. Separation location vs lip pressure for Freon (prototype) and Air (model) nozzles.

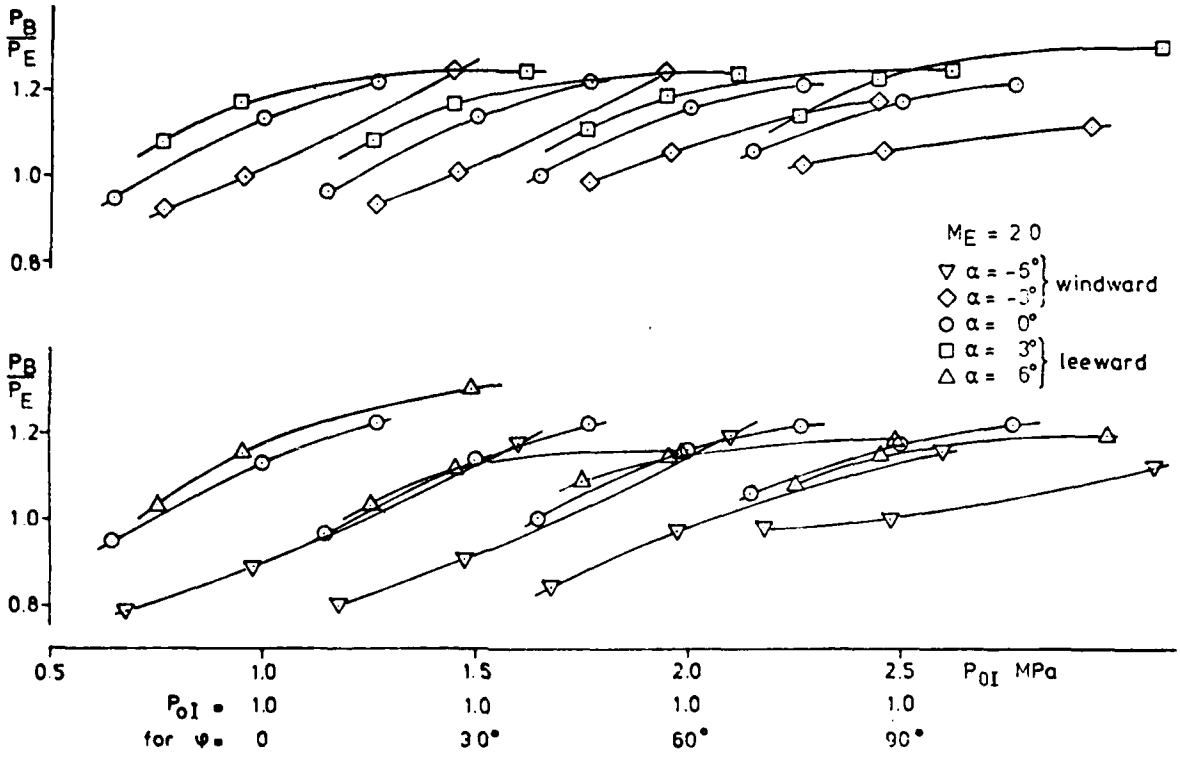


Figure 25. Base pressure ratio $P_B/P_E$ for Freon (prototype) versus stagnation pressure $P_{0I}$ at different circumferential angles $\varphi$ and angles of attack $\alpha$.

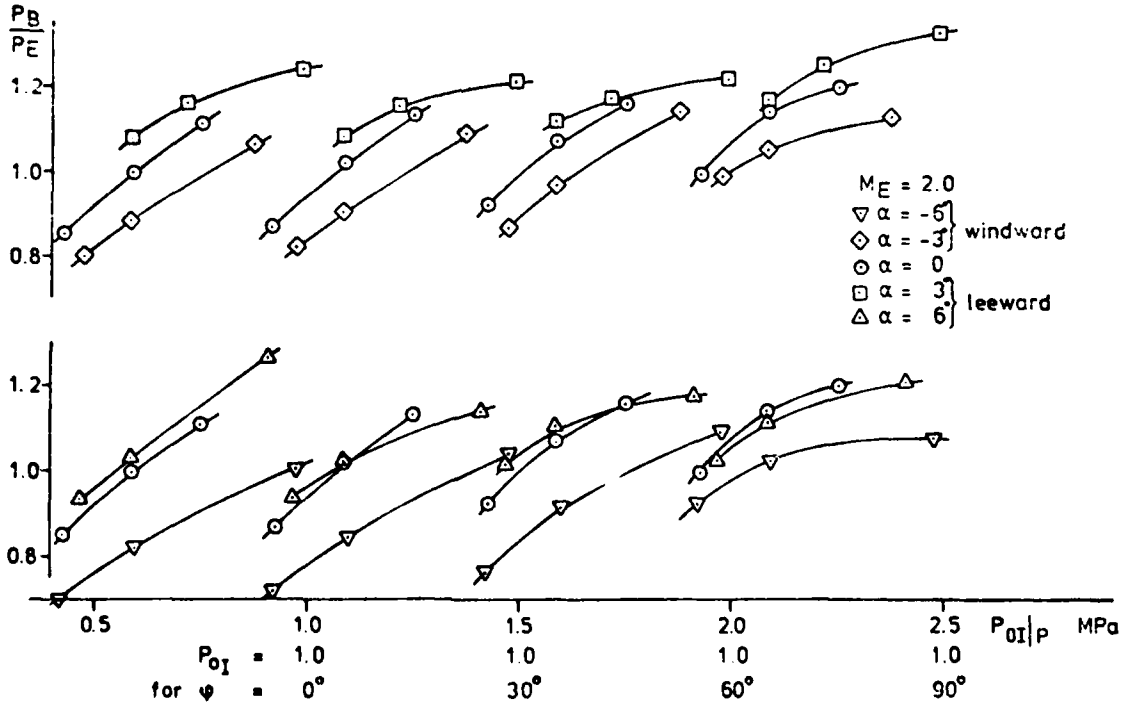


Figure 26. Base pressure ratio $P_B/P_E$ for Air (model, weak shock modeling) versus stagnation pressure $P_{0I}|_P$ in prototype plane at different circumferential angles $\varphi$ and angles of attack $\alpha$.

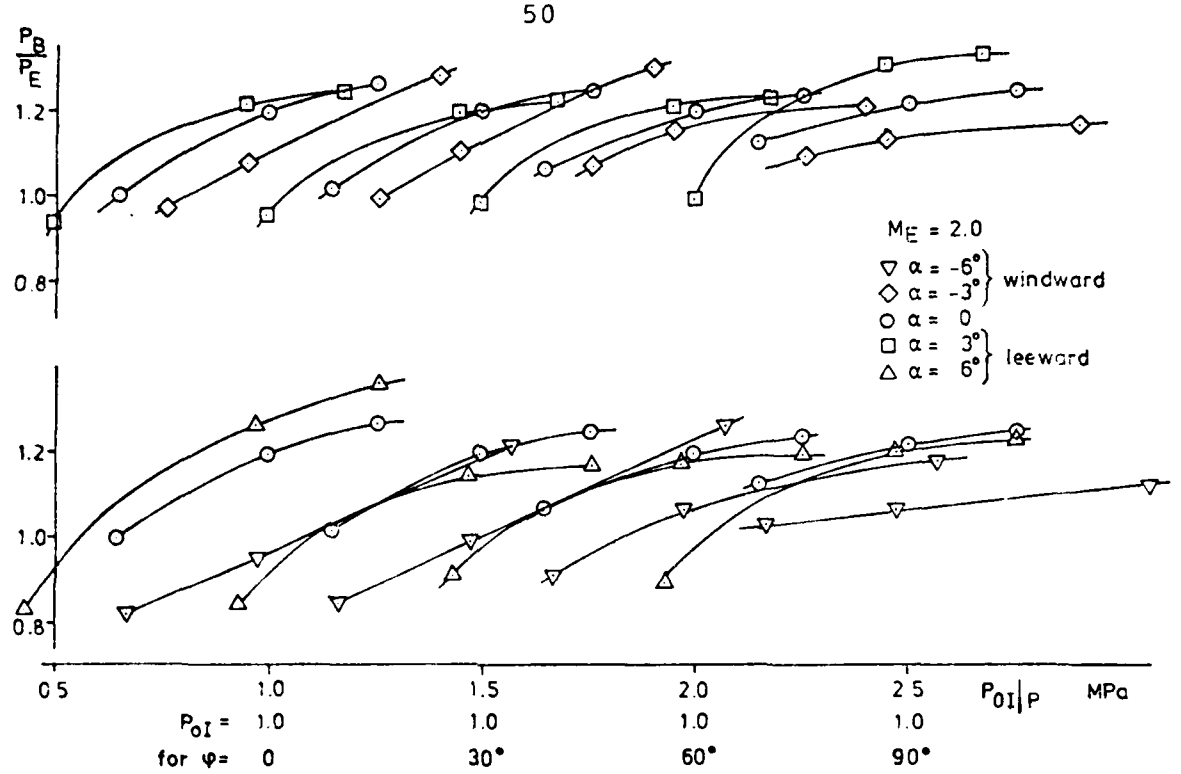


Figure 27. Base pressure ratio $P_B/P_E$ for Air (model, strong shock modeling) versus stagnation pressure $P_{0I|P}$ in prototype plane at different circumferential angles $\varphi$ and angles of attack $\alpha$.

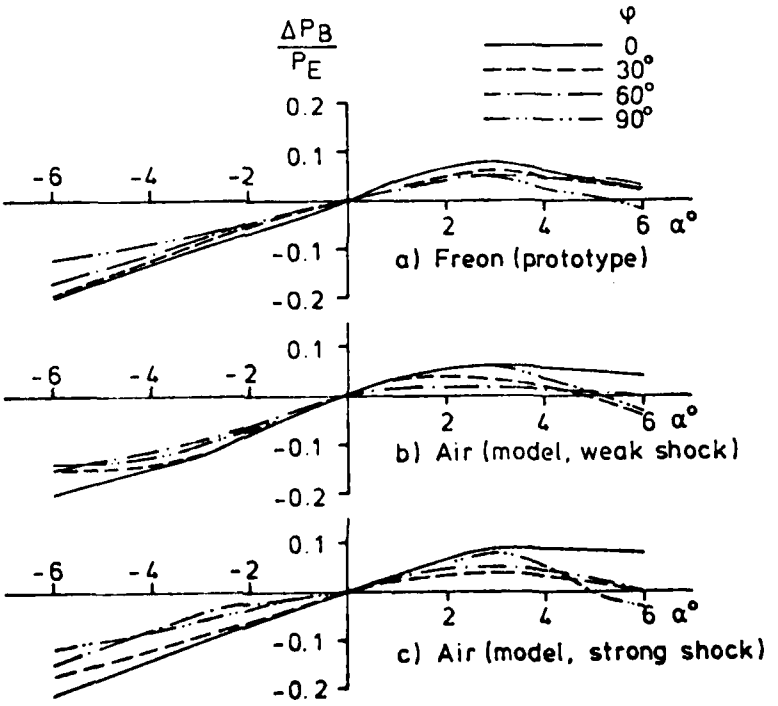


Figure 28. Effect on base pressure ratio of angle of attack $\Delta(P_B/P_E) = (P_B/P_E)_\alpha - (P_B/P_E)_{\alpha=0}$ versus angle of attack at stagnation pressure $P_{0I|P} = 0.75$ MPa and $M_E = 2.0$.

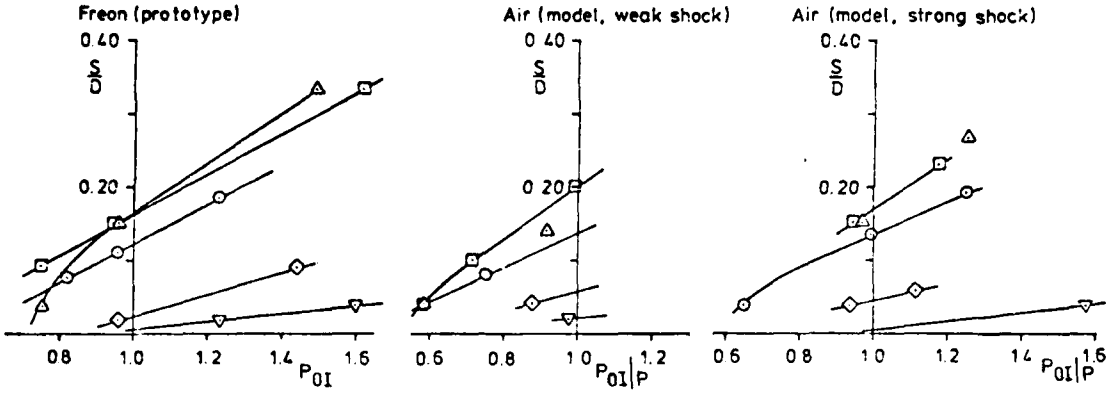


Figure 29. Separation location S/D versus jet stagnation pressure for Freon (prototype) and Air (model) nozzles. $M_E = 2.0$ ; $\varphi = 0$.

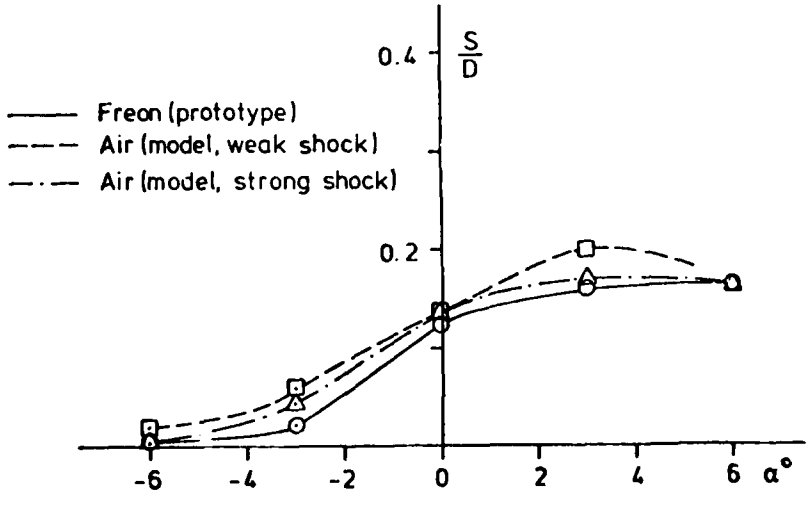


Figure 30. Separation location S/D at $\varphi = 0$ and at design pressure $P_{0I}|_P = 1.0$ MPa versus angle of attack for Freon (prototype) and Air (model) nozzles. $M_E = 2.0$

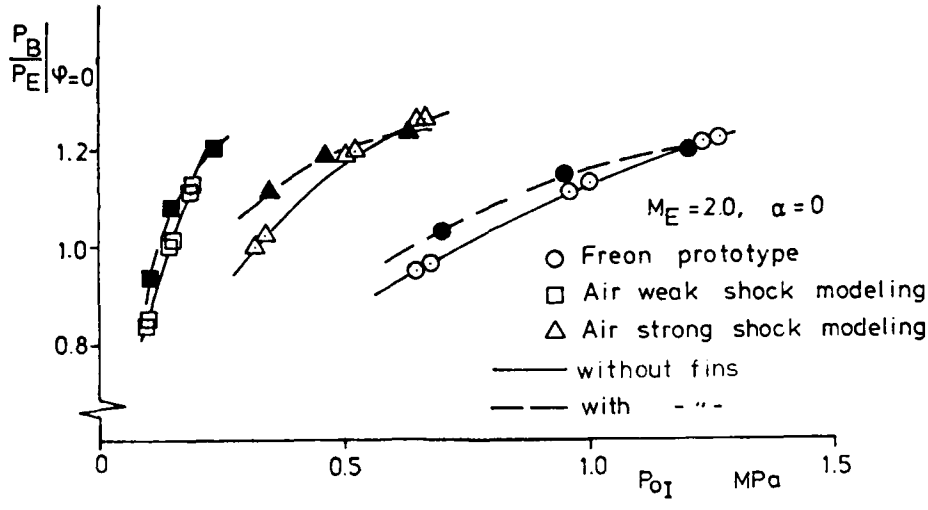


Figure 31. Base pressure ratio $P_B/P_E$ for Freon (prototype) and Air (model) nozzles versus jet stagnation pressure $P_{0I}$ with and without fins.

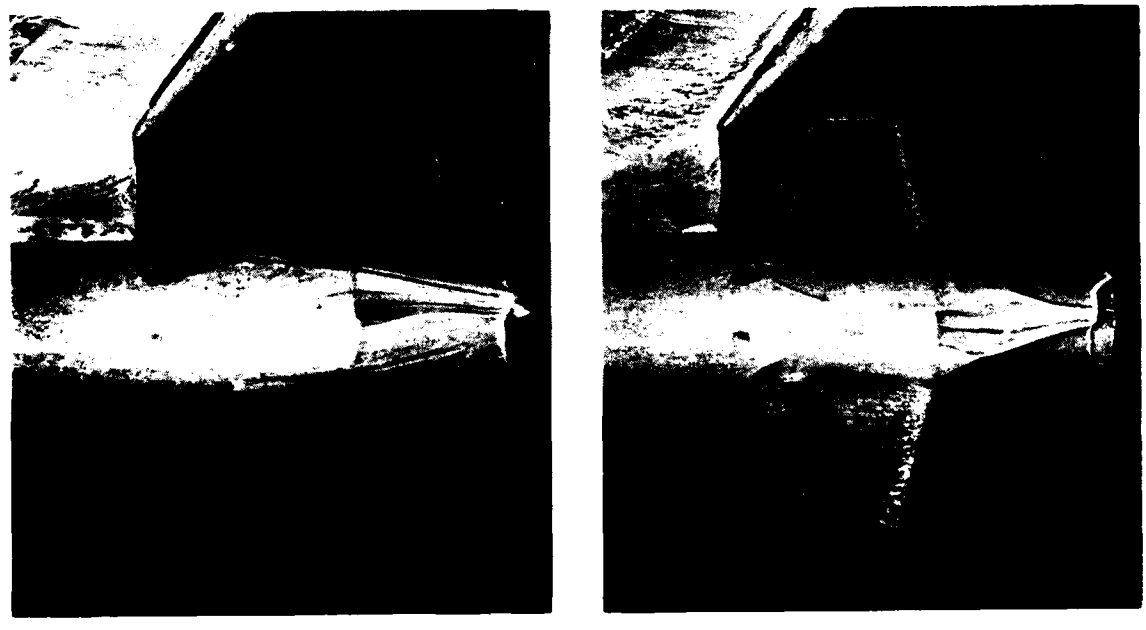

Figure 32. Oil flow pictures of the boundary layer flow with and without fins. $M_E = 2.0$; $\alpha = 0$; Air nozzle (strong shock modeling) $P_{0I} = 0.5$ MPa

# APPENDIX 1. TABLES OF BASIC TEST DATA, MODELING FROM AIR TO FREON

| Table | $M_E$ | $M_L$ | $\Theta_L$ | Test gas |
|---|---|---|---|---|
| 1 | 2.0 | 2.5 | 10 | Air |
| 2 | 2.0 | 2.5 | 20 | Air |
| 3 | 2.0 | 3.90 | 19.76 | Freon |
| 4 | 2.0 | 3.90 | 19.76 | Air |
| 5 | 2.0 | 3.19 | 14.19 | Freon |
| 6 | 2.0 | 3.19 | 14.19 | Air |
| 7 | 3.0 | 2.5 | 10 | Air |
| 8 | 3.0 | 3.90 | 19.76 | Freon |
| 9 | 3.0 | 3.19 | 14.19 | Freon |

TABLE OF BASIC TEST DATA 1

| RUN | ME | L/D | BETAE | ALFA | PL/PE | PE | | | PN/PE | | | | PB/PE |
|---|---|---|---|---|---|---|---|---|---|---|---|---|---|
| NO. | | | | | | KPA | X/D= 8.10 | 8.30 | 8.52 | 8.74 | 8.96 | 9.20 | 9.42 | 9.50 |
| 5258 | 2.00 | 1.0 | 8.0 | 0.0 | JETOFF | 12.66 | 0.998 | 1.017 | 0.758 | 0.690 | 0.692 | 0.707 | 0.720 | 0.735 |
| 5259 | 2.00 | 1.0 | 8.0 | 0.0 | 15.2 | 12.66 | 1.004 | 1.018 | 0.760 | 0.689 | 0.692 | 0.962 | 1.308 | 1.389 |
| 5260 | 2.00 | 1.0 | 8.0 | 0.0 | 9.2 | 12.66 | 1.001 | 1.016 | 0.759 | 0.688 | 0.691 | 0.706 | 1.230 | 1.318 |
| 5261 | 2.00 | 1.0 | 8.0 | 0.0 | 6.0 | 12.66 | 1.000 | 1.016 | 0.758 | 0.688 | 0.691 | 0.705 | 1.017 | 1.224 |
| 5262 | 2.00 | 1.0 | 8.0 | 0.0 | 3.0 | 12.66 | 1.000 | 1.018 | 0.759 | 0.690 | 0.693 | 0.707 | 0.736 | 0.957 |
| 5263 | 2.00 | 1.0 | 8.0 | 0.0 | 1.0 | 12.66 | 0.999 | 1.017 | 0.759 | 0.689 | 0.693 | 0.707 | 0.720 | 0.605 |
| 5264 | 2.00 | 1.0 | 8.0 | 0.0 | JETOFF | 12.66 | 0.998 | 1.016 | 0.756 | 0.688 | 0.692 | 0.707 | 0.718 | 0.728 |

TABLE OF BASIC TEST DATA 2

| RUN | ME | L/D | BETAE | ALFA | PL/PE | PE | | | PN/PE | | | | PB/PE |
|---|---|---|---|---|---|---|---|---|---|---|---|---|---|
| NO. | | | | | | KPA | X/D= 8.10 | 8.30 | 8.52 | 8.74 | 8.96 | 9.20 | 9.42 | 9.50 |
| 5265 | 2.00 | 1.0 | 8.0 | 0.0 | JETOFF | 12.66 | 0.997 | 1.015 | 0.757 | 0.687 | 0.691 | 0.705 | 0.718 | 0.724 |
| 5268 | 2.00 | 1.0 | 8.0 | 0.0 | 9.2 | 12.66 | 1.000 | 1.014 | 0.757 | 0.686 | 0.691 | 1.205 | 1.301 | 1.408 |
| 5271 | 2.00 | 1.0 | 8.0 | 0.0 | 15.2 | 12.67 | 1.000 | 1.013 | 0.757 | 0.685 | 1.007 | 1.303 | 1.280 | 1.444 |
| 5272 | 2.00 | 1.0 | 8.0 | 0.0 | 6.0 | 12.67 | 0.999 | 1.015 | 0.757 | 0.687 | 0.690 | 0.746 | 1.289 | 1.369 |
| 5273 | 2.00 | 1.0 | 8.0 | 0.0 | 3.0 | 12.67 | 0.998 | 1.015 | 0.757 | 0.687 | 0.691 | 0.705 | 0.993 | 1.214 |
| 5274 | 2.00 | 1.0 | 8.0 | 0.0 | 1.0 | 12.67 | 0.998 | 1.016 | 0.756 | 0.687 | 0.692 | 0.705 | 0.721 | 0.817 |
| 5275 | 2.00 | 1.0 | 8.0 | 0.0 | JETOFF | 12.67 | 0.998 | 1.016 | 0.756 | 0.688 | 0.692 | 0.705 | 0.718 | 0.721 |

FFA AU 1384 TABLE OF BASIC TEST DATA 3

RUN 5347 ME=2.00 POE= 97.59 KPA PE=12.47 KPA ALPHA=0.0 L/D=1.0 BETAE= 8.0 ML=3.90 THETAL=19.76

| T | TO | POI | PN/PE | | | | | | | PB/PE |
|---|---|---|---|---|---|---|---|---|---|---|
| SEC | C | MPA | X/D=8.10 | 8.30 | 8.52 | 8.74 | 8.96 | 9.20 | 9.42 | 9.50 |
| 0.0 | 120 | 1.11 | | | | | 0.690 | 0.723 | 0.712 | 0.650 |
| 1.0 | 206 | 14.60 | | | | | 0.689 | 0.723 | 0.978 | 1.163 |
| 1.9 | 224 | 16.60 | | | | | 0.709 | 0.727 | 1.201 | 1.290 |
| 2.9 | 232 | 16.75 | 0.989 | | | | 0.694 | 0.726 | 1.220 | 1.292 |
| 3.8 | 236 | 16.84 | | 1.003 | | | 0.690 | 0.723 | 1.216 | 1.290 |
| 4.8 | 240 | 16.86 | | | | | 0.689 | 0.723 | 1.212 | 1.286 |
| 5.7 | 243 | 16.89 | | | 0.742 | | 0.689 | 0.723 | 1.195 | 1.284 |
| 6.6 | 246 | 16.93 | | | | | 0.689 | 0.723 | 1.204 | 1.283 |
| 7.6 | 248 | 16.93 | | | | 0.676 | 0.689 | 0.723 | 1.204 | 1.281 |
| 8.5 | 250 | 16.96 | | | | | 0.689 | 0.723 | 1.201 | 1.286 |
| 9.5 | 252 | 16.95 | | | | | 0.689 | 0.722 | 1.199 | 1.277 |
| 10.4 | 253 | 16.97 | | | | | 0.689 | 0.722 | 1.196 | 1.275 |

RUN 5348 ME=2.00 POE= 97.60 KPA PE=12.47 KPA ALPHA=0.0 L/D=1.0 BETAE= 8.0 ML=3.90 THETAL=19.76

| T | TO | POI | PN/PE | | | | | | | PB/PE |
|---|---|---|---|---|---|---|---|---|---|---|
| SEC | C | MPA | X/D=8.10 | 8.30 | 8.52 | 8.74 | 8.96 | 9.20 | 9.42 | 9.50 |
| 0.0 | 253 | 15.84 | | | | | 0.693 | 0.726 | 1.169 | 1.255 |
| 1.0 | 255 | 15.93 | | | | | 0.693 | 0.726 | 1.167 | 1.254 |
| 1.9 | 257 | 15.97 | | | | | 0.714 | 0.726 | 1.164 | 1.253 |
| 2.9 | 258 | 16.00 | 0.994 | | | | 0.698 | 0.726 | 1.163 | 1.252 |
| 3.8 | 259 | 16.02 | | 1.010 | | | 0.694 | 0.724 | 1.161 | 1.251 |
| 4.8 | 260 | 16.03 | | | | | 0.693 | 0.725 | 1.161 | 1.25 |
| 5.7 | 261 | 16.05 | | | 0.747 | | 0.693 | 0.726 | 1.146 | 1.251 |
| 6.6 | 262 | 16.06 | | | | | 0.693 | 0.725 | 1.157 | 1.250 |
| 7.6 | 262 | 16.07 | | | | 0.680 | 0.693 | 0.725 | 1.158 | 1.249 |
| 8.5 | 263 | 16.08 | | | | | 0.693 | 0.725 | 1.158 | 1.247 |
| 9.5 | 263 | 16.09 | | | | | 0.693 | 0.725 | 1.158 | 1.247 |
| 10.4 | 264 | 16.10 | | | | | 0.693 | 0.725 | 1.158 | 1.249 |

FFA AU 1384 TABLE OF BASIC TEST DATA 3 CONT.

RUN 5349 ME=2.00 POE= 97.60 KPA PE=12.47 KPA ALPHA=0.0 L/D=1.0 BETAE= 8.0 ML=3.90 THETAL=19.76

| T | TO | POI | PN/PE | | | | | | | PB/PE |
|---|---|---|---|---|---|---|---|---|---|---|
| SEC | C | MPA | X/D=8.10 | 8.30 | 8.52 | 8.74 | 8.96 | 9.20 | 9.42 | 9.50 |
| 0.0 | 185 | 2.57 | | | | | 0.695 | 0.729 | 0.706 | 0.629 |
| 0.9 | 216 | 5.57 | | | | | 0.695 | 0.728 | 0.713 | 0.773 |
| 1.9 | 226 | 6.49 | | | | | 0.718 | 0.728 | 0.725 | 0.862 |
| 2.8 | 234 | 7.06 | 0.995 | | | | 0.700 | 0.728 | 0.733 | 0.916 |
| 3.8 | 239 | 7.42 | | 1.012 | | | 0.696 | 0.726 | 0.739 | 0.947 |
| 4.7 | 242 | 7.69 | | | | | 0.694 | 0.727 | 0.744 | 0.968 |
| 5.7 | 244 | 7.89 | | | 0.748 | | 0.694 | 0.727 | 0.747 | 0.982 |
| 6.6 | 246 | 8.04 | | | | | 0.694 | 0.727 | 0.752 | 0.992 |
| 7.6 | 247 | 8.15 | | | | 0.681 | 0.694 | 0.727 | 0.757 | 1.000 |
| 8.5 | 248 | 8.23 | | | | | 0.694 | 0.727 | 0.760 | 1.008 |
| 9.5 | 249 | 8.29 | | | | | 0.694 | 0.727 | 0.762 | 1.010 |
| 10.4 | 250 | 8.35 | | | | | 0.694 | 0.727 | 0.765 | 1.013 |

RUN 5351 ME=2.00 POE= 98.09 KPA PE=12.54 KPA ALPHA=0.0 L/D=1.0 BETAE= 8.0 ML=3.90 THETAL=19.76

| T | TO | POI | PN/PE | | | | | | | PB/PE |
|---|---|---|---|---|---|---|---|---|---|---|
| SEC | C | MPA | X/D=8.10 | 8.30 | 8.52 | 8.74 | 8.96 | 9.20 | 9.42 | 9.50 |
| 0.0 | 194 | 8.12 | | | | | 0.692 | 0.722 | 0.733 | 0.952 |
| 1.0 | 212 | 10.09 | | | | | 0.691 | 0.722 | 0.815 | 1.098 |
| 1.9 | 221 | 11.34 | | | | | 0.707 | 0.721 | 0.936 | 1.159 |
| 2.9 | 227 | 12.14 | 0.988 | | | | 0.695 | 0.721 | 1.019 | 1.188 |
| 3.8 | 231 | 12.66 | | 1.002 | | | 0.692 | 0.719 | 1.059 | 1.203 |
| 4.8 | 234 | 12.93 | | | | | 0.691 | 0.721 | 1.078 | 1.209 |
| 5.7 | 236 | 13.12 | | | 0.742 | | 0.691 | 0.721 | 1.074 | 1.212 |
| 6.6 | 238 | 13.22 | | | | | 0.691 | 0.721 | 1.087 | 1.214 |
| 7.6 | 240 | 13.30 | | | | 0.676 | 0.691 | 0.721 | 1.089 | 1.214 |
| 8.5 | 242 | 13.40 | | | | | 0.691 | 0.721 | 1.090 | 1.213 |
| 9.5 | 243 | 13.43 | | | | | 0.691 | 0.721 | 1.090 | 1.214 |
| 10.4 | 245 | 13.48 | | | | | 0.691 | 0.721 | 1.088 | 1.213 |

FFA AU 1384 TABLE OF BASIC TEST DATA 3 CONT.

RUN 5352 ME=2.00 POE= 98.11 KPA PE=12.54 KPA ALPHA=0.0 L/D=1.0 BETAE= 8.0 ML=3.90 THETAL=19.76

| T | TO | POI | PN/PE | | | | | | | PB/PE |
|---|---|---|---|---|---|---|---|---|---|---|
| SEC | C | MPA | X/D=8.10 | 8.30 | 8.52 | 8.74 | 8.96 | 9.20 | 9.42 | 9.50 |
| 0.0 | 183 | 5.11 | | | | | 0.692 | 0.721 | 0.708 | 0.715 |
| 0.9 | 221 | 8.78 | | | | | 0.691 | 0.721 | 0.735 | 0.953 |
| 1.9 | 236 | 10.68 | | | | | 0.707 | 0.720 | 0.811 | 1.086 |
| 2.8 | 243 | 11.88 | 0.987 | | | | 0.695 | 0.720 | 0.911 | 1.141 |
| 3.8 | 247 | 12.63 | | 1.001 | | | 0.691 | 0.718 | 0.986 | 1.168 |
| 4.8 | 250 | 13.10 | | | | | 0.691 | 0.719 | 1.027 | 1.182 |
| 5.7 | 252 | 13.41 | | | 0.743 | | 0.690 | 0.719 | 1.036 | 1.190 |
| 6.6 | 253 | 13.60 | | | | | 0.690 | 0.719 | 1.055 | 1.195 |
| 7.6 | 254 | 13.74 | | | | 0.676 | 0.690 | 0.719 | 1.064 | 1.198 |
| 8.5 | 255 | 13.83 | | | | | 0.690 | 0.719 | 1.070 | 1.199 |
| 9.5 | 256 | 13.91 | | | | | 0.690 | 0.719 | 1.073 | 1.201 |
| 10.4 | 256 | 13.98 | | | | | 0.690 | 0.719 | 1.077 | 1.203 |

RUN 5353 ME=2.00 POE= 98.11 KPA PE=12.54 KPA ALPHA=0.0 L/D=1.0 BETAE= 8.0 ML=3.90 THETAL=19.76

| T | TO | POI | PN/PE | | | | | | | PB/PE |
|---|---|---|---|---|---|---|---|---|---|---|
| SEC | C | MPA | X/D=8.10 | 8.30 | 8.52 | 8.74 | 8.96 | 9.20 | 9.42 | 9.50 |
| 0.0 | 195 | 4.94 | | | | | 0.691 | 0.720 | 0.703 | 0.689 |
| 0.9 | 223 | 6.89 | | | | | 0.691 | 0.720 | 0.719 | 0.848 |
| 1.9 | 234 | 8.06 | | | | | 0.707 | 0.720 | 0.735 | 0.952 |
| 2.8 | 241 | 8.77 | 0.986 | | | | 0.695 | 0.720 | 0.759 | 1.005 |
| 3.8 | 245 | 9.23 | | 1.000 | | | 0.691 | 0.717 | 0.777 | 1.034 |
| 4.7 | 248 | 9.60 | | | | | 0.691 | 0.719 | 0.790 | 1.053 |
| 5.7 | 250 | 9.84 | | | 0.742 | | 0.690 | 0.719 | 0.798 | 1.067 |
| 6.6 | 252 | 10.01 | | | | | 0.690 | 0.719 | 0.811 | 1.075 |
| 7.6 | 252 | 10.14 | | | | 0.675 | 0.690 | 0.719 | 0.820 | 1.082 |
| 8.5 | 253 | 10.24 | | | | | 0.690 | 0.719 | 0.828 | 1.087 |
| 9.5 | 253 | 10.32 | | | | | 0.690 | 0.719 | 0.834 | 1.089 |
| 10.4 | 254 | 10.38 | | | | | 0.690 | 0.718 | 0.839 | 1.092 |

FFA AU 1334 TABLE OF BASIC TEST DATA 3 CONCLUDED

RUN 5357 ME=2.00 POE=100.14 KPA PE=12.80 KPA ALPHA=0.0 L/D=1.0 BETAE= 8.0 ML=3.90 THETAL=19.76

| T | TO | POI | PN/PE | | | | | | | PB/PE |
|---|---|---|---|---|---|---|---|---|---|---|
| SEC | C | MPA | X/D=8.10 | 8.30 | 8.52 | 8.74 | 8.96 | 9.20 | 9.42 | 9.50 |
| 0.0 | 165 | 8.38 | | | | | 0.691 | 0.720 | 0.717 | 0.853 |
| 1.0 | 196 | 8.48 | | | | | 0.690 | 0.719 | 0.739 | 0.993 |
| 1.9 | 207 | 8.42 | | | | | 0.704 | 0.719 | 0.740 | 0.991 |
| 2.9 | 213 | 8.49 | 0.988 | | | | 0.693 | 0.719 | 0.754 | 0.984 |
| 3.8 | 218 | 8.61 | | 1.003 | | | 0.690 | 0.717 | 0.752 | 0.985 |
| 4.8 | 221 | 8.69 | | | | | 0.689 | 0.718 | 0.746 | 0.986 |
| 5.7 | 223 | 8.73 | | | 0.741 | | 0.689 | 0.719 | 0.741 | 0.985 |
| 6.6 | 225 | 8.76 | | | | | 0.689 | 0.719 | 0.740 | 0.983 |
| 7.6 | 227 | 8.78 | | | | 0.674 | 0.689 | 0.718 | 0.738 | 0.981 |
| 8.5 | 228 | 8.80 | | | | | 0.689 | 0.718 | 0.736 | 0.982 |
| 9.5 | 230 | 8.80 | | | | | 0.689 | 0.718 | 0.735 | 0.976 |
| 10.4 | 231 | 8.80 | | | | | 0.689 | 0.718 | 0.735 | 0.973 |

FFA AU 1384 TABLE OF BASIC TEST DATA 4

RUN 5366 ME=2.00 POE= 99.13 KPA PE=12.67 KPA ALPHA=0.0 L/D=1.0 BETAE= 8.0 ML=3.90 THETAL=19.76

| T | TO | POI | PN/PE | | | | | | | PB/PE |
|---|---|---|---|---|---|---|---|---|---|---|
| SEC | C | MPA | X/D=8.10 | 8.30 | 8.52 | 8.74 | 8.96 | 9.20 | 9.42 | 9.50 |
| 0.0 | 191 | 13.32 | | | | | 0.684 | 0.724 | 0.756 | 0.766 |
| 1.0 | 204 | 13.45 | | | | | 0.684 | 0.723 | 0.752 | 0.787 |
| 1.9 | 209 | 13.50 | | | | | 0.701 | 0.723 | 0.753 | 0.793 |
| 2.9 | 212 | 13.52 | 0.985 | | | | 0.688 | 0.723 | 0.752 | 0.794 |
| 3.8 | 213 | 13.53 | | 1.001 | | | 0.684 | 0.721 | 0.752 | 0.795 |
| 4.8 | 214 | 13.54 | | | | | 0.684 | 0.722 | 0.751 | 0.796 |
| 5.7 | 215 | 13.55 | | | 0.732 | | 0.684 | 0.723 | 0.749 | 0.798 |
| 6.6 | 216 | 13.55 | | | | | 0.684 | 0.723 | 0.750 | 0.798 |
| 7.6 | 216 | 13.55 | | | | 0.672 | 0.683 | 0.723 | 0.750 | 0.799 |
| 8.5 | 216 | 13.55 | | | | | 0.683 | 0.723 | 0.751 | 0.804 |
| 9.5 | 216 | 13.56 | | | | | 0.684 | 0.722 | 0.751 | 0.800 |
| 10.4 | 216 | 13.56 | | | | | 0.684 | 0.722 | 0.751 | 0.800 |



RUN 5367 ME=2.00 POE= 99.15 KPA PE=12.67 KPA ALPHA=0.0 L/D=1.0 BETAE= 8.0 ML=3.90 THETAL=19.76

| T | TO | POI | PN/PE | | | | | | | PB/PE |
|---|---|---|---|---|---|---|---|---|---|---|
| SEC | C | MPA | X/D=8.10 | 8.30 | 8.52 | 8.74 | 8.96 | 9.20 | 9.42 | 9.50 |
| 0.0 | 208 | 12.74 | | | | | 0.684 | 0.722 | 0.752 | 0.742 |
| 1.0 | 218 | 12.87 | | | | | 0.684 | 0.722 | 0.753 | 0.771 |
| 1.9 | 222 | 12.92 | | | | | 0.702 | 0.722 | 0.752 | 0.778 |
| 2.9 | 225 | 12.94 | 0.984 | | | | 0.688 | 0.722 | 0.751 | 0.779 |
| 3.8 | 226 | 12.95 | | 0.999 | | | 0.685 | 0.719 | 0.749 | 0.780 |
| 4.8 | 227 | 12.96 | | | | | 0.684 | 0.721 | 0.749 | 0.781 |
| 5.7 | 228 | 12.97 | | | 0.733 | | 0.684 | 0.722 | 0.747 | 0.781 |
| 6.6 | 228 | 12.98 | | | | | 0.684 | 0.722 | 0.748 | 0.782 |
| 7.6 | 228 | 12.98 | | | | 0.672 | 0.684 | 0.722 | 0.748 | 0.782 |
| 8.5 | 228 | 12.98 | | | | | 0.684 | 0.722 | 0.747 | 0.788 |
| 9.5 | 229 | 12.99 | | | | | 0.684 | 0.721 | 0.748 | 0.785 |
| 10.4 | 229 | 12.99 | | | | | 0.684 | 0.722 | 0.748 | 0.784 |

FFA AU 1384 TABLE OF BASIC TEST DATA 5

RUN 5337 ME=2.00 POE=101.85 KPA PE=13.02 KPA ALPHA=0.0 L/D=1.0 BETAE= 8.0 RL=3.19 THETAL=14.19

| T | TO | POI | PN/PE | | | | | | | PB/PE |
|---|---|---|---|---|---|---|---|---|---|---|
| SEC | C | MPA | X/D=8.10 | 8.30 | 8.52 | 8.74 | 8.96 | 9.20 | 9.42 | 9.50 |
| 0.0 | 190 | 2.31 | | | | | 0.688 | 0.807 | 0.995 | 1.108 |
| 1.0 | 220 | 7.07 | | | | | 0.687 | 0.848 | 1.228 | 1.304 |
| 1.9 | 226 | 6.92 | | | | | 0.702 | 0.786 | 1.244 | 1.308 |
| 2.9 | 230 | 7.01 | 0.987 | | | | 0.691 | 0.789 | 1.247 | 1.311 |
| 3.8 | 234 | 7.15 | | 0.998 | | | 0.688 | 0.816 | 1.247 | 1.311 |
| 4.8 | 236 | 7.35 | | | | | 0.688 | 0.869 | 1.247 | 1.313 |
| 5.7 | 239 | 7.56 | | | 0.743 | | 0.689 | 0.934 | 1.239 | 1.315 |
| 6.6 | 241 | 7.74 | | | | | 0.689 | 0.984 | 1.247 | 1.317 |
| 7.6 | 243 | 7.86 | | | | 0.676 | 0.690 | 1.010 | 1.250 | 1.318 |
| 8.5 | 244 | 8.08 | | | | | 0.690 | 1.033 | 1.251 | 1.318 |
| 9.5 | 243 | 8.27 | | | | | 0.690 | 1.060 | 1.252 | 1.322 |
| 10.4 | 240 | 8.29 | | | | | 0.691 | 1.068 | 1.251 | 1.322 |

RUN 5338 ME=2.00 POE=101.85 KPA PE=13.02 KPA ALPHA=0.0 L/D=1.0 BETAE= 8.0 RL=3.19 THETAL=14.19

| T | TO | PGI | PN/PE | | | | | | | PB/PE |
|---|---|---|---|---|---|---|---|---|---|---|
| SEC | C | MPA | X/D=8.10 | 8.30 | 8.52 | 8.74 | 8.96 | 9.20 | 9.42 | 9.50 |
| 0.0 | 206 | 10.44 | | | | | 0.698 | 0.952 | 0.972 | 1.103 |
| 1.0 | 220 | 9.98 | | | | | 0.699 | 1.184 | 1.233 | 1.347 |
| 1.9 | 227 | 8.26 | | | | | 0.705 | 1.108 | 1.256 | 1.328 |
| 2.9 | 232 | 7.73 | 0.996 | | | | 0.692 | 1.020 | 1.252 | 1.316 |
| 3.8 | 235 | 7.71 | | 1.004 | | | 0.688 | 0.992 | 1.250 | 1.314 |
| 4.8 | 237 | 7.59 | | | | | 0.688 | 0.993 | 1.247 | 1.312 |
| 5.7 | 238 | 7.57 | | | 0.748 | | 0.688 | 0.989 | 1.239 | 1.311 |
| 6.6 | 239 | 7.61 | | | | | 0.688 | 0.995 | 1.244 | 1.311 |
| 7.6 | 240 | 7.66 | | | | 0.678 | 0.688 | 1.003 | 1.245 | 1.313 |
| 8.5 | 241 | 7.71 | | | | | 0.689 | 1.014 | 1.245 | 1.309 |
| 9.5 | 241 | 7.78 | | | | | 0.689 | 1.026 | 1.244 | 1.311 |
| 10.4 | 242 | 7.85 | | | | | 0.689 | 1.033 | 1.244 | 1.313 |

FFA AU 1384 TABLE OF BASIC TEST DATA 5 CONT.

RUN 5340 ME=2.00 POE= 97.92 KPA PE=12.51 KPA ALPHA=0.0 L/D=1.0 BETAE= 8.0 ML=3.19 THETAL=14.19

| T | TO | POI | PN/PE | | | | | | | PB/PE |
|---|---|---|---|---|---|---|---|---|---|---|
| SEC | C | MPA | X/D=8.10 | 8.30 | 8.52 | 8.74 | 8.96 | 9.20 | 9.42 | 9.50 |
| 0.0 | 219 | 3.94 | | | | | 0.687 | 0.721 | 1.090 | 1.207 |
| 0.9 | 222 | 4.03 | | | | | 0.687 | 0.721 | 1.098 | 1.215 |
| 1.9 | 224 | 4.13 | | | | | 0.710 | 0.721 | 1.112 | 1.224 |
| 2.8 | 226 | 4.26 | 0.989 | | | | 0.693 | 0.721 | 1.127 | 1.232 |
| 3.8 | 229 | 4.44 | | 1.006 | | | 0.690 | 0.719 | 1.143 | 1.241 |
| 4.8 | 231 | 4.81 | | | | | 0.689 | 0.721 | 1.167 | 1.257 |
| 5.7 | 232 | 5.26 | | | 0.745 | | 0.690 | 0.723 | 1.178 | 1.273 |
| 6.6 | 234 | 7.11 | | | | | 0.689 | 0.791 | 1.227 | 1.304 |
| 7.6 | 229 | 7.27 | | | | 0.678 | 0.689 | 0.967 | 1.245 | 1.316 |
| 8.5 | 225 | 6.46 | | | | | 0.690 | 0.871 | 1.242 | 1.307 |
| 9.5 | 223 | 5.65 | | | | | 0.690 | 0.766 | 1.228 | 1.295 |
| 10.4 | 223 | 5.08 | | | | | 0.690 | 0.732 | 1.205 | 1.277 |

RUN 5343 ME=2.00 POE= 97.47 KPA PE=12.46 KPA ALPHA=0.0 L/D=1.0 BETAE= 8.0 ML=3.19 THETAL=14.19

| T | TO | POI | PN/PE | | | | | | | PB/PE |
|---|---|---|---|---|---|---|---|---|---|---|
| SEC | C | MPA | X/D=8.10 | 8.30 | 8.52 | 8.74 | 8.96 | 9.20 | 9.42 | 9.50 |
| 0.0 | 117 | 0.96 | | | | | 0.694 | 0.726 | 0.709 | 0.707 |
| 0.9 | 193 | 3.89 | | | | | 0.694 | 0.726 | 1.039 | 1.192 |
| 1.9 | 206 | 3.77 | | | | | 0.710 | 0.726 | 1.084 | 1.207 |
| 2.8 | 211 | 3.59 | 0.992 | | | | 0.698 | 0.726 | 1.046 | 1.190 |
| 3.8 | 215 | 3.58 | | 1.008 | | | 0.695 | 0.724 | 1.022 | 1.184 |
| 4.7 | 213 | 3.85 | | | | | 0.694 | 0.725 | 1.029 | 1.190 |
| 5.7 | 221 | 3.77 | | | 0.745 | | 0.694 | 0.725 | 1.041 | 1.201 |
| 6.6 | 223 | 3.88 | | | | | 0.694 | 0.725 | 1.072 | 1.210 |
| 7.6 | 226 | 4.01 | | | | 0.681 | 0.694 | 0.725 | 1.099 | 1.220 |
| 8.5 | 227 | 4.15 | | | | | 0.694 | 0.725 | 1.119 | 1.228 |
| 9.5 | 229 | 4.31 | | | | | 0.695 | 0.725 | 1.138 | 1.240 |
| 10.4 | 23 | 0.01 | | | | | 0.690 | 0.721 | 0.701 | 0.713 |

FFA AU 1384 TABLE OF BASIC TEST DATA 5 CONCLUDED

RUN 5344 ME=2.00 POE= 97.47 KPA PE=12.46 KPA ALPHA=0.0 L/D=1.0 BETAE= 8.0 ML=3.19 THETAL=14.19

| T | TO | POI | PN/PE | | | | | | | PB/PE |
|---|---|---|---|---|---|---|---|---|---|---|
| SEC | C | MPA | X/D=8.10 | 8.30 | 8.52 | 8.74 | 8.96 | 9.20 | 9.42 | 9.50 |
| 0.0 | 206 | 2.40 | | | | | 0.696 | 0.727 | 0.780 | 1.031 |
| 0.9 | 210 | 2.35 | | | | | 0.696 | 0.727 | 0.769 | 1.021 |
| 1.9 | 212 | 2.30 | | | | | 0.712 | 0.727 | 0.760 | 1.010 |
| 2.8 | 214 | 2.25 | 0.993 | | | | 0.700 | 0.727 | 0.754 | 1.000 |
| 3.8 | 216 | 2.19 | | 1.010 | | | 0.696 | 0.724 | 0.750 | 0.990 |
| 4.7 | 217 | 2.13 | | | | | 0.696 | 0.726 | 0.746 | 0.979 |
| 5.7 | 218 | 2.10 | | | 0.746 | | 0.696 | 0.726 | 0.742 | 0.971 |
| 6.6 | 219 | 2.06 | | | | | 0.695 | 0.726 | 0.741 | 0.965 |
| 7.6 | 220 | 2.01 | | | | 0.682 | 0.696 | 0.726 | 0.739 | 0.956 |
| 8.5 | 221 | 1.96 | | | | | 0.696 | 0.725 | 0.736 | 0.950 |
| 9.5 | 221 | 1.92 | | | | | 0.696 | 0.725 | 0.734 | 0.937 |
| 10.4 | 221 | 1.83 | | | | | 0.696 | 0.725 | 0.732 | 0.922 |

FFA AU 1384 TABLE OF BASIC TEST DATA 6

RUN 5368 ME=2.00 PDE= 99.20 KPA PE=12.68 KPA ALPHA=0.0 L/D=1.0 BETAE= 8.0 RL=3.19 THETAL=14.19

| T | TO | POI | PN/PE | | | | | | | PB/PE |
|---|---|---|---|---|---|---|---|---|---|---|
| SEC | C | MPA | X/D=8.10 | 8.30 | 8.52 | 8.74 | 8.96 | 9.20 | 9.42 | 9.50 |
| 0.0 | 152 | 1.96 | | | | | 0.690 | 0.720 | 0.735 | 0.600 |
| 1.0 | 168 | 2.03 | | | | | 0.689 | 0.720 | 0.736 | 0.604 |
| 1.9 | 176 | 2.05 | | | | | 0.705 | 0.720 | 0.735 | 0.606 |
| 2.9 | 181 | 2.07 | 0.985 | | | | 0.693 | 0.719 | 0.733 | 0.609 |
| 3.8 | 185 | 2.08 | | 1.001 | | | 0.690 | 0.717 | 0.729 | 0.610 |
| 4.8 | 189 | 2.10 | | | | | 0.689 | 0.719 | 0.727 | 0.612 |
| 5.7 | 192 | 2.11 | | | 0.738 | | 0.689 | 0.719 | 0.725 | 0.614 |
| 6.6 | 194 | 2.12 | | | | | 0.689 | 0.719 | 0.724 | 0.615 |
| 7.6 | 197 | 2.12 | | | | 0.675 | 0.689 | 0.719 | 0.724 | 0.616 |
| 8.5 | 199 | 2.13 | | | | | 0.689 | 0.719 | 0.723 | 0.622 |
| 9.5 | 200 | 2.14 | | | | | 0.689 | 0.719 | 0.723 | 0.620 |
| 10.4 | 202 | 2.14 | | | | | 0.689 | 0.719 | 0.723 | 0.620 |

RUN 5369 ME=2.00 PDE= 99.20 KPA PE=12.68 KPA ALPHA=0.0 L/D=1.0 BETAE= 8.0 RL=3.19 THETAL=14.19

| T | TO | POI | PN/PE | | | | | | | PB/PE |
|---|---|---|---|---|---|---|---|---|---|---|
| SEC | C | MPA | X/D=8.10 | 8.30 | 8.52 | 8.74 | 8.96 | 9.20 | 9.42 | 9.50 |
| 0.0 | 209 | 3.62 | | | | | 0.690 | 0.719 | 0.737 | 0.723 |
| 0.9 | 217 | 3.69 | | | | | 0.689 | 0.719 | 0.730 | 0.742 |
| 1.9 | 221 | 3.72 | | | | | 0.706 | 0.719 | 0.727 | 0.748 |
| 2.8 | 223 | 3.75 | 0.985 | | | | 0.693 | 0.719 | 0.725 | 0.751 |
| 3.8 | 225 | 3.76 | | 1.000 | | | 0.689 | 0.716 | 0.725 | 0.753 |
| 4.7 | 226 | 3.77 | | | | | 0.689 | 0.718 | 0.724 | 0.755 |
| 5.7 | 227 | 3.78 | | | 0.739 | | 0.689 | 0.718 | 0.724 | 0.756 |
| 6.6 | 227 | 3.79 | | | | | 0.689 | 0.718 | 0.724 | 0.757 |
| 7.6 | 228 | 3.79 | | | | 0.675 | 0.689 | 0.718 | 0.724 | 0.759 |
| 8.5 | 228 | 3.79 | | | | | 0.689 | 0.718 | 0.724 | 0.760 |
| 9.5 | 228 | 3.80 | | | | | 0.689 | 0.718 | 0.724 | 0.763 |
| 10.4 | 228 | 3.80 | | | | | 0.689 | 0.718 | 0.724 | 0.763 |

FFA AU 1384 TABLE OF BASIC TEST DATA 6 CONCLUDED

RUN 5370 ME=2.00 POE= 99.20 KPA PE=12.68 KPA ALPHA=0.0 L/D=1.0 BETAE= 8.0 ML=3.19 THETAL=14.19

| T | TO | POI | PN/PE | | | | | | | PB/PE |
|---|---|---|---|---|---|---|---|---|---|---|
| SEC | C | MPA | X/D=8.10 | 8.30 | 8.52 | 8.74 | 8.96 | 9.20 | 9.42 | 9.50 |
| 0.0 | 226 | 5.84 | | | | | 0.691 | 0.719 | 0.736 | 0.840 |
| 1.0 | 230 | 5.95 | | | | | 0.689 | 0.718 | 0.738 | 0.885 |
| 1.9 | 233 | 6.01 | | | | | 0.706 | 0.718 | 0.748 | 0.897 |
| 2.9 | 235 | 6.04 | 0.986 | | | | 0.693 | 0.718 | 0.744 | 0.901 |
| 3.8 | 236 | 6.06 | | 0.998 | | | 0.689 | 0.715 | 0.758 | 0.903 |
| 4.8 | 236 | 6.07 | | | | | 0.688 | 0.717 | 0.753 | 0.905 |
| 5.7 | 237 | 6.09 | | | 0.741 | | 0.688 | 0.717 | 0.748 | 0.906 |
| 6.6 | 237 | 6.10 | | | | | 0.688 | 0.717 | 0.746 | 0.907 |
| 7.6 | 237 | 6.10 | | | | 0.675 | 0.689 | 0.717 | 0.744 | 0.908 |
| 8.5 | 237 | 6.11 | | | | | 0.689 | 0.717 | 0.744 | 0.915 |
| 9.5 | 237 | 6.12 | | | | | 0.689 | 0.717 | 0.744 | 0.911 |
| 10.4 | 237 | 6.12 | | | | | 0.689 | 0.717 | 0.744 | 0.911 |

TABLE OF BASIC TEST DATA 7

| RUN | ME | L/D | BETAE | POI | PE | | | | PN/PE | | | | | PB/PE |
|---|---|---|---|---|---|---|---|---|---|---|---|---|---|---|
| NO. | | | | MPA | KPA | X/D= | 8.10 | 8.30 | 8.52 | 8.74 | 8.96 | 9.20 | 9.42 | 9.50 |
| 5391 | 3.00 | 1.0 | 8.0 | 0.90 | 2.79 | | 1.020 | 1.044 | 0.819 | 0.707 | 0.686 | 0.729 | 1.127 | 1.328 |
| 5393 | 3.00 | 1.0 | 8.0 | 0.66 | 2.79 | | 1.020 | 1.044 | 0.819 | 0.707 | 0.684 | 0.713 | 0.941 | 1.203 |
| 5394 | 3.00 | 1.0 | 8.0 | 0.40 | 2.79 | | 1.022 | 1.046 | 0.819 | 0.708 | 0.686 | 0.713 | 0.814 | 0.980 |
| 5395 | 3.00 | 1.0 | 8.0 | 0.30 | 2.79 | | 1.020 | 1.045 | 0.820 | 0.707 | 0.691 | 0.717 | 0.786 | 0.865 |
| 5396 | 3.00 | 1.0 | 8.0 | 0.15 | 2.79 | | 1.021 | 1.045 | 0.820 | 0.707 | 0.685 | 0.709 | 0.693 | 0.713 |
| 5397 | 3.00 | 1.0 | 8.0 | 0.08 | 2.79 | | 1.020 | 1.044 | 0.820 | 0.707 | 0.678 | 0.707 | 0.678 | 0.547 |
| 5398 | 3.00 | 1.0 | 8.0 | 1.61 | 2.79 | | 1.022 | 1.045 | 0.819 | 0.705 | 0.685 | 0.863 | 1.345 | 1.472 |
| 5399 | 3.00 | 1.0 | 8.0 | 1.74 | 2.79 | | 1.023 | 1.046 | 0.818 | 0.705 | 0.694 | 0.841 | 1.311 | 1.467 |
| 5401 | 3.00 | 1.0 | 8.0 | 2.10 | 2.79 | | 1.022 | 1.046 | 0.818 | 0.705 | 0.689 | 0.942 | 1.379 | 1.496 |
| 5402 | 3.00 | 1.0 | 8.0 | 2.51 | 2.79 | | 1.024 | 1.046 | 0.818 | 0.703 | 0.698 | 1.121 | 1.384 | 1.524 |

TABLE OF BASIC TEST DATA 8

| RUN | ME | L/D | BETAE | POI | PE | | | | PN/PE | | | | | PB/PE |
|---|---|---|---|---|---|---|---|---|---|---|---|---|---|---|
| NO. | | | | MPA | KPA | X/D= | 8.10 | 8.30 | 8.52 | 8.74 | 8.96 | 9.20 | 9.42 | 9.50 |
| 5416 | 3.00 | 1.0 | 8.0 | 6.22 | 2.72 | | 1.021 | 1.052 | 0.831 | 0.716 | 0.687 | 0.721 | 0.899 | 1.139 |
| 5417 | 3.00 | 1.0 | 8.0 | 8.22 | 2.72 | | 1.027 | 1.047 | 0.831 | 0.715 | 0.720 | 0.869 | 1.072 | 1.268 |
| 5418 | 3.00 | 1.0 | 8.0 | 5.02 | 2.72 | | 1.034 | 1.048 | 0.835 | 0.717 | 0.697 | 0.857 | 0.899 | 1.070 |
| 5419 | 3.00 | 1.0 | 8.0 | 9.45 | 2.72 | | 1.042 | 1.050 | 0.836 | 0.717 | 0.765 | 0.947 | 1.236 | 1.282 |
| 5421 | 3.00 | 1.0 | 8.0 | 3.17 | 2.72 | | 1.039 | 1.047 | 0.838 | 0.719 | 0.698 | 0.734 | 0.824 | 0.910 |
| 5422 | 3.00 | 1.0 | 8.0 | 7.22 | 2.72 | | 1.047 | 1.049 | 0.840 | 0.719 | 0.700 | 0.810 | 1.074 | 1.209 |

TABLE OF BASIC TEST DATA 9

| RUN | ME | L/D | BETAE | POI | PE | | | | PN/PE | | | | | PB/PE |
|---|---|---|---|---|---|---|---|---|---|---|---|---|---|---|
| NO. | | | | MPA | KPA | X/D= | 8.10 | 8.30 | 8.52 | 8.74 | 8.96 | 9.20 | 9.42 | 9.50 |
| 5407 | 3.00 | 1.0 | 8.0 | 0.97 | 2.80 | | 1.022 | 1.044 | 0.823 | 0.712 | 0.690 | 0.715 | 0.816 | 0.933 |
| 5408 | 3.00 | 1.0 | 8.0 | 4.02 | 2.80 | | 1.024 | 1.052 | 0.892 | 0.714 | 0.767 | 1.115 | 1.320 | 1.438 |
| 5409 | 3.00 | 1.0 | 8.0 | 1.90 | 2.80 | | 1.024 | 1.044 | 0.833 | 0.715 | 0.698 | 0.800 | 1.097 | 1.253 |
| 5411 | 3.00 | 1.0 | 8.0 | 1.52 | 2.80 | | 1.000 | 1.039 | 0.833 | 0.717 | 0.693 | 0.846 | 0.986 | 1.160 |
| 5412 | 3.00 | 1.0 | 8.0 | 3.25 | 2.80 | | 0.999 | 1.038 | 0.831 | 0.716 | 0.729 | 0.970 | 1.277 | 1.405 |
| 5413 | 3.00 | 1.0 | 8.0 | 5.29 | 2.80 | | 0.999 | 1.037 | 0.830 | 0.718 | 0.858 | 1.247 | 1.342 | 1.482 |

# APPENDIX 2. TABLES OF BASIC TEST DATA, MODELING FROM FREON TO AIR

| Run No | Nozzle $M_L$ | Nozzle $\theta_L$ | Test Gas | Angle of Attack $\alpha$ | With Fins |
|---|---|---|---|---|---|
| 5504 | 2.6 | 15 | Air | 0 | No |
| 5507 | | | Freon | | |
| 5508 | | | | | |
| 5510 | | | | | Yes |
| 5511 | | | | | |
| 5514 | | | | -3 | No |
| 5517 | | | | -6 | |
| 5520 | | | | +3 | |
| 5523 | | | | +6 | |
| 5538 | 2.03 | 10.5 | Air | 0 | Yes |
| 5540 | | | | | |
| 5541 | | | | | No |
| 5542 | | | | | |
| 5544 | | | | -3 | |
| 5547 | | | | -6 | |
| 5548 | | | | +3 | |
| 5550 | | | | +6 | |
| 5562 | 1.41 | 3.07 | | 0 | Yes |
| 5563 | | | | | |
| 5564 | | | | | No |
| 5565 | | | | | |
| 5569 | | | | -3 | |
| 5571 | | | | -6 | |
| 5573 | | | | +3 | |
| 5575 | | | | +6 | |

RUN 5504 ME=2.00 POE= 99.74 KPA PE=12.75 KPA ALPHA=0.0 L/D=1.0 BETAE= 8.0
ML=2.6 THETAL=15

| POI MPA | M | N=1 | 2 | 3 | 4 | 5 | 6 | 7 | 8 |
|---|---|---|---|---|---|---|---|---|---|
| 0.985 | 0 | 1.005 | 1.018 | 0.753 | 0.690 | 0.689 | 0.713 | 0.759 | 0.862 |
| | 3 | 0.991 | 0.992 | 0.745 | 0.684 | 0.691 | 0.697 | 0.729 | 0.872 |
| | 6 | 0.951 | 0.948 | 0.711 | 0.653 | 0.650 | 0.669 | 0.735 | |
| | 9 | 0.861 | 0.852 | 0.682 | 0.569 | 0.635 | 0.718 | 0.785 | 0.973 |
| 0.478 | 0 | 1.006 | 1.019 | 0.753 | 0.690 | 0.690 | 0.714 | 0.745 | 0.653 |
| | 3 | 0.992 | 0.992 | 0.744 | 0.683 | 0.690 | 0.697 | 0.710 | 0.660 |
| | 6 | 0.951 | 0.948 | 0.711 | 0.653 | 0.650 | 0.669 | 0.703 | |
| | 9 | 0.861 | 0.852 | 0.681 | 0.567 | 0.633 | 0.715 | 0.763 | 0.721 |

RUN 5507 ME=2.00 POE= 98.16 KPA PE=12.55 KPA ALPHA=0.0 L/D=1.0 BETAE= 8.0
ML=2.6 THETAL=15

| POI MPA | M | N=1 | 2 | 3 | 4 | 5 | 6 | 7 | 8 |
|---|---|---|---|---|---|---|---|---|---|
| 1.267 | 0 | 1.003 | 1.015 | 0.754 | 0.692 | 0.690 | 0.717 | 1.110 | 1.225 |
| | 3 | 0.989 | 0.986 | 0.744 | 0.686 | 0.693 | 0.701 | 1.129 | 1.223 |
| | 6 | 0.950 | 0.944 | 0.713 | 0.654 | 0.650 | 0.678 | 1.153 | 1.214 |
| | 9 | 0.867 | 0.854 | 0.687 | 0.571 | 0.634 | 0.725 | 1.165 | 1.220 |
| 1.002 | 0 | 1.004 | 1.017 | 0.754 | 0.693 | 0.691 | 0.717 | 0.905 | 1.131 |
| | 3 | 0.990 | 0.987 | 0.744 | 0.686 | 0.693 | 0.699 | 0.962 | 1.141 |
| | 6 | 0.950 | 0.945 | 0.713 | 0.655 | 0.650 | 0.670 | 1.043 | 1.163 |
| | 9 | 0.867 | 0.855 | 0.688 | 0.571 | 0.632 | 0.719 | 1.073 | 1.176 |
| 0.648 | 0 | 1.004 | 1.018 | 0.754 | 0.693 | 0.692 | 0.717 | 0.761 | 0.949 |
| | 3 | 0.992 | 0.987 | 0.745 | 0.686 | 0.693 | 0.699 | 0.752 | 0.961 |
| | 6 | 0.951 | 0.945 | 0.713 | 0.655 | 0.650 | 0.670 | 0.780 | 1.005 |
| | 9 | 0.868 | 0.855 | 0.688 | 0.569 | 0.632 | 0.718 | 0.826 | 1.059 |

RUN 5508 ME=2.00 POE= 98.11 KPA PE=12.54 KPA ALPHA=0.0 L/D=1.0 BETAE= 8.0
ML=2.6 THETAL=15

| POI MPA | M | N=1 | 2 | 3 | 4 | 5 | 6 | 7 | 8 |
|---|---|---|---|---|---|---|---|---|---|
| 1.230 | 0 | 1.003 | 1.016 | 0.756 | 0.692 | 0.691 | 0.716 | 1.083 | 1.215 |
| | 3 | 0.991 | 0.986 | 0.743 | 0.686 | 0.695 | 0.699 | 1.116 | 1.215 |
| | 6 | 0.949 | 0.943 | 0.715 | 0.655 | 0.650 | 0.672 | 1.144 | 1.209 |
| | 9 | 0.867 | 0.855 | 0.687 | 0.571 | 0.636 | 0.721 | 1.159 | 1.215 |
| 0.954 | 0 | 1.003 | 1.016 | 0.755 | 0.692 | 0.691 | 0.716 | 0.860 | 1.111 |
| | 3 | 0.991 | 0.986 | 0.743 | 0.685 | 0.695 | 0.699 | 0.912 | 1.121 |
| | 6 | 0.950 | 0.943 | 0.714 | 0.655 | 0.651 | 0.671 | 1.008 | 1.148 |
| | 9 | 0.867 | 0.855 | 0.687 | 0.570 | 0.636 | 0.720 | 1.030 | 1.171 |
| 0.677 | 0 | 1.003 | 1.016 | 0.754 | 0.693 | 0.691 | 0.716 | 0.765 | 0.965 |
| | 3 | 0.991 | 0.987 | 0.745 | 0.685 | 0.691 | 0.699 | 0.760 | 0.977 |
| | 6 | 0.951 | 0.944 | 0.713 | 0.655 | 0.652 | 0.672 | 0.794 | 1.020 |
| | 9 | 0.868 | 0.855 | 0.687 | 0.569 | 0.632 | 0.717 | 0.835 | 1.072 |

RUN 5510 ME=2.00 POE= 99.03 KPA PE=12.66 KPA ALPHA=0.0 L/D=1.0 BETAE= 8.0
ML=2.6 THETAL=15

| POI MPA | M | N=1 | 2 | 3 | 4 | 5 | 6 | 7 | 8 |
|---|---|---|---|---|---|---|---|---|---|
| 1.200 | 0 | 1.171 | 1.127 | 0.777 | 0.641 | 0.578 | 0.769 | 1.142 | 1.198 |
| | 3 | 1.026 | 0.938 | 0.644 | 0.661 | 0.751 | 0.748 | 1.138 | 1.180 |
| | 6 | 1.004 | 0.923 | 0.653 | 0.699 | 0.761 | 0.757 | 1.105 | 1.202 |
| | 9 | 1.217 | 1.206 | 0.885 | 0.657 | 0.595 | 0.676 | 1.128 | 1.191 |
| 0.920 | 0 | 1.175 | 1.131 | 0.779 | 0.643 | 0.581 | 0.721 | 1.065 | 1.145 |
| | 3 | 1.030 | 0.942 | 0.647 | 0.663 | 0.750 | 0.744 | 0.975 | 1.119 |
| | 6 | 1.003 | 0.923 | 0.652 | 0.702 | 0.765 | 0.758 | 0.879 | 1.110 |
| | 9 | 1.218 | 1.206 | 0.886 | 0.657 | 0.597 | 0.679 | 0.919 | 1.114 |

RUN 5511 ME=2.00 POE= 99.02 KPA PE=12.66 KPA ALPHA=0.0 L/D=1.0 BETAE= 8.0

ML=2.6 THETAL=15

| POI MPA | M | N=1 | 2 | 3 | 4 | 5 | 6 | 7 | 8 |
|---|---|---|---|---|---|---|---|---|---|
| 0.975 | 0 | 1.175 | 1.131 | 0.782 | 0.644 | 0.583 | 0.723 | 1.077 | 1.150 |
| | 3 | 1.030 | 0.942 | 0.647 | 0.663 | 0.749 | 0.745 | 1.004 | 1.127 |
| | 6 | 1.005 | 0.923 | 0.652 | 0.701 | 0.766 | 0.759 | 0.908 | 1.122 |
| | 9 | 1.217 | 1.206 | 0.885 | 0.657 | 0.597 | 0.679 | 0.947 | 1.124 |
| 0.700 | 0 | 1.175 | 1.132 | 0.782 | 0.644 | 0.585 | 0.721 | 0.900 | 1.030 |
| | 3 | 1.030 | 0.943 | 0.648 | 0.664 | 0.748 | 0.745 | 0.815 | 0.982 |
| | 6 | 1.006 | 0.924 | 0.652 | 0.701 | 0.767 | 0.759 | 0.777 | 0.971 |
| | 9 | 1.218 | 1.207 | 0.886 | 0.657 | 0.597 | 0.680 | 0.795 | 0.987 |

RUN 5514 ME=2.00 POE= 99.89 KPA PE=12.77 KPA ALPHA=-3.0 L/D=1.0 BETHA= 8.0

ML=2.6 THETAL=15

| POI MPA | M | N=1 | 2 | 3 | 4 | 5 | 6 | 7 | 8 |
|---|---|---|---|---|---|---|---|---|---|
| 1.443 | 0 | 1.025 | 1.032 | 0.774 | 0.690 | 0.688 | 0.707 | 0.934 | 1.248 |
| | 3 | 1.019 | 1.015 | 0.763 | 0.667 | 0.682 | 0.693 | 1.041 | 1.249 |
| | 6 | 0.958 | 0.947 | 0.721 | 0.620 | 0.630 | 0.668 | 1.086 | 1.177 |
| | 9 | 0.850 | 0.833 | 0.657 | 0.561 | 0.584 | 0.999 | 1.085 | 1.122 |
| 0.956 | 0 | 1.025 | 1.036 | 0.776 | 0.692 | 0.690 | 0.709 | 0.747 | 0.995 |
| | 3 | 1.019 | 1.018 | 0.767 | 0.671 | 0.685 | 0.696 | 0.736 | 1.009 |
| | 6 | 0.960 | 0.949 | 0.721 | 0.624 | 0.633 | 0.649 | 0.793 | 1.059 |
| | 9 | 0.851 | 0.833 | 0.658 | 0.559 | 0.575 | 0.672 | 1.021 | 1.058 |
| 0.768 | 0 | 1.025 | 1.036 | 0.778 | 0.693 | 0.691 | 0.710 | 0.739 | 0.921 |
| | 3 | 1.019 | 1.020 | 0.768 | 0.672 | 0.684 | 0.696 | 0.720 | 0.934 |
| | 6 | 0.961 | 0.950 | 0.721 | 0.625 | 0.634 | 0.649 | 0.710 | 0.987 |
| | 9 | 0.852 | 0.834 | 0.659 | 0.559 | 0.573 | 0.663 | 0.939 | 1.029 |

RUN 5517 ME=2.00 POE=100.18 KPA PE=12.80 KPA ALPHA=-6.0 L/D=1.0 BETHA= 8.0
ML=2.6 THETAL=15

| POI MPA | M | N=1 | 2 | 3 | 4 | 5 | 6 | 7 | 8 |
|---|---|---|---|---|---|---|---|---|---|
| 1.596 | 0 | 1.052 | 1.059 | 0.786 | 0.707 | 0.701 | 0.710 | 0.749 | 1.176 |
| | 3 | 1.041 | 1.039 | 0.783 | 0.669 | 0.687 | 0.690 | 0.754 | 1.195 |
| | 6 | 0.965 | 0.954 | 0.721 | 0.592 | 0.608 | 0.633 | 0.986 | 1.159 |
| | 9 | 0.815 | 0.798 | 0.622 | 0.501 | 0.530 | 0.951 | 0.979 | 1.126 |
| 0.973 | 0 | 1.054 | 1.062 | 0.788 | 0.711 | 0.706 | 0.712 | 0.730 | 0.885 |
| | 3 | 1.044 | 1.042 | 0.792 | 0.671 | 0.689 | 0.691 | 0.705 | 0.905 |
| | 6 | 0.969 | 0.955 | 0.722 | 0.594 | 0.612 | 0.631 | 0.673 | 0.976 |
| | 9 | 0.816 | 0.799 | 0.623 | 0.501 | 0.503 | 0.611 | 0.935 | 1.002 |
| 0.679 | 0 | 1.056 | 1.063 | 0.789 | 0.711 | 0.707 | 0.713 | 0.729 | 0.782 |
| | 3 | 1.046 | 1.043 | 0.794 | 0.671 | 0.688 | 0.692 | 0.699 | 0.797 |
| | 6 | 0.970 | 0.955 | 0.721 | 0.595 | 0.613 | 0.631 | 0.622 | 0.840 |
| | 9 | 0.816 | 0.799 | 0.623 | 0.501 | 0.502 | 0.565 | 0.811 | 0.983 |

RUN 5520 ME=2.00 POE=100.86 KPA PE=12.89 KPA ALPHA=3.0 L/D=1.0 BETAE= 8.0
ML=2.6 THETAL=15

| POI MPA | M | N=1 | 2 | 3 | 4 | 5 | 6 | 7 | 8 |
|---|---|---|---|---|---|---|---|---|---|
| 0.757 | 0 | 0.993 | 1.000 | 0.749 | 0.692 | 0.709 | 0.728 | 0.832 | 1.078 |
| | 3 | 0.975 | 0.970 | 0.742 | 0.683 | 0.694 | 0.711 | 0.946 | 1.083 |
| | 6 | 0.922 | 0.924 | 0.707 | 0.608 | 0.659 | 0.739 | 0.956 | 1.116 |
| | 9 | 0.846 | 0.865 | 0.707 | 0.626 | 0.685 | 0.783 | 0.900 | 1.143 |
| 0.944 | 0 | 0.995 | 1.001 | 0.751 | 0.694 | 0.711 | 0.729 | 1.026 | 1.174 |
| | 3 | 0.977 | 0.974 | 0.744 | 0.686 | 0.695 | 0.714 | 1.095 | 1.171 |
| | 6 | 0.925 | 0.927 | 0.709 | 0.610 | 0.662 | 0.743 | 1.098 | 1.190 |
| | 9 | 0.849 | 0.869 | 0.708 | 0.627 | 0.687 | 0.784 | 1.076 | 1.232 |
| 1.616 | 0 | 0.995 | 1.002 | 0.751 | 0.695 | 0.712 | 0.879 | 1.199 | 1.250 |
| | 3 | 0.977 | 0.974 | 0.744 | 0.687 | 0.695 | 1.052 | 1.180 | 1.247 |
| | 6 | 0.927 | 0.927 | 0.709 | 0.610 | 0.663 | 1.015 | 1.196 | 1.250 |
| | 9 | 0.849 | 0.868 | 0.707 | 0.626 | 0.686 | 0.874 | 1.249 | 1.309 |

RUN 5523 ME=2.00 POE=100.86 KPA PE=12.89 KPA ALPHA=6.0 L/D=1.0 BETAE= 8.0

ML=2.6 THETAL=15

| POI MPA | M | N=1 | 2 | 3 | 4 | 5 | 6 | 7 | 8 |
|---|---|---|---|---|---|---|---|---|---|
| 0.754 | 0 | 0.996 | 0.991 | 0.721 | 0.645 | 0.652 | 0.690 | 0.756 | 1.033 |
| | 3 | 0.917 | 0.914 | 0.688 | 0.642 | 0.662 | 0.703 | 0.898 | 1.031 |
| | 6 | 0.889 | 0.894 | 0.689 | 0.651 | 0.718 | 0.776 | 0.990 | 1.089 |
| | 9 | 0.832 | 0.869 | 0.732 | 0.654 | 0.754 | 0.770 | 0.912 | 1.082 |
| 0.956 | 0 | 0.997 | 0.992 | 0.722 | 0.648 | 0.655 | 0.692 | 0.773 | 1.157 |
| | 3 | 0.919 | 0.917 | 0.691 | 0.645 | 0.662 | 0.708 | 1.064 | 1.115 |
| | 6 | 0.891 | 0.896 | 0.689 | 0.651 | 0.720 | 0.801 | 1.090 | 1.144 |
| | 9 | 0.834 | 0.869 | 0.732 | 0.656 | 0.756 | 0.773 | 1.064 | 1.147 |
| 1.490 | 0 | 0.997 | 0.992 | 0.723 | 0.649 | 0.657 | 0.695 | 1.186 | 1.306 |
| | 3 | 0.922 | 0.921 | 0.695 | 0.647 | 0.662 | 1.002 | 1.110 | 1.154 |
| | 6 | 0.894 | 0.898 | 0.690 | 0.649 | 0.730 | 1.058 | 1.135 | 1.185 |
| | 9 | 0.835 | 0.869 | 0.732 | 0.656 | 0.757 | 0.998 | 1.136 | 1.195 |

RUN 5538 ME=2.00 POE=100.13 KPA PE=12.80 KPA ALPHA=0.0 L/D=1.0 BETAE= 8.0

ML=2.03 THETAL=10.5

| POI MPA | M | N=1 | 2 | 3 | 4 | 5 | 6 | 7 | 8 |
|---|---|---|---|---|---|---|---|---|---|
| 0.460 | 0 | 1.235 | 1.146 | 0.761 | 0.645 | 0.589 | 0.717 | 1.106 | 1.189 |
| | 3 | 1.036 | 0.928 | 0.599 | 0.692 | 0.750 | 0.750 | 1.046 | 1.181 |
| | 6 | 0.996 | 0.926 | 0.621 | 0.715 | 0.766 | 0.735 | 1.005 | 1.166 |
| | 9 | 1.194 | 1.189 | 0.767 | 0.685 | 0.606 | 0.676 | 1.064 | 1.168 |
| 0.630 | 0 | 1.239 | 1.149 | 0.763 | 0.646 | 0.589 | 0.749 | 1.174 | 1.231 |
| | 3 | 1.038 | 0.932 | 0.601 | 0.694 | 0.749 | 0.754 | 1.176 | 1.225 |
| | 6 | 0.996 | 0.927 | 0.620 | 0.714 | 0.769 | 0.738 | 1.162 | 1.217 |
| | 9 | 1.197 | 1.190 | 0.769 | 0.685 | 0.606 | 0.678 | 1.167 | 1.223 |

RUN 5540 ME=2.00 POE=100.11 KPA PE=12.79 KPA ALPHA=0.0 L/D=1.0 BETAE= 8.0
ML=2.03 THETAL=10.5

| POI MPA | M | N=1 | 2 | 3 | 4 | 5 | 6 | 7 | 8 |
|---|---|---|---|---|---|---|---|---|---|
| 0.348 | 0 | 1.225 | 1.142 | 0.764 | 0.648 | 0.592 | 0.719 | 0.955 | 1.114 |
| | 3 | 1.039 | 0.940 | 0.600 | 0.697 | 0.758 | 0.754 | 0.846 | 1.082 |
| | 6 | 1.002 | 0.932 | 0.625 | 0.722 | 0.768 | 0.739 | 0.820 | 1.073 |
| | 9 | 1.202 | 1.197 | 0.769 | 0.689 | 0.609 | 0.682 | 0.881 | 1.084 |

RUN 5541 ME=2.00 POE=100.03 KPA PE=12.78 KPA ALPHA=0.0 L/D=1.0 BETAE= 8.0
ML=2.03 THETAL=10.5

| POI MPA | M | N=1 | 2 | 3 | 4 | 5 | 6 | 7 | 8 |
|---|---|---|---|---|---|---|---|---|---|
| 0.320 | 0 | 1.033 | 1.029 | 0.733 | 0.693 | 0.700 | 0.717 | 0.768 | 0.998 |
| | 3 | 1.000 | 0.987 | 0.706 | 0.692 | 0.691 | 0.710 | 0.772 | 1.016 |
| | 6 | 0.956 | 0.946 | 0.685 | 0.659 | 0.652 | 0.649 | 0.806 | 1.064 |
| | 9 | 0.891 | 0.899 | 0.633 | 0.599 | 0.605 | 0.697 | 0.964 | 1.125 |
| 0.520 | 0 | 1.032 | 1.029 | 0.732 | 0.693 | 0.699 | 0.717 | 1.001 | 1.194 |
| | 3 | 1.000 | 0.988 | 0.706 | 0.692 | 0.691 | 0.710 | 1.047 | 1.200 |
| | 6 | 0.957 | 0.946 | 0.686 | 0.659 | 0.652 | 0.650 | 1.111 | 1.198 |
| | 9 | 0.892 | 0.899 | 0.634 | 0.599 | 0.605 | 0.717 | 1.131 | 1.219 |
| 0.665 | 0 | 1.031 | 1.029 | 0.731 | 0.693 | 0.699 | 0.717 | 1.163 | 1.263 |
| | 3 | 0.999 | 0.989 | 0.706 | 0.692 | 0.688 | 0.711 | 1.177 | 1.248 |
| | 6 | 0.958 | 0.946 | 0.686 | 0.659 | 0.653 | 0.663 | 1.160 | 1.235 |
| | 9 | 0.892 | 0.898 | 0.634 | 0.598 | 0.603 | 0.885 | 1.170 | 1.249 |

RUN 5542 ME=2.00 POE=100.00 KPA PE=12.78 KPA ALPHA=0.0 L/D=1.0 BETAE= 8.0
ML=2.03 THETAL=10.5

| POI MPA | M | N=1 | 2 | 3 | 4 | 5 | 6 | 7 | 8 |
|---|---|---|---|---|---|---|---|---|---|
| 0.339 | 0 | 1.034 | 1.027 | 0.732 | 0.694 | 0.700 | 0.719 | 0.771 | 1.022 |
| | 3 | 0.999 | 1.005 | 0.706 | 0.694 | 0.693 | 0.711 | 0.776 | 1.041 |
| | 6 | 0.955 | 0.946 | 0.685 | 0.659 | 0.652 | 0.649 | 0.820 | 1.088 |
| | 9 | 0.890 | 0.898 | 0.632 | 0.599 | 0.602 | 0.704 | 0.983 | 1.149 |
| 0.501 | 0 | 1.034 | 1.027 | 0.732 | 0.693 | 0.699 | 0.718 | 0.961 | 1.184 |
| | 3 | 0.998 | 1.005 | 0.706 | 0.694 | 0.692 | 0.711 | 1.012 | 1.195 |
| | 6 | 0.957 | 0.946 | 0.685 | 0.659 | 0.652 | 0.648 | 1.098 | 1.199 |
| | 9 | 0.890 | 0.898 | 0.633 | 0.599 | 0.601 | 0.717 | 1.123 | 1.224 |
| 0.648 | 0 | 1.034 | 1.027 | 0.732 | 0.692 | 0.699 | 0.717 | 1.149 | 1.260 |
| | 3 | 0.998 | 1.006 | 0.707 | 0.693 | 0.688 | 0.712 | 1.164 | 1.249 |
| | 6 | 0.958 | 0.947 | 0.684 | 0.658 | 0.653 | 0.652 | 1.158 | 1.240 |
| | 9 | 0.891 | 0.898 | 0.632 | 0.599 | 0.599 | 0.848 | 1.159 | 1.255 |

RUN 5544 ME=2.00 POE= 99.49 KPA PE=12.71 KPA ALPHA=-3.0 L/D=1.0 BETAE= 8.0
ML=2.03 THETAL=10.5

| POI MPA | M | N=1 | 2 | 3 | 4 | 5 | 6 | 7 | 8 |
|---|---|---|---|---|---|---|---|---|---|
| 0.386 | 0 | 1.146 | 1.064 | 0.775 | 0.685 | 0.700 | 0.713 | 0.744 | 0.971 |
| | 3 | 1.020 | 0.991 | 0.712 | 0.682 | 0.690 | 0.716 | 0.724 | 0.996 |
| | 6 | 0.971 | 0.958 | 0.663 | 0.645 | 0.639 | 0.630 | 0.718 | 1.070 |
| | 9 | 0.875 | 0.868 | 0.596 | 0.559 | 0.562 | 0.637 | 1.027 | 1.096 |
| 0.495 | 0 | 1.146 | 1.064 | 0.775 | 0.684 | 0.700 | 0.713 | 0.756 | 1.078 |
| | 3 | 1.019 | 0.993 | 0.712 | 0.682 | 0.688 | 0.717 | 0.742 | 1.107 |
| | 6 | 0.973 | 0.960 | 0.662 | 0.645 | 0.640 | 0.630 | 0.902 | 1.153 |
| | 9 | 0.876 | 0.869 | 0.598 | 0.559 | 0.562 | 0.665 | 1.066 | 1.129 |
| 0.753 | 0 | 1.146 | 1.064 | 0.775 | 0.684 | 0.700 | 0.713 | 0.919 | 1.285 |
| | 3 | 1.021 | 0.996 | 0.712 | 0.681 | 0.687 | 0.717 | 1.011 | 1.305 |
| | 6 | 0.974 | 0.960 | 0.663 | 0.645 | 0.642 | 0.636 | 1.102 | 1.210 |
| | 9 | 0.876 | 0.868 | 0.597 | 0.558 | 0.561 | 1.030 | 1.087 | 1.169 |

RUN 5547 ME=2.00 POE= 99.51 KPA PE=12.72 KPA ALPHA=-6.0 L/D=1.0 BETAE= 8.0
ML=2.03 THETAL=10.5

| POI MPA | M | N=1 | 2 | 3 | 4 | 5 | 6 | 7 | 8 |
|---|---|---|---|---|---|---|---|---|---|
| 0.332 | 0 | 1.087 | 1.067 | 0.774 | 0.693 | 0.709 | 0.713 | 0.740 | 0.820 |
| | 3 | 1.036 | 1.008 | 0.725 | 0.682 | 0.686 | 0.716 | 0.709 | 0.847 |
| | 6 | 0.974 | 0.956 | 0.659 | 0.618 | 0.618 | 0.610 | 0.616 | 0.909 |
| | 9 | 0.837 | 0.837 | 0.564 | 0.508 | 0.510 | 0.536 | 0.916 | 1.028 |
| 0.507 | 0 | 1.089 | 1.068 | 0.775 | 0.694 | 0.710 | 0.714 | 0.743 | 0.955 |
| | 3 | 1.036 | 1.010 | 0.726 | 0.683 | 0.686 | 0.716 | 0.711 | 0.989 |
| | 6 | 0.975 | 0.957 | 0.658 | 0.517 | 0.620 | 0.610 | 0.697 | 1.065 |
| | 9 | 0.837 | 0.837 | 0.564 | 0.507 | 0.510 | 0.649 | 0.972 | 1.065 |
| 0.846 | 0 | 1.090 | 1.069 | 0.775 | 0.694 | 0.710 | 0.714 | 0.759 | 1.215 |
| | 3 | 1.037 | 1.012 | 0.727 | 0.683 | 0.684 | 0.717 | 0.743 | 1.260 |
| | 6 | 0.977 | 0.958 | 0.657 | 0.617 | 0.620 | 0.611 | 1.012 | 1.178 |
| | 9 | 0.837 | 0.837 | 0.563 | 0.506 | 0.530 | 0.962 | 0.988 | 1.120 |

RUN 5548 ME=2.00 POE= 99.51 KPA PE=12.72 KPA ALPHA=3.0 L/D=1.0 BETAE= 8.0
ML=2.03 THETAL=10.5

| POI MPA | M | N=1 | 2 | 3 | 4 | 5 | 6 | 7 | 8 |
|---|---|---|---|---|---|---|---|---|---|
| 0.235 | 0 | 1.010 | 1.001 | 0.727 | 0.697 | 0.716 | 0.727 | 0.766 | 0.934 |
| | 3 | 0.977 | 0.956 | 0.684 | 0.701 | 0.702 | 0.718 | 0.782 | 0.955 |
| | 6 | 0.936 | 0.941 | 0.655 | 0.634 | 0.662 | 0.690 | 0.825 | 0.983 |
| | 9 | 0.876 | 0.881 | 0.617 | 0.602 | 0.657 | 0.778 | 0.813 | 0.992 |
| 0.491 | 0 | 1.011 | 1.002 | 0.728 | 0.698 | 0.716 | 0.727 | 1.101 | 1.217 |
| | 3 | 0.979 | 0.958 | 0.685 | 0.702 | 0.701 | 0.719 | 1.124 | 1.198 |
| | 6 | 0.940 | 0.942 | 0.654 | 0.634 | 0.664 | 0.697 | 1.135 | 1.211 |
| | 9 | 0.878 | 0.881 | 0.617 | 0.600 | 0.656 | 0.777 | 1.162 | 1.304 |
| 0.620 | 0 | 1.010 | 1.002 | 0.728 | 0.698 | 0.716 | 0.731 | 1.176 | 1.245 |
| | 3 | 0.980 | 0.959 | 0.685 | 0.702 | 0.699 | 0.750 | 1.154 | 1.222 |
| | 6 | 0.941 | 0.943 | 0.654 | 0.635 | 0.665 | 0.810 | 1.156 | 1.230 |
| | 9 | 0.878 | 0.881 | 0.618 | 0.600 | 0.656 | 0.784 | 1.223 | 1.335 |

RUN 5550 ME=2.00 POE= 99.51 KPA PE=12.72 KPA ALPHA=6.0 L/D=1.0 BETAE= 8.0
ML=2.03 THETAL=10.5

| POI MPA | M | N=1 | 2 | 3 | 4 | 5 | 6 | 7 | 8 |
|---|---|---|---|---|---|---|---|---|---|
| 0.200 | 0 | 0.997 | 0.993 | 0.709 | 0.636 | 0.668 | 0.700 | 0.767 | 0.830 |
| | 3 | 0.920 | 0.893 | 0.646 | 0.662 | 0.659 | 0.697 | 0.746 | 0.845 |
| | 6 | 0.896 | 0.904 | 0.657 | 0.652 | 0.699 | 0.745 | 0.822 | 0.909 |
| | 9 | 0.863 | 0.889 | 0.621 | 0.645 | 0.748 | 0.781 | 0.804 | 0.893 |
| 0.505 | 0 | 0.997 | 0.993 | 0.709 | 0.636 | 0.668 | 0.701 | 0.833 | 1.264 |
| | 3 | 0.922 | 0.896 | 0.647 | 0.663 | 0.657 | 0.706 | 1.084 | 1.142 |
| | 6 | 0.896 | 0.905 | 0.656 | 0.650 | 0.699 | 0.863 | 1.105 | 1.171 |
| | 9 | 0.863 | 0.889 | 0.620 | 0.643 | 0.746 | 0.819 | 1.100 | 1.198 |
| 0.664 | 0 | 0.996 | 0.993 | 0.708 | 0.636 | 0.667 | 0.701 | 1.152 | 1.357 |
| | 3 | 0.922 | 0.896 | 0.648 | 0.664 | 0.655 | 0.878 | 1.088 | 1.168 |
| | 6 | 0.899 | 0.906 | 0.653 | 0.649 | 0.703 | 1.039 | 1.123 | 1.194 |
| | 9 | 0.863 | 0.889 | 0.620 | 0.642 | 0.745 | 0.993 | 1.121 | 1.227 |

RUN 5562 ME=2.00 POE=100.82 KPA PE=12.89 KPA ALPHA=0.0 L/D=1.0 BETAE= 8.0
ML=1.41 THETAL=3.07

| POI MPA | M | N=1 | 2 | 3 | 4 | 5 | 6 | 7 | 8 |
|---|---|---|---|---|---|---|---|---|---|
| 0.135 | 0 | 1.172 | 1.110 | 0.778 | 0.629 | 0.599 | 0.708 | 0.897 | 1.042 |
| | 3 | 1.000 | 0.913 | 0.599 | 0.682 | 0.747 | 0.752 | 0.789 | 1.021 |
| | 6 | 1.003 | 0.888 | 0.686 | 0.734 | 0.765 | 0.757 | 0.784 | 1.023 |
| | 9 | 1.211 | 1.152 | 0.778 | 0.686 | 0.604 | 0.684 | 0.835 | 1.048 |
| 0.178 | 0 | 1.173 | 1.111 | 0.780 | 0.629 | 0.598 | 0.706 | 1.046 | 1.143 |
| | 3 | 1.003 | 0.915 | 0.599 | 0.682 | 0.746 | 0.752 | 0.882 | 1.132 |
| | 6 | 1.004 | 0.889 | 0.685 | 0.735 | 0.770 | 0.761 | 0.885 | 1.141 |
| | 9 | 1.215 | 1.155 | 0.778 | 0.686 | 0.606 | 0.682 | 0.972 | 1.144 |

RUN 5563 ME=2.00 POE=100.83 KPA PE=12.89 KPA ALPHA=0.0 L/D=1.0 BETAE= 8.0

ML=1.41 THETAL=3.07

| POI MPA | M | N=1 | 2 | 3 | 4 | 5 | 6 | 7 | 8 |
|---|---|---|---|---|---|---|---|---|---|
| 0.104 | 0 | 1.173 | 1.113 | 0.785 | 0.629 | 0.598 | 0.708 | 0.817 | 0.932 |
| | 3 | 1.002 | 0.913 | 0.598 | 0.683 | 0.749 | 0.753 | 0.768 | 0.911 |
| | 6 | 1.009 | 0.891 | 0.688 | 0.738 | 0.770 | 0.760 | 0.757 | 0.908 |
| | 9 | 1.220 | 1.159 | 0.781 | 0.687 | 0.607 | 0.687 | 0.801 | 0.938 |
| 0.147 | 0 | 1.174 | 1.113 | 0.785 | 0.630 | 0.598 | 0.708 | 0.939 | 1.079 |
| | 3 | 1.002 | 0.913 | 0.598 | 0.684 | 0.747 | 0.754 | 0.801 | 1.061 |
| | 6 | 1.009 | 0.890 | 0.688 | 0.738 | 0.771 | 0.761 | 0.802 | 1.065 |
| | 9 | 1.219 | 1.159 | 0.781 | 0.687 | 0.607 | 0.686 | 0.861 | 1.083 |
| 0.233 | 0 | 1.176 | 1.115 | 0.787 | 0.631 | 0.597 | 0.715 | 1.141 | 1.201 |
| | 3 | 1.003 | 0.916 | 0.599 | 0.684 | 0.746 | 0.755 | 1.103 | 1.189 |
| | 6 | 1.011 | 0.891 | 0.687 | 0.738 | 0.774 | 0.764 | 1.095 | 1.206 |
| | 9 | 1.220 | 1.159 | 0.781 | 0.688 | 0.607 | 0.685 | 1.134 | 1.197 |

RUN 5564 ME=2.00 POE=100.86 KPA PE=12.89 KPA ALPHA=0.0 L/D=1.0 BETHA= 8.0

ML=1.41 THETAL=3.07

| POI MPA | M | N=1 | 2 | 3 | 4 | 5 | 6 | 7 | 8 |
|---|---|---|---|---|---|---|---|---|---|
| 0.096 | 0 | 1.007 | 1.019 | 0.768 | 0.687 | 0.721 | 0.706 | 0.723 | 0.836 |
| | 3 | 0.973 | 0.971 | 0.704 | 0.679 | 0.689 | 0.699 | 0.716 | 0.851 |
| | 6 | 0.971 | 0.929 | 0.718 | 0.661 | 0.652 | 0.685 | 0.730 | 0.902 |
| | 9 | 0.926 | 0.866 | 0.639 | 0.604 | 0.637 | 0.718 | 0.819 | 0.974 |
| 0.149 | 0 | 1.007 | 1.019 | 0.769 | 0.687 | 0.721 | 0.705 | 0.763 | 1.020 |
| | 3 | 0.973 | 0.972 | 0.705 | 0.679 | 0.687 | 0.701 | 0.766 | 1.038 |
| | 6 | 0.972 | 0.930 | 0.718 | 0.661 | 0.654 | 0.687 | 0.844 | 1.089 |
| | 9 | 0.929 | 0.867 | 0.640 | 0.604 | 0.638 | 0.720 | 0.965 | 1.152 |
| 0.189 | 0 | 1.008 | 1.020 | 0.770 | 0.687 | 0.721 | 0.705 | 0.851 | 1.126 |
| | 3 | 0.974 | 0.973 | 0.705 | 0.679 | 0.686 | 0.700 | 0.881 | 1.144 |
| | 6 | 0.974 | 0.931 | 0.718 | 0.661 | 0.655 | 0.687 | 1.031 | 1.164 |
| | 9 | 0.929 | 0.867 | 0.640 | 0.605 | 0.638 | 0.720 | 1.105 | 1.199 |

RUN 5565 ME=2.00 POE=100.86 KPA PE=12.89 KPA ALPHA=0.0 L/D=1.0 BETAE= 8.0
ML=1.41 THETAL=3.07

| POI MPA | M | N=1 | 2 | 3 | 4 | 5 | 6 | 7 | 8 |
|---|---|---|---|---|---|---|---|---|---|
| 0.101 | 0 | 1.014 | 1.019 | 0.767 | 0.687 | 0.722 | 0.705 | 0.725 | 0.849 |
| | 3 | 0.974 | 0.972 | 0.704 | 0.678 | 0.688 | 0.699 | 0.718 | 0.866 |
| | 6 | 0.972 | 0.930 | 0.718 | 0.660 | 0.653 | 0.685 | 0.734 | 0.919 |
| | 9 | 0.928 | 0.868 | 0.639 | 0.605 | 0.636 | 0.718 | 0.825 | 0.990 |
| 0.142 | 0 | 1.014 | 1.019 | 0.768 | 0.687 | 0.723 | 0.705 | 0.754 | 0.995 |
| | 3 | 0.974 | 0.973 | 0.705 | 0.679 | 0.687 | 0.701 | 0.752 | 1.014 |
| | 6 | 0.972 | 0.931 | 0.718 | 0.660 | 0.655 | 0.687 | 0.815 | 1.068 |
| | 9 | 0.929 | 0.868 | 0.639 | 0.606 | 0.638 | 0.720 | 0.932 | 1.136 |
| 0.182 | 0 | 1.015 | 1.019 | 0.770 | 0.688 | 0.723 | 0.705 | 0.827 | 1.109 |
| | 3 | 0.974 | 0.975 | 0.706 | 0.679 | 0.684 | 0.701 | 0.848 | 1.128 |
| | 6 | 0.974 | 0.932 | 0.719 | 0.660 | 0.656 | 0.687 | 1.002 | 1.154 |
| | 9 | 0.930 | 0.869 | 0.640 | 0.607 | 0.638 | 0.720 | 1.091 | 1.195 |

RUN 5569 ME=2.00 POE=100.92 KPA PE=12.90 KPA ALPHA=-3.0 L/D=1.0 BETAE= 8.0
ML=1.41 THETAL=3.07

| POI MPA | M | N=1 | 2 | 3 | 4 | 5 | 6 | 7 | 8 |
|---|---|---|---|---|---|---|---|---|---|
| 0.114 | 0 | 1.020 | 1.037 | 0.778 | 0.674 | 0.720 | 0.693 | 0.723 | 0.801 |
| | 3 | 1.006 | 0.994 | 0.711 | 0.657 | 0.678 | 0.695 | 0.692 | 0.818 |
| | 6 | 0.975 | 0.936 | 0.709 | 0.639 | 0.638 | 0.663 | 0.658 | 0.865 |
| | 9 | 0.902 | 0.830 | 0.620 | 0.561 | 0.577 | 0.668 | 0.802 | 0.985 |
| 0.141 | 0 | 1.020 | 1.037 | 0.777 | 0.673 | 0.719 | 0.692 | 0.725 | 0.880 |
| | 3 | 1.005 | 0.994 | 0.711 | 0.657 | 0.675 | 0.695 | 0.693 | 0.899 |
| | 6 | 0.975 | 0.936 | 0.708 | 0.639 | 0.639 | 0.663 | 0.674 | 0.963 |
| | 9 | 0.902 | 0.830 | 0.619 | 0.561 | 0.576 | 0.668 | 0.913 | 1.051 |
| 0.214 | 0 | 1.018 | 1.037 | 0.777 | 0.673 | 0.719 | 0.691 | 0.738 | 1.059 |
| | 3 | 1.005 | 0.994 | 0.710 | 0.657 | 0.672 | 0.695 | 0.716 | 1.084 |
| | 6 | 0.976 | 0.935 | 0.706 | 0.637 | 0.640 | 0.663 | 0.903 | 1.139 |
| | 9 | 0.902 | 0.830 | 0.619 | 0.560 | 0.574 | 0.691 | 1.065 | 1.122 |

RUN 5571 ME=2.00 POE= 98.83 KPA PE=12.63 KPA ALPHA=-6.0 L/D=1.0 BETAE= 8.0
ML=1.41 THETAL=3.07

| POI MPA | M | N=1 | 2 | 3 | 4 | 5 | 6 | 7 | 8 |
|---|---|---|---|---|---|---|---|---|---|
| 0.099 | 0 | 1.055 | 1.075 | 0.798 | 0.691 | 0.744 | 0.700 | 0.722 | 0.702 |
| | 3 | 1.050 | 1.020 | 0.737 | 0.657 | 0.684 | 0.694 | 0.686 | 0.718 |
| | 6 | 0.983 | 0.939 | 0.698 | 0.617 | 0.621 | 0.648 | 0.619 | 0.760 |
| | 9 | 0.875 | 0.803 | 0.591 | 0.511 | 0.514 | 0.591 | 0.744 | 0.919 |
| 0.144 | 0 | 1.057 | 1.075 | 0.798 | 0.691 | 0.746 | 0.700 | 0.724 | 0.817 |
| | 3 | 1.051 | 1.021 | 0.738 | 0.657 | 0.683 | 0.694 | 0.686 | 0.841 |
| | 6 | 0.986 | 0.940 | 0.698 | 0.618 | 0.623 | 0.650 | 0.627 | 0.910 |
| | 9 | 0.879 | 0.804 | 0.591 | 0.511 | 0.515 | 0.591 | 0.931 | 1.022 |
| 0.239 | 0 | 1.058 | 1.076 | 0.798 | 0.691 | 0.747 | 0.700 | 0.725 | 1.006 |
| | 3 | 1.052 | 1.022 | 0.739 | 0.657 | 0.682 | 0.695 | 0.690 | 1.037 |
| | 6 | 0.986 | 0.941 | 0.697 | 0.618 | 0.624 | 0.650 | 0.829 | 1.091 |
| | 9 | 0.878 | 0.804 | 0.591 | 0.511 | 0.513 | 0.807 | 1.012 | 1.073 |

RUN 5573 ME=2.00 POE= 98.78 KPA PE=12.62 KPA ALPHA=3.0 L/D=1.0 BETAE= 8.0
ML=1.41 THETAL=3.07

| POI MPA | M | N=1 | 2 | 3 | 4 | 5 | 6 | 7 | 8 |
|---|---|---|---|---|---|---|---|---|---|
| 0.141 | 0 | 0.990 | 1.002 | 0.756 | 0.687 | 0.741 | 0.715 | 0.837 | 1.076 |
| | 3 | 0.960 | 0.958 | 0.697 | 0.686 | 0.698 | 0.715 | 0.900 | 1.080 |
| | 6 | 0.954 | 0.917 | 0.704 | 0.648 | 0.674 | 0.749 | 0.978 | 1.118 |
| | 9 | 0.912 | 0.868 | 0.649 | 0.624 | 0.690 | 0.788 | 0.894 | 1.162 |
| 0.174 | 0 | 0.991 | 1.002 | 0.756 | 0.687 | 0.741 | 0.715 | 0.962 | 1.160 |
| | 3 | 0.961 | 0.959 | 0.697 | 0.686 | 0.697 | 0.716 | 1.043 | 1.151 |
| | 6 | 0.954 | 0.917 | 0.704 | 0.648 | 0.675 | 0.751 | 1.092 | 1.177 |
| | 9 | 0.912 | 0.868 | 0.649 | 0.624 | 0.689 | 0.787 | 1.028 | 1.248 |
| 0.242 | 0 | 0.991 | 1.002 | 0.756 | 0.688 | 0.741 | 0.716 | 1.166 | 1.238 |
| | 3 | 0.961 | 0.960 | 0.697 | 0.686 | 0.695 | 0.735 | 1.149 | 1.210 |
| | 6 | 0.955 | 0.916 | 0.703 | 0.647 | 0.675 | 0.818 | 1.149 | 1.219 |
| | 9 | 0.912 | 0.868 | 0.648 | 0.623 | 0.688 | 0.787 | 1.204 | 1.320 |

RUN 5575 ME=2.00 POE= 98.73 KPA PE=12.62 KPA ALPHA=6.0 L/D=1.0 BETAE= 8.0

ML=1.41 THETAL=3.07

| POI MPA | M | N=1 | 2 | 3 | 4 | 5 | 6 | 7 | 8 |
|---|---|---|---|---|---|---|---|---|---|
| 0.112 | 0 | 0.987 | 0.998 | 0.725 | 0.630 | 0.692 | 0.686 | 0.759 | 0.929 |
| | 3 | 0.902 | 0.893 | 0.650 | 0.647 | 0.665 | 0.712 | 0.784 | 0.934 |
| | 6 | 0.915 | 0.897 | 0.693 | 0.674 | 0.725 | 0.774 | 0.878 | 1.014 |
| | 9 | 0.897 | 0.868 | 0.650 | 0.658 | 0.729 | 0.777 | 0.842 | 1.022 |
| 0.141 | 0 | 0.987 | 0.997 | 0.724 | 0.631 | 0.691 | 0.686 | 0.762 | 1.028 |
| | 3 | 0.902 | 0.893 | 0.650 | 0.646 | 0.663 | 0.712 | 0.865 | 1.022 |
| | 6 | 0.915 | 0.897 | 0.692 | 0.673 | 0.727 | 0.775 | 0.976 | 1.102 |
| | 9 | 0.898 | 0.868 | 0.651 | 0.657 | 0.759 | 0.777 | 0.895 | 1.110 |
| 0.222 | 0 | 0.986 | 0.997 | 0.724 | 0.632 | 0.691 | 0.687 | 0.804 | 1.262 |
| | 3 | 0.901 | 0.894 | 0.651 | 0.647 | 0.661 | 0.719 | 1.102 | 1.140 |
| | 6 | 0.915 | 0.897 | 0.690 | 0.671 | 0.728 | 0.830 | 1.119 | 1.170 |
| | 9 | 0.899 | 0.868 | 0.651 | 0.657 | 0.759 | 0.783 | 1.114 | 1.204 |